

# **Copper requirements and acquisition mechanisms in marine phytoplankton**

by

Jian Guo

A THESIS SUBMITTED IN PARTIAL FULFILMENT OF  
THE REQUIREMENTS FOR THE DEGREE OF

DOCTOR OF PHILOSOPHY

in

The Faculty of Graduate Studies

(Oceanography)

THE UNIVERSITY OF BRITISH COLUMBIA  
(Vancouver)

April 2012

© Jian Guo 2012

## Abstract

Copper nutrition is essential for the growth of marine diatoms, especially under Fe-limiting conditions. I investigated the physiology of Cu in marine phytoplankton by studying how the Fe and Cu availability interact and control Cu uptake and demand. I used short-lived Cu radioisotopes to determine the Cu requirements and steady-state Cu transport rates ( $\rho_{ss}\text{Cu}$ ) of ten species from three classes of marine phytoplankton, isolated from coastal and oceanic environments. I also determined the Cu uptake kinetics of two marine centric diatoms (*Thalassiosira oceanica* and *T. pseudonana*) grown under various Fe and Cu conditions (sufficient and limiting). Furthermore, putative genes encoding potential components of Cu transport and homeostasis were identified in *T. pseudonana*, and their expression was investigated. Copper had significant effects on growth rates and  $\rho_{ss}\text{Cu}$  of the oceanic phytoplankton, but not the coastal strains. Although Cu quotas (Cu:C) were not significantly higher in oceanic strains, there were five independent lines of evidence supporting a more important role of Cu in the physiology of oceanic phytoplankton. Distinct biphasic Cu transport rates as a function of Cu concentrations were observed in the centric diatoms, *Thalassiosira oceanica* and *T. pseudonana*, suggesting the presence of a high- and a low-affinity Cu transport system. The high-affinity Cu transport system followed Michaelis-Menten saturation kinetics, but was controlled differently by Fe and/or Cu availability. A strong interaction between Fe and Cu nutrition in controlling the expression of genes encoding Cu transport and homeostasis was observed. Most genes, including putative Cu transporters (CTR), Cu transporting P-type ATPases, Cu chaperones and putative Zn transporters in *T. pseudonana* were up-regulated by low Fe, while low Cu either had no effect or the effect was dependent on Fe availability. These results suggest a complex interaction between Cu and Fe response networks. The function of a putative Cu transporter (CTR) in *T. pseudonana* was examined using functional complementation of *Saccharomyces cerevisiae* *ctr1Δctr3Δ* mutant. Though the results were inconclusive, various explanations for these findings were discussed. This thesis highlights a complex interaction between Fe and Cu nutrition in marine phytoplankton at the protein and gene expression level.

# Preface

## Contributions of Authors

- 1) A version of chapter 2 will be published as: Guo, J., Lapi, S., Ruth, T. J. & Maldonado, M. T. 2012. The effects of iron and copper availability on the Cu stoichiometry of marine phytoplankton *J. Phycol.* 48 (in Press).

I conducted all the testing. The ideas, experiments and written manuscript were carried out in collaboration with my supervisor Dr. Maria T. Maldonado. Dr. Suzanne Lapi and Dr. Thomas J. Ruth provided the radioactive isotope  $^{67}\text{Cu}$ .

- 2) A version of chapter 3 was published as: Guo, J., Annett, A. L., Taylor, R. L., Lapi, S., Ruth, T. J. & Maldonado, M. T. 2010. Copper uptake kinetics of coastal and oceanic diatoms. *J. Phycol.* 46: 1218-28.

I conducted all the testing with the exception of data contained in Figure 3.1. These were collected by Dr. Maria T. Maldonado and Rebecca L. Taylor. The ideas, experiments and written manuscript were carried out in collaboration with my supervisor Dr. Maria T. Maldonado. Amber L. Annett provided pre-test data. Dr. Suzanne Lapi and Dr. Thomas J. Ruth provided the radioactive isotope  $^{67}\text{Cu}$ .

- 3) A version of chapter 4 was submitted as: Guo, J. Green, B. R. & Maldonado, M. T. Sequence analysis and gene expression of potential components of copper transport and homeostasis in *Thalassiosira pseudonana* grown under low copper and iron availability. (Manuscript ID: JPY-11-220-ART).

I conducted all the testing. The experiments and written manuscript were carried out in collaboration with my supervisor Dr. Maria T. Maldonado and Dr. Beverley R. Green.

# Table of Contents

<b>Abstract</b> .....	ii
<b>Preface</b> .....	iii
<b>Table of Contents</b> .....	iv
<b>List of Tables</b> .....	ix
<b>List of Figures</b> .....	xi
<b>Acknowledgments</b> .....	xiii
<b>Dedication</b> .....	xv
<b>Chapter 1 Introduction</b> .....	1
1.1 Marine phytoplankton and primary production .....	2
1.2 Trace metal nutrition of phytoplankton .....	3
1.3 Cellular Cu requirements of phytoplankton .....	4
1.4 Copper in the ocean .....	6
1.5 The effects of Fe and Cu availability on phytoplankton trace metal stoichiometry .....	7
1.6 Copper uptake kinetics .....	10
1.7 Molecular components and regulation of Cu acquisition and homeostasis ...	12
1.8 Thesis objectives .....	16
<b>Chapter 2 The effects of iron and copper availability on the copper stoichiometry of marine phytoplankton</b> .....	18
2.1 Introduction .....	19
2.2 Materials and methods .....	21
2.2.1 Studied organisms and culture manipulations .....	21
2.2.2 Growth parameter measurements .....	23
2.2.3 Cu:C ratio determinations .....	24
2.2.4 Statistical analyses .....	25
2.3 Results .....	25
2.3.1 Effect of Fe and Cu on growth rate and cell size .....	25
2.3.2 Effect of Fe and Cu availability on Cu quotas .....	33

2.3.3	Effect of Fe and Cu availability on steady-state Cu uptake	38
2.3.4	Effect of Fe and Cu availability on Cu use efficiency	41
2.4	Discussion	41
2.4.1	The effect of Fe and Cu availability on the growth rate	41
2.4.2	Cellular Cu:C ratios	43
2.4.3	Steady-state Cu uptake rates	48
2.5	Conclusions	52
<b>Chapter 3</b>	<b>Copper uptake kinetics of coastal and oceanic diatoms</b>	<b>55</b>
3.1	Introduction	56
3.2	Materials and methods	58
3.2.1	Study organisms	58
3.2.2	Media and culture manipulations	59
3.2.3	Determination of growth rates and cell sizes	60
3.2.4	Measurement of Cu uptake rates	61
3.2.5	Cu uptake kinetic parameters for cells grown under various Fe and/or Cu levels	62
3.3	Results	64
3.3.1	Cellular characteristics	64
3.3.2	Kinetics of Cu transport	65
3.3.3	Low-affinity Cu uptake kinetics	69
3.3.4	High-affinity Cu uptake kinetics	69
3.4	Discussion	72
3.4.1	Cu uptake kinetics of phytoplankton	72
3.4.2	<i>T. oceanica</i> versus <i>T. pseudonana</i> Cu uptake kinetics	74
3.4.3	Strong Cu and Fe effects on Cu Uptake Kinetics	75
3.4.4	High-affinity and low-affinity Cu transporters in eukaryotes	76
3.4.5	Oceanographic implications	77
<b>Chapter 4</b>	<b>Sequence analysis and gene expression of potential components of copper transport and homeostasis in <i>Thalassiosira pseudonana</i> grown</b>	

	<b>under low copper and iron availability</b> .....	81
4.1	Introduction .....	82
4.2	Materials and methods .....	84
	4.2.1 Candidate genes and sequence analysis .....	84
	4.2.2 Algal culturing .....	85
	4.2.3 RNA extraction and quantitative real-time PCR .....	87
	4.2.4 Statistical analysis .....	88
4.3	Results .....	88
	4.3.1 Effects of long-term acclimation to Fe and/or Cu starvation on growth rate and cell size .....	88
	4.3.2 Putative CTR Cu transporters and their gene expression .....	88
	4.3.3 Putative Cu-transporting p-type ATPases and their gene expression ..	97
	4.3.4 Putative Cu chaperones .....	100
	4.3.5 Putative ZIP transporters .....	102
	4.3.6 Relative gene expression of components of Fe uptake system .....	108
4.4	Discussion .....	110
	4.4.1 Potential components of Cu acquisition system in <i>T. pseudonana</i> ...	110
	4.4.2 Intracellular Cu transporters and Cu chaperones in <i>T. pseudonana</i> ..	112
	4.4.3 Transcriptional activation of Fe transport-related genes in response to Cu deficiency .....	113
	4.4.4 Copper and Fe deficiency induce changes in Zn transporters .....	114
<b>Chapter 5 Functional complementation of <i>Saccharomyces cerevisiae</i></b>		
	<b><i>ctr1Δctr3Δ</i>mutant (MPY17) by expression of <i>Thalassiosira pseudonana</i></b>	
	<b>CTRs</b> .....	116
5.1	Introduction .....	117
5.2	Materials and methods .....	122
	5.2.1 Organisms and growth conditions .....	122
	5.2.2 Cloning of putative CTR-like genes in <i>T. pseudonana</i> .....	123
	5.2.3 Yeast plasmid construction .....	124

5.2.4	Functional complementation in yeast .....	124
5.2.5	Amplification of <i>T. pseudonana</i> CTR-like genes from transformed yeast cells .....	124
5.3	Results and Discussion .....	125
<b>Chapter 6</b>	<b>General conclusions .....</b>	<b>129</b>
6.1	Summary of major findings and contributions .....	130
6.2	Conclusions and findings for specific dissertation hypotheses .....	134
6.2.1	Oceanic phytoplankton have a higher Cu demand for growth than coastal strains .....	134
6.2.2	The copper requirements of Fe-limited phytoplankton are higher than those of Fe-sufficient ones .....	135
6.2.3	Copper quotas are higher for eukaryotic phytoplankton of the green plastid than the red plastid superfamilies. <i>Synechococcus</i> have the lowest Cu quotas, as they evolved in a low Cu environment and are very sensitive to high Cu levels .....	136
6.2.4	Marine diatoms possess a high- and a low-affinity Cu transport system, and these systems are controlled differently by Fe and/or Cu availability .....	138
6.2.5	Copper uptake rate is determined by the concentration of total Cu and not that of free Cu <sup>+</sup> .....	139
6.2.6	The putative genes encoding high- and low-affinity Cu transport systems, as well as for Cu chaperones are present in the genome of <i>T. pseudonana</i> . Their gene expressions are affected by Cu and/or Fe availability .....	140
6.2.7	The putative high affinity, CTR-like Cu transporters in <i>T. pseudonana</i> are novel .....	140
6.4	Future research .....	142
	<b>Bibliography .....</b>	<b>145</b>
	<b>Appendix A Supplemental table 1. A list of all genes and primer sequences used</b>	

**in this study** ..... 173

## List of Tables

Table 1.1	Summary of Cu transporters, Cu chaperones and their targets in three model eukaryotic organisms . . . . .	15
Table 2.1	Species name, taxa, clone, isolation site, oceanic provenance and cell diameter ( $\mu\text{m}$ ) of the marine phytoplankton used in this study . . . . .	22
Table 2.2	Iron and copper additions to culture media . . . . .	23
Table 2.3	Growth rates ( $\text{d}^{-1}$ ) and cell diameter ( $\mu\text{m}$ ) of marine phytoplankton grown under different Fe and Cu levels . . . . .	28
Table 2.4	Statistical analyses (two-way ANOVA) of Fe effect, Cu effect, and Fe $\times$ Cu interaction on growth rates, Cu:C and steady-state Cu uptake rates ( $\rho_{\text{ss}}\text{Cu}$ ) . . . . .	31
Table 2.5	Results (p value) from the linear mixed-effect model statistical analyses on the growth rates, Cu quotas, and steady-state Cu uptake rates ( $\rho_{\text{ss}}\text{Cu}$ ) . . . . .	32
Table 2.6	Cellular concentration of Cu ( $\mu\text{M}$ ) and C (M), and Cu:C ( $\mu\text{mol Cu} \cdot \text{mol}^{-1} \text{C}$ ) ratios of phytoplankton grown under different Fe and/or Cu levels . . . . .	35
Table 2.7	Steady-state Cu uptake rates ( $\rho_{\text{ss}}\text{Cu}$ , $\times 10^{-20} \text{ mol Cu} \cdot \mu\text{m}^{-2} \cdot \text{d}^{-1}$ ) and Cu use efficiency ( $\text{mol C} \cdot \mu\text{mol Cu}^{-1} \cdot \text{d}^{-1}$ ) of phytoplankton grown under different Fe and/or Cu levels . . . . .	39
Table 2.8	Comparison of C-normalized copper quotas (Cu:C) of different phytoplankton phyla in this study with values reported by Ho et al. (2003) . . . . .	44
Table 2.9	The effects of Fe limitation on growth rate ( $\mu$ ), Cu:C ratios (both expected and observed), and steady-state Cu uptake rates ( $\rho_{\text{ss}}\text{Cu}$ ) in oceanic and coastal phytoplankton grown under replete (pCu 14) and low Cu (pCu 15) conditions . . . . .	50
Table 3.1	Culture media with various Fe and Cu additions . . . . .	60
Table 3.2	Cellular characteristics (mean $\pm$ SD) of live <i>T. oceanica</i> and <i>T. pseudonana</i> grown under different Fe and Cu levels . . . . .	64
Table 3.3	Kinetic parameters of the high- and low-affinity Cu transport system in <i>T. oceanica</i> and <i>T. pseudonana</i> grown under various Fe and Cu levels . . . . .	68

Table 3.4	Effects (p-value, TDIST and two-way ANOVA) of Cu availability, Fe availability and the interaction between Fe and Cu availability on $K_m$ and $V_{max}$ of the low- and high-affinity Cu transport system in <i>T. oceanica</i> and <i>T. pseudonana</i> . . . . .	71
Table 3.5	Measured Cu uptake rates ( $\rho_{Cu}$ ) by <i>T. oceanica</i> and <i>T. pseudonana</i> grown in Fe/Cu replete media, maximum diffusive rate of dissolved inorganic Cu ( $Cu'$ ) from the bulk solution to the surface of the diatom cell ( $J_D$ ), and the ratio of $\rho_{Cu}: J_D$ . . . . .	80
Table 4.1	Growth rate ( $d^{-1}$ ) and cell diameter ( $\mu m$ ) of <i>T. pseudonana</i> grown under different Fe and Cu concentrations . . . . .	86
Table 4.2	Statistic results (two-way ANOVA) of low Fe effect, low Cu effect, and the Fe and Cu interaction on transcript abundance of putative genes involved in Cu and Fe acquisition . . . . .	99

## List of Figures

Figure 1.1	Approximate relative differences in Cu and Fe availability in ocean and phytoplankton phyla appearance through geological time . . . . .	8
Figure 1.2	A model for Cu homeostasis in <i>S. cerevisiae</i> and in chloroplast of <i>Arabidopsis</i> . . . . .	14
Figure 2.1	Growth rates ( $d^{-1}$ ) of oceanic and coastal phytoplankton grown under different Fe and/or Cu levels (pFe_pCu) . . . . .	30
Figure 2.2	Cu:C ratios ( $\mu\text{mol Cu} \cdot \text{mol}^{-1} \text{C}$ ) of oceanic and coastal phytoplankton grown under different Fe and/or Cu levels . . . . .	37
Figure 3.1	Michaelis-Menten kinetics of Cu uptake as a function of total Cu concentrations in Fe and Cu replete <i>T. pseudonana</i> . . . . .	63
Figure 3.2	Michaelis-Menten kinetics of Cu uptake as a function of total Cu concentrations in <i>T. oceanica</i> and <i>T. pseudonana</i> cultured under different Cu and Fe levels . . . . .	67
Figure 4.1	Structural model and conserved motifs of the CTR proteins of <i>S. cerevisiae</i> ( <i>ScCTR1</i> ), <i>A. thaliana</i> ( <i>AtCOPT1</i> ), <i>C. reinhardtii</i> ( <i>ChCTR1</i> ), <i>O. lucimarinus</i> ( <i>OlCTR1</i> ) and putative CTRs of <i>T. pseudonana</i> ( <i>TpCTR</i> and <i>TpCTR/S</i> ) . . . . .	90
Figure 4.2	Alignment of putative <i>T. pseudonana</i> CTR ( <i>TpCTR</i>  24275) with other organisms, including <i>Fragilariopsis cylindrus</i> , <i>Phaeodactylum tricornutum</i> , <i>Perkinsus marinus</i> , <i>Ostreococcus lucimarinus</i> and <i>Micromonas pusilla</i> . . . . .	93
Figure 4.3	Steady-state relative gene expression of putative Cu transporters and Cu chaperones in <i>T. pseudonana</i> under different Fe and Cu levels . . . . .	95
Figure 4.4	Relative gene expression of putative Cu transporters and Cu chaperones in low Cu acclimated <i>T. pseudonana</i> supplied with excessive Cu (500 nM) . .	96
Figure 4.5	Structural models and conserved motifs of Cu-transporting p-type ATPase of <i>S. cerevisiae</i> ( <i>ScCcc2</i> ), <i>A. thaliana</i> ( <i>AtPAA1</i> ), <i>Synechococcus elongatus</i> ( <i>SePacS</i> ) and putative <i>TpCTP</i>  263051 and <i>TpCTP</i>  264357 of <i>T.</i>	

	<i>pseudonana</i> .....	98
Figure 4.6	Alignment of putative <i>Tp</i> COX17 264096 (a) and <i>Tp</i> COX11 37139 (b) from <i>T. pseudonana</i> with other known or putative homologous from <i>S. cerevisiae</i> ( <i>Sc</i> ), <i>A. thaliana</i> ( <i>At</i> ), <i>C. reinhardtii</i> ( <i>Ch</i> ), and <i>O. lucimarinus</i> ( <i>Ol</i> ) .....	101
Figure 4.7	Alignment of <i>Chlamydomonas</i> <i>gufA</i> subfamily of ZIP proteins with putative ZIPs of <i>T. pseudonana</i> and <i>O. lucimarinus</i> .....	104
Figure 4.8	Alignment of the sequences of predicted transmembrane domains (TM 4-8) of subfamily ZIPs from <i>Homo sapiens</i> ZIP1 and ZIP2, <i>Chlamydomonas</i> ZIP2 and ZIP6, with their homolog <i>Tp</i> ZIP 11826 in <i>T. pseudonana</i> .....	105
Figure 4.9	Steady-state relative gene expression of putative ZIP-like transporters in <i>T. pseudonana</i> under different Fe and/or Cu availability .....	106
Figure 4.10	The relative gene expression of putative ZIP-like transporters and putative components of Fe transport system in low Cu acclimated <i>T. pseudonana</i> supplied with excessive Cu (500 nM) .....	107
Figure 4.11	Steady-state relative gene expression of putative components for Fe transport in <i>T. pseudonana</i> under different Fe and Cu availability .....	109
Figure 5.1	Membrane topological structure model (a) and homo-trimer structure (b) of CTR family proteins .....	119
Figure 5.2	Signature motif MxxxM-x <sub>12</sub> -GxxxG in transmembrane domain (TM2 and TM3) of CTR family proteins .....	120
Figure 5.3	Non-functional complementation of the yeast mutant MPY17, which is deficient in high affinity Cu transport, by putative <i>T. pseudonana</i> CTR-like genes <i>Tp</i> CTR 24275 and <i>Tp</i> CTR 9391 .....	126
Figure 5.4	PCR products of putative CTR-like genes <i>Tp</i> CTR 24275 and <i>Tp</i> CTR 9391 from cDNA of transformed yeast cells .....	128

# Acknowledgements

From the bottom of my heart, I would like to thank sincerely my advisor, Maria (Maite) Maldonado. I thank her so much for always encouraging and supporting me with patience all these years on my research. I consider myself incredibly lucky to have Maite to be my advisor. Her energy, enthusiasm, and love of science are contagious. She always enlightened me with her ideas, and she even studied with me together whenever I got stuck and confused with my work. I would like to thank Maite not only for her professional guidance in research but also for being a friend and a sister who gave me a lot of encourage and help in my life, especially when my life was in the most difficult time. I am truly grateful!

I would like to express my deep and sincere gratitude to my committee members, Beverley Green and Robert Guy for their valuable comments, suggestions and proofreading of my dissertation. I really appreciate Beverley Green for her help and encouragement, and for allowing me to use her laboratory facilities. I have learned so much from working with her and would never have finished this work without her support.

My special thanks go to Philippe Tortell for introducing me to study in Maite's lab, and for his support and encouragement on my study. I also would like to thank him for the many thoughtful comments, ideas, and suggestions that have greatly improved this dissertation.

I would like to thank all the past and present lab members of the Maite and Philipe team. I want to thank Amber Annett, Anna Hippmann, Erin lane, David Semeniuk, David Cassis, Lauren Moccia, Rebecca Taylor, Jade Shiller and Ana Lombardi for their help in the lab, for comments and proof-reading of grammar mistakes of this dissertation, and for their friendship and generous help during my study here. I also would like to thank Dr. Meriem Alami for her kind support and suggestions on my gene cloning experiments.

I am also forever indebted to my best friends, Eryang Li, Songhua Zhu and Ye Wang, for all their love and support in my life and my research. I knew them in Vancouver, but their friendship is a gift I will always cherish.

I would like to thank the funding sources NSERC PGS D that had supported my study here. Also I would like to thank the Journal of Psychology and PSA for giving me permission to reproduce the figures in this thesis.

Lastly, but most importantly, I would like to express my deep and sincere gratitude to my parents and my brother who has been loving and supporting me unconditionally. I also owe more than thanks to my husband Yu Hu, without his endless encouragement, support, and love I would have never made it this far. I would also like to thank my dear daughter Mofei Hu, whose love and smile mean the world to me.

# Dedication

To my parents

&

my husband Yu and my daughter Mofei

# **Chapter 1**

## **Introduction**

## 1.1 Marine phytoplankton and primary production

Marine phytoplankton are single-celled algae that inhabit in the sunlit layers of the ocean. They are the main primary producers of the sea and constitute the base of most marine food webs. Phytoplankton account for approximately half of the global biospheric net primary production (Falkowski 1994, Field et al. 1998). They provide food for animals at all trophic levels from tiny zooplankton, like protozoa, to the largest marine mammals, like blue whales. Moreover, through the process of photosynthesis, phytoplankton take up inorganic carbon and dissolved nutrients, such as phosphate and nitrate, and convert these into organic material. When phytoplankton die, they sink as whole cells or aggregates, or they are eaten by zooplankton and sink as zooplankton fecal pellets. Part of this sink carbon can be remineralized and re-used by phytoplankton, but a large fraction of fixed carbon sediments to the seafloor. It is estimated that 45 gigatons of organic carbon are produced by phytoplankton and 16 gigatons are lost to the sediments each year (Falkowski et al 1998). Carbon is thus effectively removed by phytoplankton from the ocean-atmosphere climate system. This “biological pump” by which the ocean sequesters carbon plays a central role in the global carbon cycle. Thereby, phytoplankton productivity has a significant impact on the atmosphere, the marine biogeochemical C cycle and the global climate.

Phytoplankton growth is greatly influenced by the physical and chemical environment, e.g. light, temperature, turbulence and nutrients. Changes in nutrient availability will affect phytoplankton biomass, physiology, and community composition. In general, phytoplankton need macro-nutrients in a well defined stoichiometric ratio (Carbon: Nitrogen: Phosphorus = 106:16:1, Redfield et al. 1963). They also need small amounts of micro-nutrients (such as Fe, Zn, Cu, Mn and Ni) for growth. If an essential nutrient is available at a limiting concentration and all other required nutrients are at adequate concentrations, then phytoplankton growth and primary production will be controlled by the bioavailability of the limiting nutrient.

## 1.2 Trace metal nutrition of phytoplankton

Trace metals (Fe, Mn, Zn, Co, Cu, Ni, Se and Mo) are very important nutrients for phytoplankton growth. The availability of trace elements can influence the abundance and succession of phytoplankton at both limiting (Martin et al. 1988) and toxic concentrations (Brand et al. 1986). Trace metals play critical roles in many metabolic pathways, such as photosynthesis, respiration and the assimilation of macronutrients. They may also affect the composition of phytoplankton communities because of the large differences in trace metal requirements among phytoplankton phyla and even among species of the same genera isolated from different environments (Brand et al. 1983, Sunda and Huntsman 1995a, Crawford et al. 2003). The metal assimilation pathways of phytoplankton are regulated by metal supply and demand. When metal availability does not meet the requirement, adaptive cellular mechanisms for metal uptake and distribution come into play (Morel et al. 2003). When metal concentrations are too high, the activity of the free metal may be lowered by the production of metal chelating agents intracellularly (Ahner and Morel 1995) and/or extracellularly (Croot et al. 2000).

Among micronutrients, Fe is needed in the greatest amount in most phytoplankton (Ho et al. 2003). Due to its redox properties, Fe is a component of many enzymes and electron transferring proteins involved in photosynthesis and respiration, as well as other biological reactions such as assimilation of nitrate, and detoxification of oxygen radicals (See Morel et al. 1991, Geider and LaRoche 1994, Raven et al. 1999 for reviews).

Iron is abundant in the earth's crust, but its stable oxidation state is the ferric ion ( $\text{Fe}^{3+}$ ), which is insoluble in seawater. In the surface oceans, the main sources of Fe are aeolian and riverine inputs, as well as upwelling from deep waters (Coale et al. 1996a, Johnson et al. 1997, Wu and Luther 1996, Duce and Tindale 1991, Lam and Bishop 2008). Thus, the dissolved Fe concentrations in coastal areas are higher (100 to 1000 fold) than those in the open ocean due to the proximity to land and the physical processes associated with coastal regions (e.g. coastal upwelling and river inputs etc.) (Sunda and Huntsman,

1995a). In addition, the speciation of dissolved Fe in seawater is an important determinant of its bioavailability, since inorganic Fe is readily available to phytoplankton. However, most of the dissolved Fe (>99%) in surface waters is bound to strong organic complexes (Rue and Bruland 1995, Wu and Luther, 1995). In the open ocean, the mean dissolved Fe concentration is 70 pM (Johnson et al. 1997). However, due to organic complexation, the resulting inorganic dissolved Fe concentration is 0.7 pM, too low to support phytoplankton growth of even the smallest phytoplankton. Iron-enrichment experiments in bottle incubations (Martin et al. 1989, Boyd et al. 1996) and in mesoscale enrichment experiments (Martin et al. 1994, Coale et al. 1996b, Boyd et al. 2000, Gervais et al. 2002) have shown that Fe limits marine algal growth and that Fe additions result in macronutrient consumption and increased photosynthetic biomass. At present, it is believed that marine primary productivity is limited by extremely low dissolved Fe concentrations in at least 30% of the world oceans (Bruland and Lohan, 2003); including the subarctic Pacific, the equatorial Pacific and the Southern ocean (Martin and Fitzwater 1988, Coale et al. 1996a, 1996b, Boyd et al. 2000, Tsuda et al. 2003). In response to Fe limitation, phytoplankton may 1) decrease their size, 2) lower their Fe requirements and/or 3) perform rapid sequestration of Fe from the environment (Ryther and Kramer 1961, Brand et al. 1983, Sunda et al. 1991, Sunda and Hustman 1995a, Maldonado and Price 1996, Hudson and Morel, 1990, Strzepek and Harrison, 2004). Two of these adaptations (2 & 3) involve Cu, another essential micronutrient for phytoplankton.

### **1.3 Cellular Cu requirements of phytoplankton**

Copper has two oxidation states,  $\text{Cu}^+$  and  $\text{Cu}^{2+}$ . These two states make Cu a valuable cellular constituent. Cu performs an important role in respiration as a co-factor of cytochrome c oxidase. It is also an important component of the photosynthetic apparatus in freshwater green algae (Merchant and Bogorad, 1986) and in some marine diatoms (Peers and Price 2006). In the freshwater green alga *Chlamydomonas*, the Cu-containing enzyme plastocyanin accounts for at least half of the intracellular Cu in this organism (Merchant et al. 2006). The expression of plastocyanin is inhibited under low Cu, when

instead its Fe containing replacement, cytochrome  $c_6$ , is induced (Merchant et al. 1991, Li and Merchant, 1995). The involvement of plastocyanin in the photosynthetic apparatus of marine eukaryotic phytoplankton was recently discovered in an oceanic diatom, *Thalassiosira oceanica* (Peers and Price, 2006). The Cu replacement for Fe containing enzymes decreases intracellular Fe requirements, and may explain the success of oceanic phytoplankton in open ocean waters where Fe concentrations are too low to support phytoplankton growth of coastal species. However, whether the use of plastocyanin is common in other oceanic phytoplankton is still unknown.

Copper is also involved in the high-affinity Fe transport system of some Fe-limited diatoms (Maldonado and Price 1999 & 2001), as previously demonstrated in the yeast *Saccharomyces cerevisiae* (Askwith et al. 1994) and the green alga *Chlamydomonas reinhardtii* (La Fontaine et al. 2002). This uptake system allows phytoplankton to access the greatest pool of dissolved Fe, organically bound Fe. In this high-affinity Fe uptake system, extracellular  $Fe^{3+}$  is reduced to the more-soluble  $Fe^{2+}$  by reductases embedded in the cell's plasma membrane (Maldonado and Price, 2000 & 2001). The activity of these reductases result in the dissociation of  $Fe^{2+}$  from the ligand, as the vast majority of these organic ligands have a much higher affinity for  $Fe^{3+}$  than  $Fe^{2+}$ . Multi-Cu containing oxidases oxidize  $Fe^{2+}$  back to  $Fe^{3+}$  before it reacts with the Fe transporter (Maldonado et al. 2006). The transcription level of the putative gene encoding the multi-Cu containing oxidase increases by 60-fold when the coastal diatom *Thalassiosira pseudonana* is cultured in Fe-deplete medium (Maldonado et al. 2006). The reduction and oxidation steps impart high specificity to the high-affinity Fe transport system. Iron limitation thus likely increases the need for Cu in phytoplankton.

These described Cu uses (replacing Fe with Cu in some metabolic functions, and the role of Cu in the high-affinity Fe transport system) in marine diatoms imply a link between Fe and Cu nutrition, and suggest that Cu is important for the growth of Fe-limited and/or oceanic phytoplankton (Peers et al. 2005, Wells et al. 2005, Maldonado et al. 2006 and Annett et al, 2008). However, the interaction between Cu and Fe, at a physiological and

molecular level, when phytoplankton are grown with limiting Fe and/or Cu levels, is not well documented.

## 1.4 Copper in the ocean

Copper is supplied to the surface oceans from aerosol deposition, upwelling, riverine and anthropogenic inputs (Nriagu 1979, Bashkin 2002). The total dissolved Cu concentration in non-polluted seawaters ranges from 0.5 to 6 nM, with an average concentration of 4 nM (Millero 2006, page 91). The concentration of Cu tends to increase slightly from open oceans to coastal waters (Boyle et al. 1981, Van der Loeff et al. 1997). The total Cu concentration in surface-water of the open ocean is ~1 nM (Bruland and Lohan, 2003), and that of non-polluted coastal waters is ~4-6 nM (Moffett et al, 1997). Moreover, recent laboratory experiments demonstrate that the growth of some oceanic diatoms is reduced when Cu levels are between 1-5 nM (pCu 14.5 to 15) (Peers and Price 2005, Annett et al. 2008) suggesting that Cu availability in the open ocean may be limiting at times.

In seawater, dissolved Cu can exist in several forms: free  $\text{Cu}^{2+}$ , inorganic complexes and organic complexes. Several investigations in the open ocean of the Atlantic showed that in surface waters Cu combines with organic ligands (Sunda and Ferguson 1983, Huizenga and Kester 1983, van den Berg 1984, Kramer 1986). Furthermore, up to 99.8% of  $\text{Cu}^{2+}$  was bound to strong class organic ligands (L1) in non-polluted coastal waters (e.g. San Francisco Bay, reviewed by Buck et al, 2007) and the open ocean of the Northeast Pacific (Coale and Bruland 1988, 1990), so that free  $\text{Cu}^{2+}$  concentration is greatly reduced. A recent study in the subarctic NW Pacific and the Bering Sea (Moffet and Dupont 2007) indicates that Cu is strongly complexed and that the free  $\text{Cu}^{2+}$  concentrations in these surface waters are  $2-4 \times 10^{-14}$  M (pCu 13.7 to 13.4). The combined evidence indicates that in the ocean the vast majority of dissolved Cu is bound to very strong organic ligands. Indeed, the Cu-binding ligands include two distinct classes: L1 and L2, with high (Log  $K'=12-14$ ) and low (Log  $K'=9-12$ ) conditional stability constant, respectively (Coale and Bruland 1988, 1990, Van den Berg et al. 1987). However, their sources and structures

are still unclear.

Copper is considered toxic and can damage the cell when intracellular Cu content is excessive (Brand et al. 1986, Ruter et al. 1979 and Sunda and Huntsman 1998a). For example, the growth rate of many dinoflagellates and cyanobacteria is inhibited when free Cu concentrations are higher than  $10^{-11}$  mol L<sup>-1</sup> (Brand et al. 1986). In addition, Cu can induce antagonistic effects on the uptake of other essential micronutrients (e.g. Mn<sup>2+</sup> and Zn<sup>2+</sup>). In response to Cu stress, some phytoplankton are known to release extracellular Cu-binding ligands. Marine *Synechococcus* cyanobacteria produce strong ligands with high conditional stability constants in the range of those of L1 ligands (Moffett et al. 1990, Moffett and Brand 1996, Gordon et al. 1996, Wiramanaden et al. 2008), while some eukaryotic phytoplankton are known to release Cu-binding ligands with low conditional stability constants in the range of those of L2 ligands (Gledhill et al. 1999, Moffett & Brand 1996, Croot et al. 2000). However, whether phytoplankton are also able to produce and release organic complexes in response to low Cu is unknown.

## **1.5 The effects of Fe and Cu availability on phytoplankton trace metal stoichiometry**

Earth's atmospheric oxygen originated from photosynthesis (Cloud 1973, Walker et al. 1983), starting to accumulate in the atmosphere by ~ 2.32 billion years ago (Bekker et al, 2004). This oxygenation of the Earth's atmosphere changed the redox state of the metals in the oceans (Zerkle et al, 2006). As a result, abundant Fe<sup>2+</sup> oxidized to Fe<sup>3+</sup>, becoming more insoluble, and thus less abundant in seawater. In contrast, in oxygenated seawater, Cu was released from particulates (e.g. CuS) and became more soluble. Thus, in the Archean ocean, while Fe was more abundant ( $\sim 1 \times 10^{-4}$  M) Cu was more scarce ( $\sim 1 \times 10^{-22}$  M) (Saito et al, 2003). This contrasts with the modern ocean where Cu concentrations (higher than  $1 \times 10^{-9}$  M) exceed those of Fe (lower than  $1 \times 10^{-9}$  M) in open ocean waters (Figure 1.1).

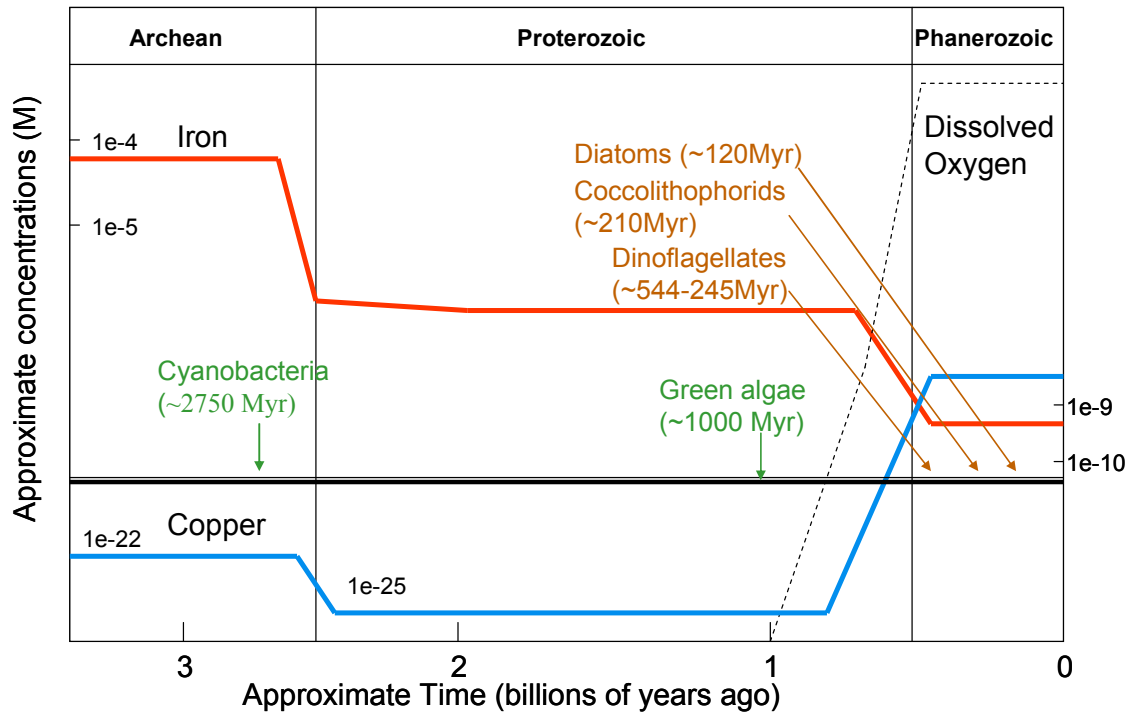


Figure 1.1 Approximate relative differences in Cu and Fe availability in ocean and phytoplankton phyla appearance through geological time (Redrawn from Saito et al, 2003 and Quigg et al, 2003).

The bioavailability of metal elements in the local environment of an organism influences the selection of a trace element in the active site of an enzyme, as postulated by Da Silva and Williams (Da Silva and Williams, 1991, p. 9-10). The atmospheric oxygen evolution has affected the choice of metals used in the photosynthetic electron transport chain; one example is the Cu-containing plastocyanin versus the Fe-containing equivalent, cytochrome  $c_6$ . Indeed, the availability of Fe and Cu regulates the expression of these two proteins in many cyanobacteria and chlorophytes (Wood 1978, Sandmann et al., 1983, Merchant 1998). In the anaerobic Archean ocean, when Cu concentration was low and that of Fe was higher, the utilization of Fe in electron-transfer reactions was favored, thus cytochrome  $c_6$  evolved. Later on, when Cu availability increased, plastocyanin was favored to ferry electrons from the cytochrome  $b_6/f$  complex to  $P_{700}$  (see review of Raven et al. 1999, Palenik et al. 2003).

Differences in trace elemental stoichiometries among phytoplankton phyla reflect environmental selection pressures on components of the photosynthetic apparatus where metal substitutions are possible (Quigg et al. 2003). Phytoplankton phyla evolved at different geological times: prokaryotic cyanobacteria originated in the Archean ocean (~2750 Myr), and eukaryotic algae originated in the Palaeozoic (~1000 Myr) and the Modern oceans (from ~540 to ~120 Myr). In the modern ocean, cyanobacteria are the vast majority of phytoplankton and are very sensitive to high levels of Cu in the environment (Brand et al. 1986, Ahner et al. 1997, Mann et al. 2002). This may be due to their origin in the Archean ocean, when Cu concentrations were extremely low. To deal with the relatively higher Cu levels in the modern ocean, cyanobacteria have developed the ability to produce strong organic ligands to bind high dissolved Cu, and reduce its toxicity (Moffett and Brand 1997, Moffett 1995). A systematic difference in the trace metal stoichiometries between phytoplankton with chlorophyll a/b antennas (chlorophytes and prasinophytes) and those with chlorophyll a/c antennas was observed (Quigg et al. 2003). Marine phytoplankton with chlorophyll a/c antennas (diatoms, dinoflagellates, haptophytes) have relatively higher Mn, Co and Cd quotas (metal:P ratio)

and lower Fe, Zn and Cu quotas compared to those with chlorophyll a/b antennas, suggesting a critical role of the environmental changes arising from the redox state of the ocean on the trace element requirement of phytoplankton with different acquired plastids (Quigg et al. 2003). In addition, the availabilities of many micronutrients (e.g. Fe and Cu) are relatively lower in oceanic than in coastal waters. Indeed, pronounced differences exist between the trace metal requirements of coastal and oceanic isolates of the same genera, emphasizing a significant habitat effect (Sunda and Huntsman 1995b, Maldonado and Price 1996, Annett et al. 2009).

## 1.6 Copper uptake kinetics

Numerous studies have focused on the toxicity of Cu in marine phytoplankton (Rueter et al., 1979, Brand et al. 1986, Pistocchi et al. 1997 and Miao et al., 2005), but only few studies have examined the kinetics of Cu uptake (Chang and Reinfelder 2000, Croot et al. 2003 and Quigg et al., 2006). Moreover, little information exists linking Cu uptake kinetics of phytoplankton to limiting Fe and Cu levels.

In contrast, many studies have investigated Cu uptake kinetics and transport in yeast and freshwater algae. In yeast *Saccharomyces cerevisiae*, Cu uptake is mediated by either a high- or a low-affinity system, depending on Cu availability. High affinity Cu uptake is specific for  $\text{Cu}^+$  over other metal ions (Dancis et al. 1994a and Lin and Kosman 1990). The half-saturation constant ( $K_m$ ) of this high-affinity Cu uptake system is about 1–4  $\mu\text{M}$  dissolved Cu in yeast (Dancis et al. 1994a, De Rome and Gadd 1987, Lin and Kosman 1990). In the freshwater microalgae *Scenedesmus subspicatus*, Cu uptake is also mediated by two systems: a high-affinity ( $K_m=0.07$  pM free  $[\text{Cu}^{2+}]$ ) and a low-affinity system ( $K_m=2.8$  pM free  $[\text{Cu}^{2+}]$ ) (Knauer et al. 1997). In contrast, in *Chlamydomonas*, the  $K_m$  was invariant (0.2 $\mu\text{M}$ , dissolved Cu), but the maximum rate of Cu uptake ( $V_{\text{max}}$ ) achieved by the cells was 20 fold faster in Cu deficient than in Cu sufficient conditions (Hill et al, 1996). These parameters suggested that the same transporter operates in both Cu-replete and Cu-deficient condition, but the number of Cu transporters at the cell surface is higher

under Cu-deficient conditions.

So far, marine phytoplankton studies have shown that Cu uptake in some marine phytoplankton under non-Cu limited conditions is determined by the activity of the free metal ion and follows Michaelis–Menten kinetics (Sunda and Huntsman, 1995b, and Croot et al. 2003). For example, under high Cu level, the marine blue-green alga *Synechococcus* (WH1708) and the dinoflagellate *Amphidinium carterae* have similar half saturation constants ( $K_m$ ) for transport (15.8 pM and 3.9 pM for free  $\text{Cu}^{2+}$ , respectively) (Croot et al., 2003). These  $K_m$  values are similar to that of the low-affinity transport system of the freshwater microalgae *S. subspicatus* (Knauer et al. 1997). This is not surprising, since the cultures were not Cu limited and thus only the low-affinity Cu uptake system should be active. So far, no kinetic studies have focused on the mechanism of Cu acquisition by marine phytoplankton when Cu is limiting. Thus, we do not know whether a high-affinity Cu transport system exists in marine phytoplankton.

The free ion uptake model suggests that metal uptake in phytoplankton is determined by the activity of the free metal ion and not by the total complexed metal concentration (Sunda 1994). However, whether phytoplankton can access Cu bound to strong organic ligands is not known. The process of uptake of a trace metal from the environment is comprised of three steps: diffusion of metal ions from the bulk solution to the cell surface; metal ion binding with transporters on the cell membrane; and internalization into the cells by transporters (Morel 1983, Campbell 1995). In the free ion uptake model, it is assumed that the limiting step is the metal ion transport across the cell membrane but not the ion concentration in the bulk solution. However, when the metal ion concentration is low, such as the Fe concentration in most open oceans, the metal ion diffusion from the bulk solution to the cell surface becomes the limiting step. It has been shown that marine phytoplankton can reductively release and acquire Fe from organic Fe complexes (Maldonado and Price, 2001). In addition, it has been demonstrated that cupric reductase activity exists at the cell surface of marine phytoplankton (Jones et al., 1987), and some studies hint that organically bound Cu may be bioavailable (Quigg et al, 2006, Annett et

al. 2008, Semeniuk et al. 2009). Thus phytoplankton may use organically complexed Cu in a similar manner to that of Fe. Some phytoplankton can release extracellular ligands to bind Cu. The cyanobacterium *Synechococcus* can produce a strong Cu complexing ligand to relieve Cu toxicity when ambient free Cu concentration is high (Moffett and Brand 1996). *Dunaliella* sp. and *T. pseudonana* can produce glutathione (GLO, GSH) inside the cell when exposed to steady-state high concentration of Cu (Ahner et al. 2002). Moreover, the coccolithophore *Emiliana huxleyi* can release glutathione and other thiol-containing compounds in response to Cu additions (Leal et al. 1999, Dupont and Ahner 2005). These thiols may be the pools of Cu binding ligands which exist in the surface ocean (Le Gall & van den Berg 1998, Leal et al. 1999, Tang et al. 2000, and Ross et al. 2003), and thus, when Cu is low, the Cu within these complexes might be accessible to phytoplankton in need of Cu.

## **1.7 Molecular components and regulation of Cu acquisition and homeostasis**

At the molecular level, very little information is available on Cu acquisition and homeostasis in marine phytoplankton (Davis et al. 2006). In contrast, a wealth of information exists for organisms such as yeasts, humans and plants. In the high-affinity uptake system of the yeast *S. cerevisiae* (Figure 1.2a), Cu is reduced from  $\text{Cu}^{2+}$  to  $\text{Cu}^+$  by the plasma membrane reductase FRE1 (Hassett and Kosman, 1995), which also functions in Fe transport (Georgatsou et al, 1997). After the Cu is reduced,  $\text{Cu}^+$  is taken up by Cu transport proteins (Ctr1p and Ctr3p) which are encoded by the CTR1 and CTR3 genes (Dancis et al. 1994b, Labbe et al. 1997 and Pena et al. 2000). The expression of these genes is regulated by intracellular Cu concentration. When Cu is replete, the expression of CTR1, CTR3, and FRE1 is inhibited (Dancis, et al. 1994a, Hassett and Kosman 1995 and Labbe et al. 1997), and Cu uptake occurs via the low-affinity system, through the transporters encoded by CTR2, FET4, and SMF1 (Kampfenkel et al. 1995, Hassett et al. 2000 and Liu et al. 1997).

Inside the yeast cell, Cu is delivered to specific destinations by Cu chaperones (Figure 1.2a), including a) Atx1p and Ccc2p which deliver Cu to Fet3p, the multicopper oxidase required for the high-affinity Fe transport system (Lin et al. 1997, Pufahl et al. 1997); b) Cox17p which is required for Cu delivery to mitochondrial cytochrome c oxidase (Glerum et al. 1996) and c) Ccs1p which targets Cu to Cu/Zn superoxide dismutase, a primary antioxidant enzyme in the cytosol (Culotta et al. 1997). Mac1p, a Cu-responsive transcriptional activator in *S. cerevisiae*, down-regulates the high-affinity Cu uptake transporters when Cu levels are elevated (Pena et al. 1998) and activates the expression of the Cu transport genes CTR1, CTR3 and FRE1 when intracellular Cu levels decrease (Georgatsou et al. 1997).

The homologs of these components were found in *Arabidopsis* and *Chlamydomonas* (Table 1.1). In addition, Cu is transported into the chloroplast by a Cu-transport P-type ATPase in plants and some algae (Figure 1.2b). PAA1 and PAA2 are P-type ATPase Cu transporters in *Arabidopsis*. PAA1 localizes to the chloroplast periphery and PAA2 localizes to the thylakoid membranes (Abdel-Ghany et al. 2005). However, so far, homologs of all these components have not been studied in marine phytoplankton. For Cu-induced response at the transcript level there is only one genomic study on the marine diatom *T. pseudonana* grown under Cu replete and toxic conditions (Davis et al., 2006). In response to elevated Cu concentrations, 11 novel Cu-induced genes were identified, but the function of these genes is not clear; the suggestive roles of many predicted amino acid sequences are in ameliorating Cu toxicity (Davis et al., 2006). The mechanisms for Cu acquisition, distribution, storage and regulation in marine phytoplankton are just beginning to be investigated.

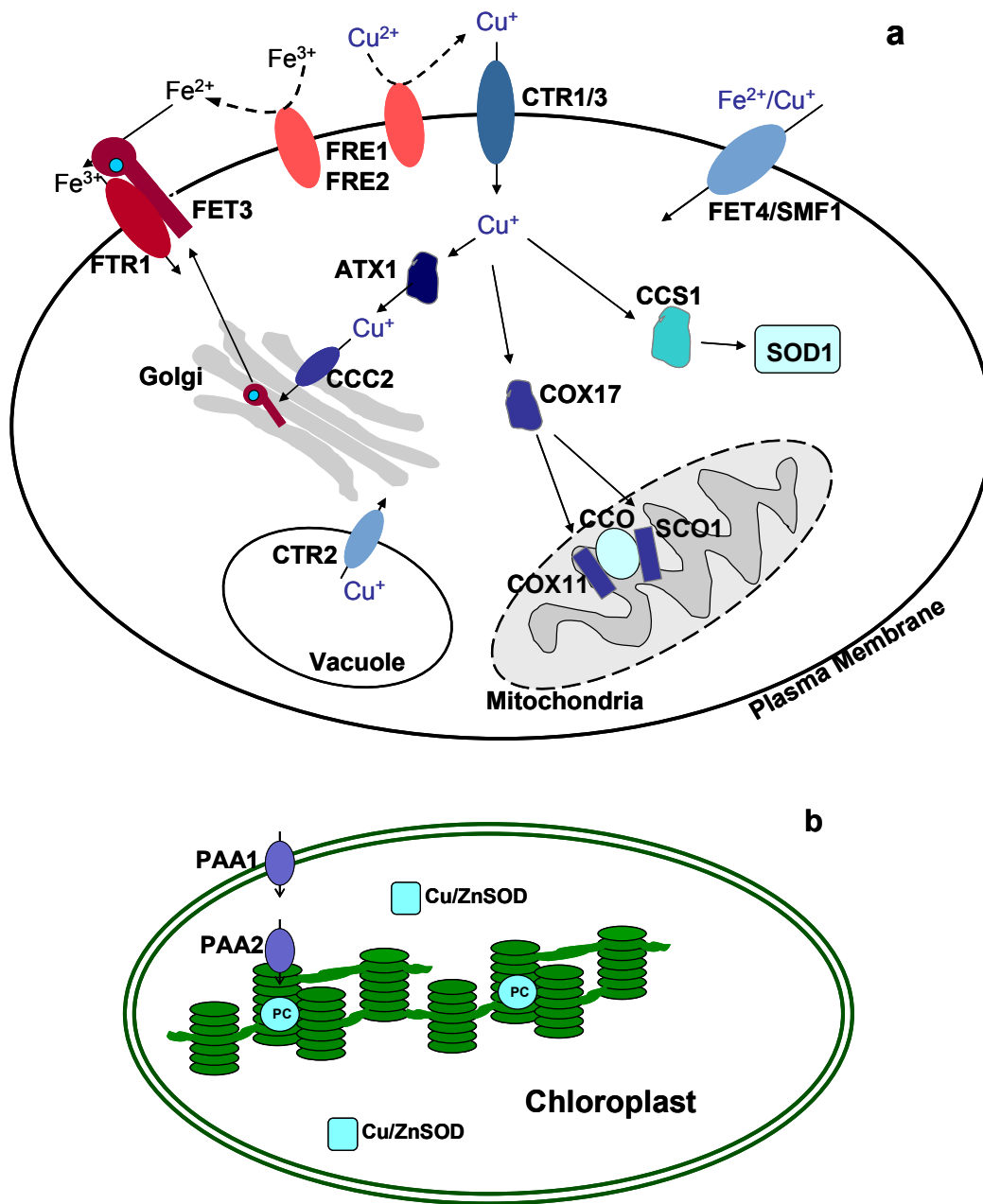


Figure 1.2 A model for Cu uptake and distribution in *S. cerevisiae* (a) and in chloroplasts of *Arabidopsis* (b) (Redrawn from Puig and Thiele 2002, Rutherford and Bird 2004, Puig et al. 2007).

Table 1.1 Summary of Cu transporters, Cu chaperones and their targets in three model eukaryotic organisms.

	<i>Saccharomyces</i>	<i>Arabidopsis</i>	<i>Chlamydomonas</i>
Transporter on plasma membrane	<i>ScCTR1</i> and 3	<i>AtCOPT1</i>	<i>CrCTR1</i> and 2
Chaperone for mitochondrion	<i>ScCOX17</i>	<i>AtCOX17</i>	<i>CrCOX17</i>
Target in mitochondrion	Cyt-c Oxidase	Cyt-c Oxidase	Cyt-c Oxidase
Chaperone for golgi	<i>ScATX1</i>	<i>AtCCH</i>	<i>CrATX1</i>
Transporter on golgi	<i>ScCCC2</i>	<i>AtRAN1</i>	<i>CrCTP1</i>
Target in golgi	<i>ScFET3</i>	<i>AtETR1</i>	<i>CrFox1</i>
Chaperone for cytosol Cu/Zn-SOD	<i>ScLYS7 (ScCCS)</i>	<i>AtCCS1</i>	?
Transport into chloroplast	N/A	<i>AtPAA1/2</i>	<i>CrCTP2</i> and 3
Target in chloroplast	N/A	Plastocyanin Cu/Zn-SOD	Plastocyanin

## 1.8 Thesis objectives

Until recently, the vast majority of studies investigating the effects of Cu on phytoplankton have focused on its toxicity. Less attention has been paid to Cu as an essential micronutrient for phytoplankton. In the last 5 years, the importance of Cu for phytoplankton metabolism has become apparent, especially for phytoplankton in the open ocean and those experiencing Fe limitation. The overall goal of my dissertation is to further our understanding of the mechanisms of Cu acquisition and homeostasis in marine eukaryotic phytoplankton. Given the interaction between Fe and Cu nutrition, I have studied how both Fe and/or Cu availability (at optimal and limiting levels) control these mechanisms.

More specifically, in this thesis I investigated the role of Fe and/or Cu availability in controlling a) growth rates and Cu stoichiometry of diverse marine phytoplankton (Chapter 2), and b) Cu uptake kinetics of marine diatoms (Chapter 3). In addition, using the genome of the recently sequenced marine diatom, *Thalassiosira pseudonana*, I identified and characterized the genes encoding the potential components of Cu transport and homeostasis in diatoms (Chapter 4 and 5).

In Chapter 2, I investigated the growth rates, Cu:C ratios and steady-state Cu uptake rates of 10 phytoplankton species from three phyla and two oceanic provenances (coastal and oceanic) under optimal and limiting Fe and/or Cu concentrations. The study hypotheses were that a) the Cu requirements of Fe-limited phytoplankton are higher than those of Fe-sufficient ones; b) oceanic phytoplankton have higher Cu requirements than coastal strains; and c) the Cu requirements of phytoplankton from different phyla differ greatly and reflect whether they belong to the green or red lineage.

In Chapter 3, using the radiotracer  $^{67}\text{Cu}$ , I measured Cu uptake rates under different Cu concentrations for the marine diatoms *T. oceanica*, an oceanic isolate, and *T. pseudonana*,

a coastal strain. The diatoms were grown under optimal or low Fe and/or Cu conditions. These data were used to determine Cu uptake kinetics (the  $K_m$  and  $V_{max}$  values) to elucidate Cu transport systems in these organisms. My hypotheses were a) there is a high- and a low-affinity Cu uptake system in marine phytoplankton when Cu is low and high, respectively; b) distinct Cu uptake systems operate in oceanic and coastal diatom; c) the Cu within organic Cu-complexes is available for uptake by marine diatoms; and d) low Fe availability enhances Cu transport rate.

My final objective was to investigate the components of Cu acquisition and homeostasis mechanisms in a marine diatom, as well as their regulation and function under various Fe and/or Cu concentrations. In Chapter 4, 11 genes encoding Cu and Zn transporters, as well as Cu chaperones were identified, including two putative high-affinity Cu transport CTR genes (*TpCTR|24275* and *TpCTR|9391*). The expression at the transcription level of these 11 genes, and five genes encoding the components of the high-affinity Fe transport system, were studied in response to changes of Fe and/or Cu concentrations.

In Chapter 5, I tested the functional complementation of *Saccharomyces cerevisiae ctr1Δctr3Δ* double-mutant strain (MPY17) by expression of *T. pseudonana* CTRs in order to test the true function of these putative high-affinity Cu transport CTR diatom genes. I assessed the ability of *TpCTR|24275* and *TpCTR|9391* to complement the inability of *S. cerevisiae* mutant MPY17 cells to grow on non-fermentable carbon sources due to their high-affinity Cu transport deficiency.

## **Chapter 2**

### **The effects of iron and copper availability on the copper stoichiometry of marine phytoplankton**

## 2.1 Introduction

Copper (Cu) is a required redox element in enzymes involved in various metabolic pathways, such as respiration (e.g. cytochrome oxidase) in phytoplankton (see reviews by Raven et al. 1999, and Merchant et al. 2006). Copper is also needed for the oxidation of organic nitrogen (Palenik et al. 1988-1989) and the detoxification of superoxide radicals using a Cu/Zn superoxide dismutase in some phytoplankton (Chadd et al. 1996). Most recently, Cu has been established as an important micro-nutrient for iron-limited green algae and marine diatoms (La Fontaine et al. 2002, Peers et al. 2005, Maldonado et al. 2006). This finding is important because 30% of the global ocean is iron (Fe) limited. In Fe limited waters phytoplankton still divide at  $\sim 0.3 \text{ d}^{-1}$  (Welschmeyer et al. 1991), and thus must have evolved either a unique mechanism of Fe uptake and/or a lower Fe demand for growth (Sunda and Huntsman 1995a, Maldonado and Price 1996). The involvement of Cu in the photosynthetic apparatus was recently discovered in the oceanic diatom *Thalassiosira oceanica* Hasle. In this organism, the Cu-containing enzyme plastocyanin replaces the Fe-containing enzyme cytochrome  $c_6$  in photosynthesis (Peers and Price 2006). The replacement of Fe-containing enzymes with Cu-containing enzymes may explain the success of oceanic phytoplankton in open ocean waters where Fe concentrations are too low to support growth of coastal phytoplankton.

The involvement of Cu in the high-affinity Fe transport system of some marine diatoms may also increase their demand for Cu (Maldonado et al. 2006). Some marine diatoms up-regulate a high-affinity Fe uptake system in order to acquire enough Fe for growth under Fe limiting conditions (Maldonado and Price 1999, 2001). The Fe transport system in diatoms is similar to that of the yeast *Saccharomyces cerevisiae* (Askwith et al. 1994) and the green algae *Chlamydomonas reinhardtii* P.A.D angeard (La Fontaine et al. 2002). During uptake, phytoplankton release the Fe from organic complexes by enzymatically reducing  $\text{Fe}^{3+}$  to  $\text{Fe}^{2+}$  (Maldonado and Price 2001, Shaked et al. 2005). Before the reduced  $\text{Fe}^{2+}$  is transported into the cell, a multi-Cu containing oxidase oxidizes  $\text{Fe}^{2+}$  back to  $\text{Fe}^{3+}$  before being internalized. Thus, Fe limitation may increase the need for Cu in

phytoplankton (Maldonado et al. 2006). The interaction between Fe and Cu nutrition has only been studied in marine diatoms (Peers et al. 2005, Wells et al. 2005, Maldonado et al. 2006, Annett et al. 2008, Semeniuk et al. 2009). Measurements of intracellular Cu levels and steady-state Cu uptake rates ( $\rho_{ss}\text{Cu}$ ) indicated that oceanic diatoms have higher Cu quotas than coastal species, and that in some cases, Fe limitation imparted a higher cellular Cu demand (Annett et al. 2008). Beyond the work cited above, the Cu requirements and  $\rho_{ss}\text{Cu}$  of diverse phytoplankton grown under different Fe and/or Cu level are still unknown.

In the present study, we investigated the growth rates, cellular Cu:C ratios (using  $^{67}\text{Cu}$  and  $^{14}\text{C}$ ) and  $\rho_{ss}\text{Cu}$  of 10 species of marine phytoplankton grown under different Fe and/or Cu level. Since previous studies have indicated that trace metal stoichiometry differs significantly among taxa (Ho et al. 2003, Quigg et al. 2003, Saito et al. 2003), we chose phytoplankton species that are abundant in the sea and represent three different phyla. Given that oceanic and coastal diatoms have different Fe and Cu requirements (Peers et al. 2005, Maldonado et al. 2006, Annett et al. 2008), we also chose pairs of phytoplankton from coastal and oceanic environments. Using linear mixed-effect model statistical analyses, this study allows us to establish the effect of phylum, regime (coastal vs. oceanic), and/or environmental conditions (Fe and Cu) on the growth rates, Cu quotas and  $\rho_{ss}\text{Cu}$  of these marine phytoplankton. We combined our new results with recently published measurements (Annett et al. 2008) so that a total of four phyla and 12 species, from coastal and oceanic environment, were compared statistically.

## 2.2 Materials and methods

### 2.2.1 Studied organisms and culture manipulations

Ten phytoplankton species from three phyla (Table 2.1) were cultured in this study. Cultures were obtained from Bigelow Laboratory for Ocean Sciences (CCMP), West Boothbay Harbor, ME, USA, and the Canadian Center for the Culture of Microorganisms (CCCM), Vancouver, BC, Canada. These cultures were assigned a coastal or oceanic provenance according to their geographic location of isolation (Table 2.1). Despite the fact that our ‘Sargasso Sea’ *Synechococcus* isolate (WH7803; also called NEPCC549, DC2, CCMP1334) has a low phycourobilin to phycoerythrobilin chromophore ratio (PUB/PEB ~0.4, Toledo et al. 1999), which is typical of coastal strains, similar strains have been shown to dominate in open ocean blooms (Campbell and Carpenter 1987, Morel 1997, Coble et al. 2004). In addition, our growth rate data suggest that this strain behaves more like an oceanic than a coastal *Synechococcus*, at least in terms of the effects of Cu and/or Fe limitation (see results below). Thus, *Synechococcus* sp. WH7803 was assigned an oceanic provenance.

Phytoplankton were cultured in 28 mL polycarbonate tubes in the well-defined artificial seawater medium-AQUIL (Price et al. 1989) with different Fe and Cu concentrations (Table 2). The AQUIL medium was prepared and was identical in chemical composition to that described by Maldonado et al. (2006). Cultures were kept in exponential growth phase using semi-continuous batch cultures and a 24 hour light regime. The eukaryotic phytoplankton were grown under  $19\pm 1^\circ\text{C}$  and a saturating light intensity of  $150 \mu\text{mol quanta} \cdot \text{m}^{-2} \cdot \text{s}^{-1}$ , while the *Synechococcus* strains were grown under  $24^\circ\text{C}$  and  $50 \mu\text{mol quanta} \cdot \text{m}^{-2} \cdot \text{s}^{-1}$ . Due to their distinct pigments, the cultures of the oceanic *Synechococcus* strain (WH7803) were pink, while those of the coastal strain were green. Sterile, trace metal-clean techniques were used throughout all the experiments.

Table 2.1 Species name, taxa, clone, isolation site, oceanic provenance and cell diameter ( $\mu\text{m}$ ) of the marine phytoplankton used in this study. Data for *T. oceanica* and *T. pseudonana* are from Annett et al. 2008.

Species	Class	Clone	Isolation location	Provenance	Diameter ( $\mu\text{m}$ )
<i>Synechococcus</i> sp.	Cyanophyceae	WH7803	Sargasso Sea	oceanic	1-3
<i>Synechococcus lividus</i> Copeland	Cyanophyceae	NEPCC 550	Brazil	coastal	1-3
<i>Phaeocystis pouchetii</i> (Hariot) Lagerheim	Prymnesiophyceae	NEPCC 225	49°52'N 142°40'W	oceanic	2.5-6
<i>Phaeocystis cordata</i> A. Zingone & M. J. Chrétiennot-Dinet	Prymnesiophyceae	CCMP 2495	Gulf of Naples, Mediterranean Sea	coastal	3-5
<i>Emiliana huxleyi</i> (Lohmann) W. W. Hay & H. P. Mohler	Prymnesiophyceae	NEPCC 732a	Station Papa, Subarctic Pacific	oceanic	6-12
<i>Emiliana huxleyi</i> (Lohmann) W. W. Hay & H. P. Mohler	Prymnesiophyceae	NEPCC646	Oslo Fjord, Norway	coastal	3-6
<i>Chrysochromulina polylepis</i> Manton & Parke	Prymnesiophyceae	NEPCC 242	49°36'N 140°37'W	oceanic	2.5-6
<i>Chrysochromulina Kappa</i> Parke & Manton	Prymnesiophyceae	CCMP 288	Gulf of Maine, North Atlantic	coastal	3-6
<i>Prorocentrum dentatum</i> Stein	Dinophyceae	CCMP1517	South Pacific	oceanic	8-17
<i>Prorocentrum minimum</i> (Pavillard) J. Schiller	Dinophyceae	NEPCC 541	Great South Bay, NY	coastal	6-16
<i>Thalassiosira oceanica</i> Hasle <sup>a</sup>	Bacillariophyceae	CCMP1003	Sargasso Sea	oceanic	5-8
<i>Thalassiosira pseudonana</i> Hasle & Heimdal <sup>a</sup>	Bacillariophyceae	3H, NEPCC 58	Moriches Bay, NY	coastal	3-6

### 2.2.2 Growth parameter measurements

Cells were acclimated to 4 or 6 different Fe and/or Cu culture conditions, depending on the species (Table 2.2). To monitor the growth of the cultures, *in vivo* fluorescence was measured daily with a Turner 10-AU Fluorometer (Turner Designs, Sunnyvale, CA, USA). Natural logarithm of fluorescence versus time was used to calculate specific growth rate ( $d^{-1}$ ). Cultures were considered acclimated to specific Fe and Cu levels when the growth rates in five successive transfers varied by less than 15% (Brand et al. 1981). The culture cell density and diameter ( $\mu m$ ) of the eukaryotic phytoplankton for each treatment were determined on live samples using a Coulter Z2 Particle Count and Size Analyzer (Beckman Coulter Inc., Brea, CA, USA). The cell surface area and volume were calculated assuming a spherical cell shape.

Table 2.2 Iron and copper additions to culture media. The Fe and Cu contamination in our media was  $\sim 1$  nM (Maldonado et al. 2006). The metals were added bound to 100  $\mu M$  EDTA. MINEQL + 4.61 (Environmental Research Software) was used to calculate free metal concentrations ( $pMe = -\log [Me^{n+}]$ )

Treatment	[Fe <sub>total</sub> ] (pFe)	[Cu <sub>total</sub> ] (pCu)
Replete	1.37 $\mu M$ (19)	10.2 nM (14)
Low	12.5 nM (21)	1.96 nM (15)
Low	2.28 nM (22)	
No addition	1.0 nM <sup>a</sup> (22.3)	

<sup>a</sup> from Fe contamination

### 2.2.3 Cu:C ratio determinations

Two radioactive tracers ( $^{67}\text{Cu}$  and  $^{14}\text{C}$ ) were used to determine the cellular Cu and C concentration in phytoplankton during mid-exponential phase of growth. The carrier-free, gamma-emitting radionuclide  $^{67}\text{Cu}$ , with a half-life of 62 hours, was produced at the MDS Nordion site on the Tri-University Meson Facility campus (TRIUMF) in Vancouver.  $^{67}\text{Cu}$  additions to the medium were precomplexed with EDTA (10 nM) for  $\geq 30$  min to avoid metal precipitation or major variation in free ion concentrations in the growth media. The precomplexed radioactive  $^{67}\text{CuEDTA}$  addition ( $0.08\text{--}0.16 \text{ MBq} \cdot \text{L}^{-1} \text{ } ^{67}\text{Cu}$ ) and  $^{14}\text{C}$  ( $0.74 \text{ MBq} \cdot \text{L}^{-1} \text{ H}^{14}\text{CO}_3$ ) were added to the media when cultures were in mid-exponential phase. After the radioactive tracers were added, duplicate initial samples (1 mL) of the culture medium were taken to determine the specific activity of these two radioactive isotopes (e.g.  $\text{MBq } ^{67}\text{Cu} / [\text{Cu}]_{\text{total}}$ ). Phytoplankton were cultured for 24–48 hours in the radioactive media. The cells were then filtered onto polycarbonate Poretics filters of either 0.8, 2.0, or 3.0  $\mu\text{m}$  porosity, depending on their cell size. The filtered cells were first soaked for 5 minutes with 5 mL of 1 mM diethylenetriaminepentaacetic acid (DTPA) solution (dissolved in sterile synthetic ocean water, pH adjusted to 8.14; Croot et al. 1999) to bind the extracellular adsorbed  $^{67}\text{Cu}$  and then rinsed with 5 mL synthetic ocean water (SOW). The filters with radioactive cells were then placed in scintillation vials and  $^{67}\text{Cu}$  activity was first measured in a PerkinElmer 1480 WIZARD 3'' Gamma Counter (PerkinElmer Inc., Waltham, MA, USA), followed by an immediate addition of scintillation cocktail. After the  $^{67}\text{Cu}$  had decayed ( $\sim 3$  weeks),  $^{14}\text{C}$  activities were measured in a scintillation counter (Beckman–Coulter LS 6500, Beckman Counter, Inc. Brea, CA, USA). Culture samples (1 mL) fixed with Lugol's solution were also taken to determine the cell density at the time of harvest.

The cellular Cu ( $\mu\text{M}$ ) and C (M) concentrations were determined using appropriate specific activities and the radioactivity on the filters where the cells were collected. In the calculation, growth rate and incubation time were incorporated according to the method of Morel (1987), given that the cultures did not undergo eight cell divisions in radioactive

media and thus were not uniformly labeled. For these experiments, at least triplicate cultures were used for each treatment. These data allowed us to calculate Cu:C ratios, Cu steady-state uptake rates ( $\rho_{ss}\text{-Cu}$ ,  $\text{mol Cu} \cdot \mu\text{m}^{-2} \cdot \text{d}^{-1}$ ) and Cu use efficiencies ( $\text{mol C} \cdot \mu\text{mol Cu}^{-1} \cdot \text{d}^{-1}$ ). The  $\rho_{ss}\text{-Cu}$  were calculated from cellular Cu ( $\text{mol Cu} \cdot \text{cell}^{-1}$ ), cell surface area ( $\mu\text{m}^{-2}$ ) and specific growth rate ( $\text{d}^{-1}$ ), according to Morel (1987). The Cu use efficiencies of low Cu cultures were calculated from Cu:C and specific growth rate.

#### **2.2.4 Statistical analyses**

Software SigmaStat 3.5 and SYSTAT, version 12 (Systat Software, Inc. San Jose, CA, USA), were used for all statistical analyses. Two-way ANOVA was used to analyze the differences between treatment means within each species. Linear mixed-effect model (Glantz and Slinker 2001) was used to examine group-wide trends. The data from this study and data from two diatoms (*Thalassiosira oceanica* and *T. pseudonana* 3H) from our research group (Annett et al. 2008) were included in this group-wide analysis. Thus, 12 species from four phyla were statistically compared. In this mixed-effect model, growth rates, Cu:C ratios and steady-state Cu uptake rates were analyzed as continuous dependent variables. Copper level (pCu14 vs. pCu15), Fe level (pFe19 vs. pFe21), species regime (coastal vs. oceanic), and species phylum (4 phyla) were analyzed as fixed effects (Table 2.5). The random effect in this mixed-effect model was species, since all species studied here were chosen randomly among many isolates.

## **2.3 Results**

### **2.3.1 Effect of Fe and Cu on growth rate and cell size**

The growth rates ( $\text{d}^{-1}$ ) and the cell diameters ( $\mu\text{m}$ ) of 10 phytoplankton species grown under different Fe and Cu treatments (Table 2.3, Figure 2.1) were determined. In general,

the availability of Fe had a greater effect on their growth rates and cell size than the availability of Cu. Two-way ANOVA statistical analysis indicated that Fe level had a significant effect ( $p < 0.001$ , Table 2.3, 2.4) on the growth rates of all tested phytoplankton, except for the coastal strain of *Emiliana huxleyi*. The reduction in growth rates under low Fe ranged from 13% to 61% (Table 2.3). Low Fe availability (pFe21) reduced the growth rate of the coastal strain of *Synechococcus* to a greater extent than that of the Sargasso Sea strain (57-59% vs. 30-44%, respectively). A similar trend was also observed for the two strains of *Phaeocystis* (21-42% for coastal strain vs. 16-18% for oceanic strain). Only when the Fe concentration was decreased to pFe22, was the growth rate of the oceanic *Phaeocystis* reduced significantly (23-46%). Surprisingly, the opposite Fe effect was observed on the strains of *Prorocentrum*, *Emiliana* and *Chrysochromulina*, in which more growth rate reduction was observed in the oceanic strains (59-61%, 28-30% and 23-31%, respectively) than in the coastal strains (13-29%, 0-6% and 0-25%, respectively). Moreover, the coastal strain of *E. huxleyi* was able to maintain maximum growth rates even in the absence of a Fe addition to the medium. When all species, including the diatoms from Annett et al. (2008), were analyzed as a group by the mixed-effect model, Fe availability and regime had a significant interaction on the growth rates (Fe  $\times$  Regime effect,  $p = 0.001$ , Table 2.5). Thus, coastal and oceanic phytoplankton groups exhibited significantly different growth response to Fe availability.

The mixed-effect model indicated that the growth response of the 4 phytoplankton phyla was significantly different for Fe availability (Fe  $\times$  Phylum effect,  $p < 0.001$  vs. Cu  $\times$  Phylum effect,  $p = 0.864$ , Table 2.4). Regardless of Cu concentration, Prymnesiophyceae exhibited a lower average growth rate reduction (16%) in response to low Fe (pFe21) than did Cyanophyceae (48%), Dinophyceae (41%) or Bacillariophyceae (22%).

The availability of Cu in the medium had less of an effect on phytoplankton growth rates than that of Fe. Two-way ANOVA statistical analysis indicated that low Cu availability reduced the growth rates of five species out of the ten studied: the Sargasso Sea *Synechococcus* sp. (WH7803), the coastal and oceanic *Phaeocystis* species, as well as the

coastal *Emiliana* and *Prorocentrum* (Table 2.4), reducing their growth rate between 17% to 44% when Cu level decreased from pCu14 to pCu15 at all Fe levels (Table 2.3). When the diatoms data (Annett et al. 2008) are included, the mixed-effect model showed that the Cu effect on growth rates was significant only for the oceanic group (Cu effect,  $p = 0.002$ , Table 2.5). In contrast to Fe, no clear phylogenetic trends were found for the growth response to various Cu levels in the medium.

There was also a statistically significant interaction between Fe and Cu on the growth of two *Phaeocystis* species (Table 2.4), where the Cu effect depended on the medium Fe level. Low Cu reduced the growth rate of the oceanic strain *P. pouchetii* (32% reduction) when Fe was limited, but reduced the growth rate of the coastal strain *P. cordata* (44%) when Fe was sufficient (Table 2.3).

As for the effects of Fe and Cu on the cell size, Fe level had significant effect on most species except for *Phaeocystis pouchetii*, *P. cordata* and *Chrysochromulina kappa*, while Cu level had no obvious effect on cell size (Table 2.3).

Table 2.3 Growth rates ( $d^{-1}$ ) and cell diameter ( $\mu m$ ) of marine phytoplankton grown under different Fe and Cu levels. Data are presented as mean  $\pm$  SD. The percent reductions in growth rates are those calculated from Fe-sufficient to low Fe media with the same Cu level, and from Cu-sufficient to low Cu media with same Fe level. \*\* ( $P < 0.001$ ) and \* ( $P < 0.05$ ) denotes the statistically slower growth rates in Fe and/or Cu limited cultures by the 2-way ANOVA (Pairwise Multiple Comparison Procedures, Holm-Sidak method).

Species (Oceanic)	pFe_pCu	Growth Rate ( $d^{-1}$ ) (n)	% Reduction from Fe sufficient	% Reduction from Cu sufficient	Cell diameter ( $\mu m$ ) (n)	Species (Coastal)	pFe_pCu	Growth Rate ( $d^{-1}$ ) (n)	% Reduction from Fe sufficient	% Reduction from Cu sufficient	Cell diameter ( $\mu m$ ) (n)	
<i>Synechococcus sp. WH7803</i>	19_14	1.05 $\pm$ 0.15 (19)				<i>Synechococcus lividus</i>	19_14	1.55 $\pm$ 0.19 (19)				
	19_15	1.02 $\pm$ 0.15 (16)		3			19_15	1.64 $\pm$ 0.18 (20)			-6	
	21_14	0.73 $\pm$ 0.09 (9)	30**				21_14	0.66 $\pm$ 0.15 (18)	57**			
	21_15	0.57 $\pm$ 0.13 (8)	44**	22*			21_15	0.68 $\pm$ 0.14 (14)	59**		-2	
<i>Phaeocystis pouchetii</i>	19_14	0.94 $\pm$ 0.07 (17)			4.3 $\pm$ 0.03 (3)	<i>Phaeocystis cordata</i>	19_14	0.43 $\pm$ 0.08 (11)			3.5 $\pm$ 0.02 (3)	
	19_15	0.90 $\pm$ 0.08 (18)		4	4.1 $\pm$ 0.04 (3)		19_15	0.24 $\pm$ 0.05 (8)			44**	3.5 $\pm$ 0.03 (4)
	21_14	0.77 $\pm$ 0.08 (18)	18**		3.8 $\pm$ 0.13 (4)		21_14	0.25 $\pm$ 0.04 (8)	42**			3.4 $\pm$ 0.02 (4)
	21_15	0.76 $\pm$ 0.08 (17)	16**	1	3.8 $\pm$ 0.15 (4)		21_15	0.19 $\pm$ 0.01 (7)	21	25		3.3 $\pm$ 0.08 (4)
	22_14	0.72 $\pm$ 0.10 (18)	23**		4.1 $\pm$ 0.07 (4)							
	22_15	0.49 $\pm$ 0.06 (11)	46**	32**	4.0 $\pm$ 0.09 (4)							
<i>Emiliana huxleyi</i>	19_14	0.39 $\pm$ 0.06 (11)			10.1 $\pm$ 0.04 (4)	<i>Emiliana huxleyi</i>	19_14	0.64 $\pm$ 0.07 (13)			4.5 $\pm$ 0.03 (3)	
	19_15	0.37 $\pm$ 0.05 (10)		5	10.4 $\pm$ 0.04 (4)		19_15	0.53 $\pm$ 0.05 (9)			17 *	4.5 $\pm$ 0.05 (3)
	21_14	0.28 $\pm$ 0.08 (8)	28**		8.5 $\pm$ 0.09 (4)		21_14	0.68 $\pm$ 0.10 (11)	-6			4.4 $\pm$ 0.01 (3)
	21_15	0.26 $\pm$ 0.05 (8)	30**	7	9.1 $\pm$ 0.06 (4)		21_15	0.50 $\pm$ 0.13 (8)	6	25**		4.1 $\pm$ 0.06 (3)
							22.3_14	0.65 $\pm$ 0.07 (11)	-2			3.8 $\pm$ 0.01 (4)
							22.3_15	0.54 $\pm$ 0.07 (12)	-2		17 *	3.6 $\pm$ 0.08 (3)

Species (Oceanic)	pFe_pCu	Growth Rate (d <sup>-1</sup> ) (n)	% Reduction from Fe sufficient	% Reduction from Cu sufficient	Cell diameter (μm) (n)	Species (Coastal)	pFe_pCu	Growth Rate (d <sup>-1</sup> ) (n)	% Reduction from Fe sufficient	% Reduction from Cu sufficient	Cell diameter (μm) (n)
<i>Chrysochromulina polylepis</i>	19_14	0.92±0.07 (19)			4.4±0.02 (3)	<i>Chrysochromulina kappa</i>	19_14	0.82±0.08 (12)			4.4±0.03 (3)
	19_15	0.94±0.06 (19)		-2	4.3±0.02 (3)		19_15	0.81±0.07 (12)		2	4.4±0.00 (3)
	21_14	0.74±0.08 (19)	19**		3.7±0.21 (4)		21_14	0.82±0.04 (11)	0		4.4±0.03 (3)
	21_15	0.75±0.13 (16)	20**	-2	3.7±0.03 (4)		21_15	0.81±0.07 (12)	0	1	4.4±0.03 (3)
	22_14	0.71±0.13 (15)	23**		3.7±0.14 (4)		22.3_14	0.71±0.09 (12)	13**		4.1±0.03 (4)
	22_15	0.65±0.13 (10)	31**	8	3.4±0.04 (4)		22.3_15	0.61±0.14 (11)	25**	13*	3.8±0.02 (4)
<i>Prorocentrum dentatum</i>	19_14	0.34±0.08 (7)			10.5±0.26 (3)	<i>Prorocentrum minimum</i>	19_14	0.31±0.04 (10)			10.3±0.05 (4)
	19_15	0.28±0.14 (7)		18	11.1±0.10 (4)		19_15	0.31±0.04 (12)		0	10.4±0.11 (4)
	21_14	0.14±0.03 (7)	59**		8.51±0.09 (4)		21_14	0.27±0.03 (11)	13*		
	21_15	0.11±0.02 (7)	61**	25	9.16±0.06 (4)		21_15	0.22±0.06 (10)	29**	18*	
<i>Thalassiosira oceanica</i> <sup>a</sup>	19_14	1.16±0.25 (43)				<i>Thalassiosira pseudonana</i> <sup>a</sup>	19_14	2.03±0.42 (87)			
	19_15	1.13±0.22 (32)		2.9			19_15	1.97±0.45 (96)		3.6	
	20.5_14	1.18±0.26 (38)	-1.8				20.5_14	1.26±0.38 (92)	38**		
	20.5_15	0.96±0.22 (49)	14*	18**			20.5_15	1.26±0.34 (91)	38**	-0.22	
	21.5_14	0.72±0.08 (16)	38**								
	21.5_15	0.68±0.12 (13)	40**	5.5							

<sup>a</sup>data from Annett et al. 2008

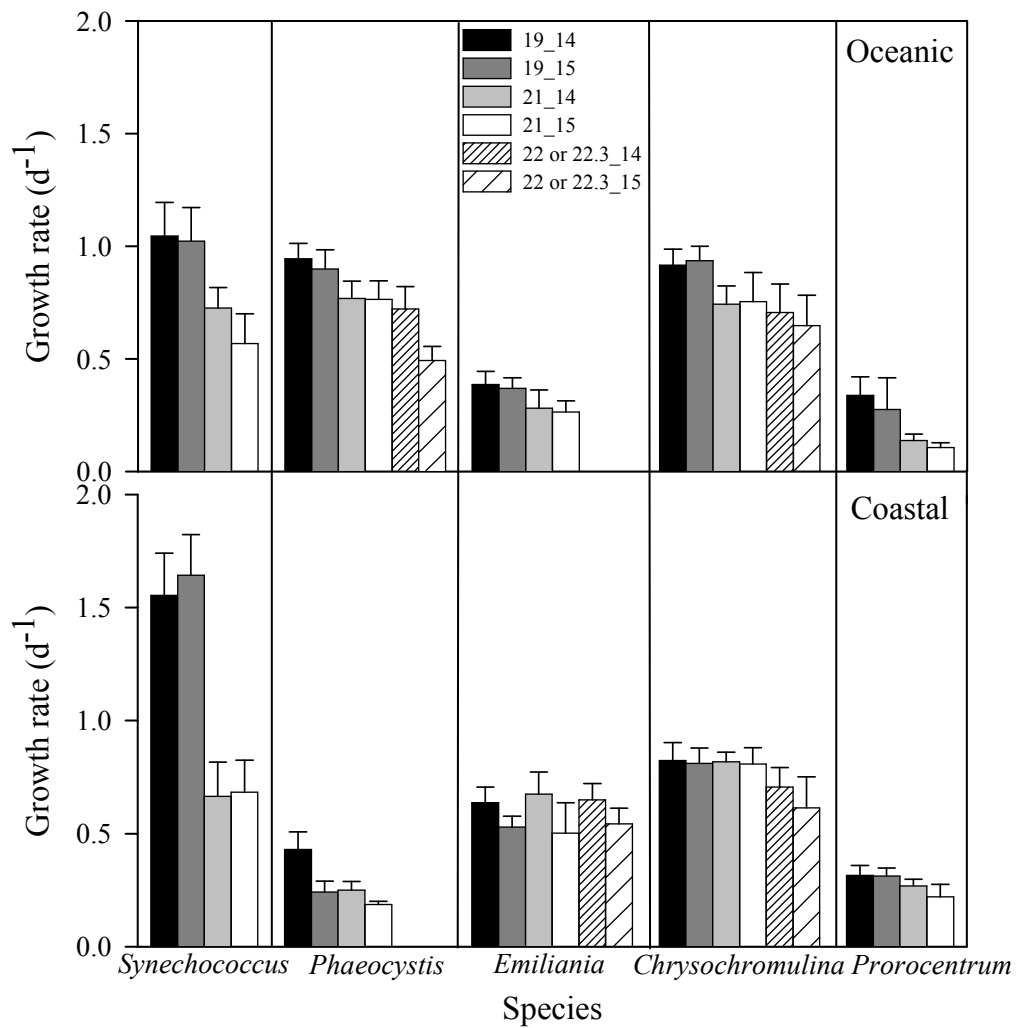


Figure 2.1 Growth rates ( $d^{-1}$ ) of oceanic and coastal phytoplankton grown under different Fe and/or Cu levels (pFe\_pCu). Species of upper level and lower level are oceanic and coastal phytoplankton, respectively. Error bars denote standard deviation. All data and statistical analyses of these data are presented in Table 2.3.

Table 2.4 Statistical analyses (two-way ANOVA) of Fe effect, Cu effect, and Fe × Cu interaction on growth rates, Cu:C and steady-state Cu uptake rates ( $\rho_{ss}Cu$ ). All the Fe and Cu treatments for each species were included in the analysis. Only significant effects are listed ( $p < 0.05$ ). Negative effects are indicated with (-) symbol, otherwise the single effects are positively correlated with the independent variable. Note that the diatom data are not included here, but are reported in Annett et al. 2008 (see Table 2.4).

Species	Growth rates	Cu:C	$\rho_{ss}Cu$
<i>Synechococcus</i> sp. WH7803 (oceanic)	Fe, Cu	Cu	N/A
<i>Synechococcus lividus</i> (coastal)	Fe	Fe(-), Cu	N/A
<i>Phaeocystis pouchetii</i> (oceanic)	Fe, Cu, Fe×Cu	Fe, Cu	Fe
<i>Phaeocystis cordata</i> (coastal)	Fe, Cu, Fe×Cu	Fe, Cu, Fe×Cu	Fe, Cu, Fe×Cu
<i>Emiliana huxleyi</i> (oceanic)	Fe	Cu	Cu
<i>Emiliana huxleyi</i> (coastal)	Cu	Cu	Fe, Cu, Fe×Cu
<i>Chrysochromulina polylepis</i> (oceanic)	Fe	Cu, Fe×Cu	Fe, Cu
<i>Chrysochromulina Kappa</i> (coastal)	Fe	Fe(-), Cu, Fe×Cu	Cu
<i>Prorocentrum dentatum</i> (oceanic)	Fe	Cu	Fe, Cu, Fe×Cu
<i>Prorocentrum minimum</i> (coastal)	Fe, Cu	Fe, Cu	Fe, Cu, Fe×Cu

Table 2.5 Results (p value) from the linear mixed-effect model statistical analyses on the growth rates, Cu quotas, and steady-state Cu uptake rates ( $\rho_{ss}Cu$ ). The mixed-effect model included data for the four treatments (pFe 19\_pCu 14; pFe19\_pCu15; pFe21\_pCu14; pFe21\_pCu15) that were common for all tested species, as well as the diatom data from Annett et al. 2008. Three mixed-effect model analyses were run: 1) included all the species, 2) included only the coastal species, and 3) included only the oceanic species. Statistically significant results ( $\alpha = 0.05$ ) are given in bold.

Effect	Significance level								
	Growth rate			Cu:C			Steady-state Cu uptake		
	All species	Coastal	Oceanic	All species	Coastal	Oceanic	All species	Coastal	Oceanic
Fe	<b>&lt;0.001</b>	<b>&lt;0.001</b>	<b>&lt;0.001</b>	0.316	0.985	<b>&lt;0.001</b>	0.318	<b>0.049</b>	<b>&lt;0.001</b>
Cu	0.170	0.549	<b>0.002</b>	<b>&lt;0.001</b>	<b>&lt;0.001</b>	<b>&lt;0.001</b>	<b>&lt;0.001</b>	0.192	<b>&lt;0.001</b>
Fe × Cu	0.447	0.895	0.118	0.106	0.835	<b>&lt;0.001</b>	0.274	0.657	<b>&lt;0.001</b>
Regime	0.945			0.391			0.499		
Fe × Regime	<b>0.001</b>			0.252			0.074		
Cu × Regime	0.380			<b>&lt;0.001</b>			<b>0.001</b>		
Fe × Cu × Regime	0.151			0.516			0.614		
Phylum	0.144	0.165	0.420	0.220	0.241	0.059	<b>0.001</b>	0.141	0.071
Fe × Phylum	<b>&lt;0.001</b>	<b>&lt;0.001</b>	<b>&lt;0.001</b>	0.329	0.503	<b>0.032</b>	0.914	0.200	<b>&lt;0.001</b>
Cu × Phylum	0.864	0.548	<b>0.010</b>	<b>0.026</b>	<b>0.022</b>	<b>&lt;0.001</b>	<b>&lt;0.001</b>	0.579	<b>&lt;0.001</b>
Fe × Cu × Phylum	0.831	0.854	<b>0.038</b>	0.116	0.644	<b>&lt;0.001</b>	<b>0.031</b>	0.297	<b>&lt;0.001</b>

### 2.3.2 Effect of Fe and Cu availability on Cu quotas

Cellular Cu:C ratios of experimental species varied from 0.04 to 3.8  $\mu\text{mol Cu} \cdot \text{mol}^{-1} \text{C}$  among all treatments (Table 2.6, Figure 2.2). Comparisons of the Cu quotas of experimental species grown with sufficient Fe and Cu concentrations (pFe19\_pCu14) indicated that the Sargasso Sea cyanobacterium *Synechococcus* sp (WH7803) had the highest Cu quotas (3.8  $\mu\text{mol Cu} \cdot \text{mol}^{-1} \text{C}$ ) and the oceanic dinoflagellate *Prorocentrum* had the lowest Cu quotas (0.36  $\mu\text{mol Cu} \cdot \text{mol}^{-1} \text{C}$ ). The order from the highest to the lowest Cu quotas for eukaryotic species was *Phaeocystis* (oceanic: 1.38  $\mu\text{mol Cu} \cdot \text{mol}^{-1} \text{C}$ ; coastal: 2.94  $\mu\text{mol Cu} \cdot \text{mol}^{-1} \text{C}$ ), *Chrysochromulina* (oceanic: 1.1  $\mu\text{mol Cu} \cdot \text{mol}^{-1} \text{C}$ ; coastal: 2.8  $\mu\text{mol Cu} \cdot \text{mol}^{-1} \text{C}$ ), *Emiliania* (oceanic: 1.0  $\mu\text{mol Cu} \cdot \text{mol}^{-1} \text{C}$ ; coastal: 1.4  $\mu\text{mol Cu} \cdot \text{mol}^{-1} \text{C}$ ) and *Prorocentrum* (oceanic: 0.36  $\mu\text{mol Cu} \cdot \text{mol}^{-1} \text{C}$ ; coastal: 0.54  $\mu\text{mol Cu} \cdot \text{mol}^{-1} \text{C}$ ).

As observed for diatoms (Annett et al. 2008), we expected higher Cu:C ratios for the oceanic than the coastal strains, when grown under Fe and Cu replete conditions. However, no clear habitat trend was observed for the Cu quotas (Table 2.6). The oceanic and coastal *Emiliania* had similar Cu quotas when grown under sufficient Fe/Cu conditions. The Cu quotas of the coastal strains of *Phaeocystis*, *Chrysochromulina* and *Prorocentrum* were ~2 times higher than those of the oceanic isolates. In contrast, the Cu quota of the Sargasso Sea *Synechococcus* (WH7803) was 8 times higher than that of the coastal isolate (*S. lividus*).

Copper levels had a significant effect ( $p < 0.001$ ) on the Cu quotas of all experimental species (Table 2.4, and 2.6). When Cu concentration decreased from pCu14 to pCu15, the Cu quotas decreased 1.2-25 fold, with an average reduction of 4.5 fold at all Fe levels. The highest reduction in the Cu quota was observed in the oceanic *Emiliania*, while the lowest reduction was observed in oceanic *Phaeocystis* (Table 2.6, Figure 2.2). The mixed-effect model showed an interaction between Cu availability and regime on the Cu:C ratios ( $\text{Cu} \times \text{Regime}$ ,  $p < 0.001$ , Table 2.5). Regardless of the Fe concentration,

when the Cu concentration decreased the Cu:C ratios declined 5.5 fold, on average, for the oceanic species and 3.8 fold, on average, for the coastal.

The mixed-effect model also revealed that Cu availability elicited a different response in the four phyla (Cu × Phylum effect,  $p = 0.026$ , Table 2.5). Regardless of Fe concentration (pFe19 and pFe21) and regime (oceanic and coastal), when the Cu concentration decreased the reductions of the Cu:C by Cyanobacteria and Bacillariophyceae were 3.9 and 3.2 fold, respectively, and were lower than the reductions by Prymnesiophyceae and Dinophyceae (5.3 and 5.0 fold, respectively).

The mixed-effect model indicated that Fe availability only had a significant effect on the Cu:C ratios of the oceanic species group (Fe effect,  $p < 0.001$ , for oceanic group; Table 2.5), but this Fe effect was also dependent on Cu availability (Fe × Cu effect,  $p < 0.001$  for oceanic group, Table 2.5) and phylum (Fe × Phylum effect,  $p = 0.032$  for the oceanic group; Fe × Cu × Phylum effect,  $p < 0.001$ , for the oceanic group; Table 2.5). For example, under high Cu conditions, the Cu:C ratios of oceanic Cyanophyceae, Dinophyceae and Prymnesiophyceae did not change significantly when Fe concentration decreased to pFe 21, while those of oceanic Bacillariophyceae increased 1.6 fold. In contrast, under low Cu conditions, the Cu:C ratios of oceanic Prymnesiophyceae increased 2.5 fold when the Fe concentration decreased (Table 2.6, Figure 2.2).

Table 2.6 Cellular concentration of Cu ( $\mu\text{M}$ ) and C (M), and Cu:C ( $\mu\text{mol Cu} \cdot \text{mol}^{-1} \text{C}$ ) ratios of phytoplankton grown under different Fe and/or Cu levels. All data are reported as mean  $\pm$  SD. Datas for *T. oceanica* and *T. pseudonana* are cited from Annett et al. 2008.

Species (Oceanic)	pFe_pCu (n)	Cellular Cu ( $\mu\text{M}$ )	Cellular C (M)	Cu:C	Species (Coastal)	pFe_pCu (n)	Cellular Cu ( $\mu\text{M}$ )	Cellular C (M)	Cu:C
<i>Synechococcus sp. WH7803</i>	19_14 (4)			3.80 $\pm$ 0.35	<i>Synechococcus lividus</i>	19_14 (14)			0.45 $\pm$ 0.09
	19_15 (4)			0.79 $\pm$ 0.11		19_15 (10)			0.11 $\pm$ 0.01
	21_14 (4)			4.30 $\pm$ 0.99		21_14 (7)			0.49 $\pm$ 0.07
	21_15 (4)			0.98 $\pm$ 0.14		21_15 (3)			0.21 $\pm$ 0.04
<i>Phaeocystis pouchetii</i>	19_14 (3)	24.9 $\pm$ 10.6	17.9 $\pm$ 0.83	1.38 $\pm$ 0.54	<i>Phaeocystis cordata</i>	19_14 (3)	23.9 $\pm$ 4.01	8.1 $\pm$ 0.11	2.94 $\pm$ 0.50
	19_15 (3)	18.6 $\pm$ 10.1	20.7 $\pm$ 11.9	0.92 $\pm$ 0.04		19_15 (4)	5.8 $\pm$ 0.96	8.2 $\pm$ 1.55	0.71 $\pm$ 0.12
	21_14 (4)	19.6 $\pm$ 4.07	13.9 $\pm$ 2.58	1.46 $\pm$ 0.12		21_14 (4)	15.8 $\pm$ 5.42	8.6 $\pm$ 1.74	1.82 $\pm$ 0.44
	21_15 (4)	14.9 $\pm$ 3.22	12.3 $\pm$ 1.95	1.20 $\pm$ 0.12		21_15 (4)	3.2 $\pm$ 0.80	7.1 $\pm$ 1.70	0.45 $\pm$ 0.06
	22_14 (4)	6.3 $\pm$ 1.03	6.03 $\pm$ 0.51	1.08 $\pm$ 0.24					
	22_15 (4)	6.6 $\pm$ 1.13	9.35 $\pm$ 2.52	0.73 $\pm$ 0.09					
<i>Emiliana huxleyi</i>	19_14 (4)	2.8 $\pm$ 0.63	3.2 $\pm$ 0.50	1.00 $\pm$ 0.25	<i>Emiliana huxleyi</i>	19_14 (3)	13.0 $\pm$ 4.30	9.1 $\pm$ 0.66	1.40 $\pm$ 0.35
	19_15 (4)	0.2 $\pm$ 0.03	5.0 $\pm$ 1.20	0.04 $\pm$ 0.00		19_15 (3)	1.6 $\pm$ 0.15	5.4 $\pm$ 0.33	0.29 $\pm$ 0.04
	21_14 (4)	5.9 $\pm$ 1.50	4.2 $\pm$ 1.20	1.50 $\pm$ 0.62		21_14 (3)	14.0 $\pm$ 0.62	10.0 $\pm$ 0.88	1.40 $\pm$ 0.11
	21_15 (4)	0.9 $\pm$ 0.19	4.4 $\pm$ 1.20	0.21 $\pm$ 0.03		21_15 (3)	3.0 $\pm$ 0.63	12.0 $\pm$ 1.40	0.25 $\pm$ 0.04
						22_3_14 (4)	9.8 $\pm$ 1.90	7.3 $\pm$ 1.70	1.40 $\pm$ 0.42
						22_3_15 (3)	1.9 $\pm$ 0.34	4.8 $\pm$ 0.93	0.41 $\pm$ 0.15
<i>Chrysochromulina polylepis</i>	19_14 (3)	15.0 $\pm$ 1.50	13.0 $\pm$ 1.40	1.15 $\pm$ 0.02	<i>Chrysochromulina kappa</i>	19_14 (3)	27.0 $\pm$ 9.50	9.3 $\pm$ 2.30	2.80 $\pm$ 0.27
	19_15 (3)	12.0 $\pm$ 2.20	17.0 $\pm$ 1.90	0.70 $\pm$ 0.08		19_15 (3)	9.3 $\pm$ 1.90	8.4 $\pm$ 0.82	1.10 $\pm$ 0.13
	21_14 (4)	19.0 $\pm$ 5.50	12.0 $\pm$ 2.50	1.60 $\pm$ 0.49		21_14 (3)	26.0 $\pm$ 0.93	9.5 $\pm$ 0.63	2.80 $\pm$ 0.24
	21_15 (4)	12.0 $\pm$ 2.50	22.0 $\pm$ 3.50	0.58 $\pm$ 0.22		21_15 (3)	8.9 $\pm$ 0.92	7.5 $\pm$ 0.97	1.10 $\pm$ 0.16
	22_14 (4)	9.7 $\pm$ 1.00	7.9 $\pm$ 0.60	1.23 $\pm$ 0.05		22_3_14 (4)	32.0 $\pm$ 2.90	5.2 $\pm$ 0.23	6.20 $\pm$ 0.31
	22_15 (4)	8.4 $\pm$ 2.60	7.1 $\pm$ 2.20	1.20 $\pm$ 0.16		22_3_15 (4)	11.0 $\pm$ 1.30	6.1 $\pm$ 1.30	1.90 $\pm$ 0.20

Species (Oceanic)	pFe_pCu (n)	Cellular Cu ( $\mu$ M)	Cellular C (M)	Cu:C	Species (Coastal)	pFe_pCu (n)	Cellular Cu ( $\mu$ M)	Cellular C (M)	Cu:C
<i>Prorocentrum dentatum</i>	19_14 (3)	3.7 $\pm$ 0.89	11 $\pm$ 1.9	0.36 $\pm$ 0.17	<i>Prorocentrum minimum</i>	19_14 (4)	12.0 $\pm$ 2.80	18.0 $\pm$ 2.40	0.67 $\pm$ 0.07
	19_15 (4)	0.8 $\pm$ 0.33	7.2 $\pm$ 2.00	0.11 $\pm$ 0.01		19_15 (4)	3.5 $\pm$ 0.79	18.0 $\pm$ 1.60	0.20 $\pm$ 0.03
	21_14 (4)			0.34 $\pm$ 0.06		21_14 (4)			0.41 $\pm$ 0.06
	21_15 (4)			0.11 $\pm$ 0.01		21_15 (4)			0.04 $\pm$ 0.02
<i>Thalassiosira oceanica</i>	19_14 (4)			2.93 $\pm$ 0.38	<i>Thalassiosira pseudonana</i>	19_14 (10)			1.88 $\pm$ 0.77
	19_15 (6)			0.94 $\pm$ 0.51		19_15 (8)			1.96 $\pm$ 0.39
	20.5_14 (3)			4.66 $\pm$ 0.49		20.5_14 (8)			2.67 $\pm$ 1.86
	20.5_15 (8)			0.64 $\pm$ 0.17		20.5_15 (10)			1.95 $\pm$ 2.62
	21.5_14 (6)			6.32 $\pm$ 2.40					
21.5_15 (6)			0.73 $\pm$ 0.41						

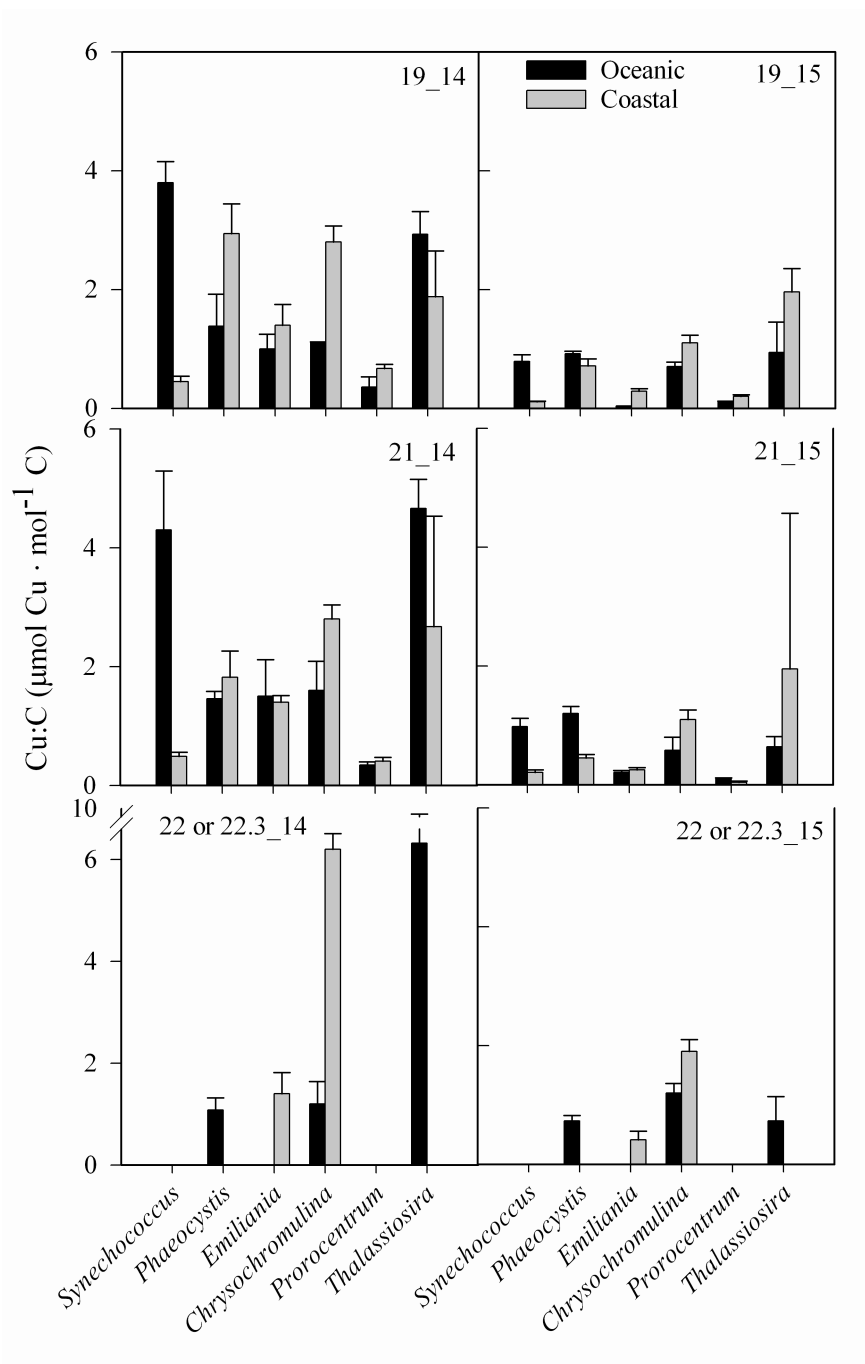


Figure 2.2 Cu:C ratios ( $\mu\text{mol Cu} \cdot \text{mol}^{-1} \text{C}$ ) of oceanic and coastal phytoplankton grown under different Fe and/or Cu levels. The Fe and Cu levels (pFe\_pCu) are indicated on the top, right corner of the graph. The Cu:C ratios of the *Thalassiosira* strains are those reported in Annett et al. 2008. Error bar denote standard deviation of at least triplicate cultures. Statistical analyses of these data are presented in Table 2.4 and 2.5.

### 2.3.3 Effect of Fe and Cu availability on steady-state Cu uptake

Among the eight eukaryotic species we examined, oceanic *Phaeocystis* (*P. pouchetii*) had the fastest Cu uptake rate ( $1.86 \times 10^{-20}$  mol Cu  $\cdot$   $\mu\text{m}^{-2} \cdot \text{d}^{-1}$ ), and oceanic *Emiliania huxleyi* and *Prorocentrum dentatum* had the slowest Cu uptake rates ( $0.22$  and  $0.26 \times 10^{-20}$  mol Cu  $\cdot$   $\mu\text{m}^{-2} \cdot \text{d}^{-1}$ , respectively) under Fe/Cu sufficient conditions (Table 2.7). Two Way ANOVA analyses indicated that Fe and Cu availability had significant interactive effects on  $\rho_{\text{ss}}\text{Cu}$  of most species (Table 2.4). When Fe levels decreased from pFe 19 to pFe21, most of the  $\rho_{\text{ss}}\text{Cu}$  decreased, except for two *E. huxleyi* strains which kept the same  $\rho_{\text{ss}}\text{Cu}$  at high Cu but increased its  $\rho_{\text{ss}}\text{Cu}$  at low Cu. When the Cu concentration decreased from pCu14 to pCu15, the  $\rho_{\text{ss}}\text{Cu}$  of experimental species decreased 1.4-22 fold (average 5.3 fold) under all Fe levels. The highest reduction was observed in oceanic *E. huxleyi* (22 fold). This Cu effect on the  $\rho_{\text{ss}}\text{Cu}$  was also supported by the mixed-effect model when all phytoplankton are treated as a group (Cu effect,  $p < 0.001$ , Table 2.5).

Similar trends to those observed for the Cu:C ratios were also revealed for  $\rho_{\text{ss}}\text{Cu}$  by the mixed-effect model. For example, the  $\rho_{\text{ss}}\text{Cu}$  of oceanic and coastal species had different responses to Cu availability (Cu  $\times$  Regime effect,  $p = 0.001$ , Table 2.5), whereby the  $\rho_{\text{ss}}\text{Cu}$  of oceanic species decreased to a greater extent than those of the coastals ( $\sim 5.4$  vs. 4.7 fold, respectively; Table 2.7). Moreover, in response to low Cu, the reduction of  $\rho_{\text{ss}}\text{Cu}$  by Prymnesiophyceae (11 fold) was higher than that by Dinophyceae (5.7 fold) and Bacillariophyceae (3 fold) (Cu  $\times$  phylum  $p < 0.001$ , Table 2.5).

Table 2.7 Steady-state Cu uptake rates ( $\rho_{ss}Cu$ ,  $\times 10^{-20}$  mol Cu  $\cdot \mu\text{m}^{-2} \cdot \text{d}^{-1}$ ) and Cu use efficiency (mol C  $\cdot \mu\text{mol Cu}^{-1} \cdot \text{d}^{-1}$ ) of phytoplankton grown under different Fe and/or Cu levels. All data are reported as mean  $\pm$  SD. Only the  $\rho_{ss}Cu$  of the coastal *Synechococcus* ( $2.42 \times 10^{-20}$  mol Cu  $\mu\text{m}^{-2} \text{d}^{-1}$ ) under Fe/Cu sufficient conditions was calculated given that we determined its cell density and size by flow-cytometry. Datas for *T. oceanica* and *T. pseudonana* are cited from Annett et al. 2008.

Species (Oceanic)	pFe_pCu (n)	$\rho_{ss}Cu$	Cu use efficiency	Species (Coastal)	pFe_pCu (n)	$\rho_{ss}Cu$	Cu use efficiency
<i>Synechococcus sp.</i> WH7803	19_15 (4)		1.54 $\pm$ 0.36	<i>Synechococcus lividus</i>	19_14 (14)	2.42 $\pm$ 0.60	
	21_15 (4)		0.54 $\pm$ 0.19		19_15 (10)		13.6 $\pm$ 2.07
					21_15 (3)		3.14 $\pm$ 0.59
<i>Phaeocystis pouchetii</i>	19_14 (3)	1.86 $\pm$ 0.76		<i>Phaeocystis cordata</i>	19_14 (3)	0.54 $\pm$ 0.07	
	19_15 (3)	1.30 $\pm$ 0.64	1.15 $\pm$ 0.04		19_15 (4)	0.10 $\pm$ 0.01	0.40 $\pm$ 0.06
	21_14 (4)	1.08 $\pm$ 0.19			21_14 (4)	0.23 $\pm$ 0.06	
	21_15 (4)	0.77 $\pm$ 0.11	0.70 $\pm$ 0.11		21_15 (4)	0.03 $\pm$ 0.01	0.41 $\pm$ 0.05
	22_14 (4)	0.34 $\pm$ 0.11					
	22_15 (4)	0.32 $\pm$ 0.04	9.86 $\pm$ 0.52				
<i>Emiliana huxleyi</i>	19_14 (4)	0.22 $\pm$ 0.08		<i>Emiliana huxleyi</i>	19_14 (3)	0.75 $\pm$ 0.25	
	19_15 (4)	0.01 $\pm$ 0.00	7.57 $\pm$ 0.11		19_15 (3)	0.06 $\pm$ 0.01	1.82 $\pm$ 0.29
	21_14 (4)	0.29 $\pm$ 0.08			21_14 (3)	0.74 $\pm$ 0.03	
	21_15 (4)	0.04 $\pm$ 0.01	1.29 $\pm$ 0.19		21_15 (3)	0.14 $\pm$ 0.03	2.81 $\pm$ 0.61
					22.3_14 (4)	0.43 $\pm$ 0.09	
				22.3_15 (3)	0.07 $\pm$ 0.02	1.55 $\pm$ 0.49	
<i>Chrysochromulina polylepis</i>	19_14 (3)	1.12 $\pm$ 0.06		<i>Chrysochromulina kappa</i>	19_14 (3)	1.72 $\pm$ 0.54	
	19_15 (3)	0.81 $\pm$ 0.15	1.37 $\pm$ 0.19		19_15 (3)	0.60 $\pm$ 0.09	0.82 $\pm$ 0.16
	21_14 (4)	0.98 $\pm$ 0.32			21_14 (3)	1.58 $\pm$ 0.18	
	21_15 (4)	0.57 $\pm$ 0.09	1.43 $\pm$ 0.45		21_15 (3)	0.60 $\pm$ 0.06	0.86 $\pm$ 0.12
	22_14 (4)	0.52 $\pm$ 0.02			22.3_14 (4)	1.44 $\pm$ 0.07	
	22_15 (4)	0.33 $\pm$ 0.07	0.60 $\pm$ 0.13		22.3_15 (4)	0.37 $\pm$ 0.02	0.28 $\pm$ 0.01

Species (Oceanic)	pFe_pCu (n)	$\rho_{ss}\text{Cu}$	Cu use efficiency	Species (Coastal)	pFe_pCu (n)	$\rho_{ss}\text{Cu}$	Cu use efficiency
<i>Prorocentrum dentatum</i>	19_14 (3)	0.26±0.06		<i>Prorocentrum minimum</i>	19_14 (4)	0.73±0.17	
	19_15 (4)	0.06±0.02	4.15±0.88		19_15 (4)	0.22±0.06	1.89±0.27
	21_14 (4)	0.05±0.02			21_14 (4)	0.10±0.04	
	21_15 (4)	0.01±0.00	0.89±0.18		21_15 (4)	0.01±0.00	4.78±2.20
<i>Thalassiosira oceanica</i>	19_14 (4)	4.64±0.28		<i>Thalassiosira pseudonana</i>	19_14 (10)	2.92±0.29	
	19_15 (6)	1.27±0.32	1.20		19_15 (8)	3.48±0.52	1.00
	20.5_14 (3)	7.98±0.42			20.5_14 (8)	2.51±0.73	
	20.5_15 (8)	1.26±0.10	1.51		20.5_15 (10)	1.78±0.73	0.65
	21.5_14 (6)	6.60±0.72					
	21.5_15 (6)	0.69±0.15	9.27				

### 2.3.4 Effect of Fe and Cu availability on Cu use efficiency

Given that phytoplankton may have luxury trace metal uptake under trace metal sufficiency, we only calculated Cu use efficiency for the low Cu treatments. The highest Cu use efficiency was observed for the coastal *Synechococcus* ( $13.6 \text{ mol C} \cdot \mu\text{mol Cu}^{-1} \cdot \text{d}^{-1}$ ), and the lowest for coastal *Chrysochromulina kappa* ( $0.28 \text{ mol C} \cdot \mu\text{mol Cu}^{-1} \cdot \text{d}^{-1}$ ). In general, for all species tested, the Cu use efficiency stayed the same or decreased with Fe-limitation (pFe19 vs. 21). The exception was *Prorocentrum minimum*, whose Cu use efficiency increased significantly  $\sim 2.5$  fold ( $p < 0.05$ ) when Fe was low (Table 2.7).

## 2.4 Discussion

### 2.4.1 The effect of Fe and Cu availability on the growth rate

Low Fe availability had a significant effect on phytoplankton growth rates. Moreover, this effect was dependent on whether the strain was isolated from a coastal or an oceanic environment and its taxonomic class. The Sargasso Sea *Synechococcus* and the oceanic *Phaeocystis* were able to grow better than their coastal counterparts at the same low concentration of Fe, indicating that these oceanic strains need less Fe concentrations for growth. This trend is consistent with previous results (Brand 1991, Sunda et al. 1991, Sunda and Huntsman 1995a, Maldonado et al. 2006, Annett et al. 2008). However, the coastal strains of Prymnesiophyceae *Emiliana*, *Chrysochromulina* and Dinophyceae *Prorocentrum* were able to maintain faster growth rates than the oceanic strains at similar limiting Fe concentrations. At present, we are unable to explain these findings. In addition, regardless of regime, Prymnesiophyceae strains exhibited less average reduction (16%) in growth rate due to low Fe (pFe21) than did phytoplankton from Cyanophyceae (48%), Dinophyceae (41%) and Bacillariophyceae (22%). This suggests that Prymnesiophyceae require the least amount of Fe for growth, while Cyanophyceae and

Dinophyceae require the most.

Lowering Cu levels had no obvious effect on the growth rates of all species when treated as a group (Cu effect,  $p = 0.170$ , Table 2.5). However, it had a significant effect on the growth rates of the oceanic strains (Cu effect,  $p = 0.002$ , Table 2.5), indicating that Cu has an important physiological role in these oceanic phytoplankton. In addition, the effect of low Cu on the growth of oceanic phytoplankton was dependant on Fe availability and phylum (Fe  $\times$  Cu  $\times$  Phylum,  $p = 0.038$  for oceanic group, Table 2.5). For example low Cu significantly reduced the growth rate of the oceanic Cyanophyceae (22%) and Bacillariophyceae (18%) when Fe was low (pFe21), but did not change the growth rate of oceanic Dinophyceae and Prymnesiophyceae regardless of the Fe availability (pFe19 or pFe21). Only when the Fe level decreased to pFe22, did the growth rate of the oceanic *Phaeocystis* (Prymnesiophyceae) decrease by 32% at low Cu condition (Table 2.3). These results suggest that the oceanic *Phaeocystis* and the Sargasso Sea *Synechococcus* also require higher Cu concentrations for growth when Fe is low, as observed previously in marine diatoms (Peers et al. 2005, Maldonado et al. 2006, Annett et al. 2008, Semeniuk et al. 2009).

Interestingly, the coastal *E. huxleyi* was the most sensitive species to low Cu and the least sensitive to low Fe. While this species maintained maximum growth rates even in the absence of a Fe addition to the medium, it significantly decreased its growth rate when Cu level was lowered—regardless of the Fe concentration. This indicates that Cu has a particularly important role for the growth of this coastal strain of *E. huxleyi*. Plastocyanin, a photosynthetic Cu-containing electron carrier, transfers electrons from cytochrome *b<sub>6</sub>f* complex to the P700 reaction centre and has been found in plants, green algae, some cyanobacteria and the oceanic diatom *T. oceanica* (Boulter et al. 1977, Sandmann et al. 1983, Laudenbach et al. 1990, Peers and Price 2006). It is encoded by the gene *petE*. Two *petE* encoding ESTs (CX773129 and CX773088) have been found in an oceanic strain of *E. huxleyi* CCMP371 (Nosenko et al. 2006). The genome of *E. huxleyi* CCMP1516 (isolated 100 Km off shore from S. America) also encodes

plastocyanin/azurin-like proteins and a Cu/Zn SOD (<http://genome.jgipsf.org/Emihu1/Emihu1.home.html>). Copper may thus be required for the photosynthetic apparatus and/or involved in the detoxification of superoxide radicals in *E. huxleyi*.

#### 2.4.2 Cellular Cu:C ratios

Cellular Cu quotas range from 0.36 to 3.8  $\mu\text{mol Cu} \cdot \text{mol}^{-1} \text{C}$  in Fe/Cu sufficient cultures (pFe19\_pCu14, Table 2.6). These Cu:C ratios are in accord with previous studies of diverse phytoplankton (0.74 to 9.93  $\mu\text{mol Cu} \cdot \text{mol}^{-1} \text{C}$ , calculated from measurements of Cu:P and C:P, Ho et al. 2003), marine diatoms (0.58 to 4.3  $\mu\text{mol Cu} \cdot \text{mol}^{-1} \text{C}$ , Sunda and Huntsman 1995b, Annett et al. 2008) and *Emiliana* (1.3 to 2.4  $\mu\text{mol Cu} \cdot \text{mol}^{-1} \text{C}$ , Muggli and Harrison 1996) (Table 2.8). In our study, the average Cu quotas of Bacillariophyceae, Cyanophyceae, Prymnesiophyceae and Dinophyceae under Fe/Cu sufficient condition were  $2.41 \pm 0.74$ ,  $2.13 \pm 2.37$ ,  $1.78 \pm 0.86$  and  $0.52 \pm 0.22$   $\mu\text{mol Cu} \cdot \text{mol}^{-1} \text{C}$ , respectively (Table 2.8). This order, from high to low, is in disagreement with that found in Ho et al. study (2003), where the average Cu quotas (Cu:C) of Dinophyceae ( $4.18 \pm 4.06$   $\mu\text{mol Cu} \cdot \text{mol}^{-1} \text{C}$ ) were higher than those of Bacillariophyceae ( $2.83 \pm 0.74$   $\mu\text{mol Cu} \cdot \text{mol}^{-1} \text{C}$ ) and Prymnesiophyceae ( $1.32 \pm 0.56$   $\mu\text{mol Cu} \cdot \text{mol}^{-1} \text{C}$ ) under 20 nM total Cu condition (pCu = 13.8).

Table 2.8 Comparison of C-normalized copper quotas (Cu:C) of different phytoplankton phyla in this study with values reported by Ho et al. (2003). The Cu:C ratios of Ho et al. (2003) were calculated from the P-normalized Cu quotas (Cu:P) and P-normalized C quotas (C:P) reported in Table 2 in Ho et al. (2003). The \* indicates that the C data used from Ho et al. (2003) are those of the HCl treated samples. R = red plastid superfamily, G = green plastid superfamily.

Species	C:P (mol · mol <sup>-1</sup> )	Cu:P (mmol · mol <sup>-1</sup> )	Cu:C (umol · mol <sup>-1</sup> )	Cu:C (umol · mol <sup>-1</sup> ) This study
<b>Chlorophyceae (G)</b>				
<i>Dunaliella tertiolecta</i>	222	0.67	3.02	
<i>Nannochloris atomus</i>	173	0.23	1.33	
Mean ± SD	198 ± 35	0.45 ± 0.31	2.17 ± 1.19	
<b>Prasinophyceae (G)</b>				
<i>Pyramimonas parkeae</i>	209*	0.62	2.97	
<i>Pycnococcus provasoli</i>	191	0.53	2.77	
<i>Tetraselmis sp.</i>	199	0.51	2.56	
Mean ± SD	200 ± 9	0.55 ± 0.06	2.77 ± 0.20	
<b>Dinophyceae</b>				
<i>Gymnodinium chlorophorum</i> (G)	137	1.36	9.93	
<i>Prorocentrum minimum</i> (R)	135	0.28	2.07	
<i>Amphidinium carterae</i> (R)	136	0.54	3.97	
<i>Thoracosphaera heimii</i> (R)	81*	0.06	0.74	
Mean ± SD	122 ± 28	0.56 ± 0.24	4.18 ± 4.06	0.52 ± 0.22
<b>Prymesiophyceae (R)</b>				
<i>Emiliana huxleyi</i>	76*	0.07	0.92	
<i>Gephyrocapsa oceanica</i>	64*	0.11	1.72	
Mean ± SD	70 ± 8	0.09 ± 0.03	1.32 ± 0.56	1.78 ± 0.86
<b>Bacillariophyceae (R)</b>				
<i>Ditylum brightwellii</i>	45	0.06	1.33	
<i>Thalassiosira weissflogii</i>	86	0.17	1.98	
<i>Nitzschia breviostris</i>	42	0.18	4.29	
<i>Thalassiosira eccentrica</i>	75	0.28	3.73	
Mean ± SD	62 ± 22	0.17 ± 0.09	2.83 ± 1.40	2.41 ± 0.74

Changes in ocean redox state have been suggested to have influenced trace metal stoichiometry in marine phytoplankton (Quigg et al. 2003, Ho et al. 2003, and Saito et al. 2003). Differences in the Cu quotas of marine eukaryotic phytoplankton have been observed between the red and the green plastid superfamilies, with the former having, in general, lower Cu quotas than the latter (Quigg et al. 2003, Ho et al. 2003). In addition, metal preferences (e.g. for Fe) and sensitivities (e.g. to Cu) of Cyanophyceae have been suggested to reflect their evolution in an ancient sulfidic ocean, where the availability of Fe was high and that of Cu was low (Saito et al. 2003). Our limited data set supports the notion that *Synechococcus* spp. have relatively high Fe requirements, as the two *Synechococcus* strains exhibited the greatest reduction in growth rates due to Fe limitation. However, contrary to our expectation of high Cu sensitivities of *Synechococcus*, we measured the highest Cu:C quotas in the Sargasso Sea *Synechococcus* under optimal Fe and Cu conditions. In spite of these high Cu:C ratios, this strain achieved fast growth rates ( $\sim 1.0 \text{ d}^{-1}$ ), suggesting that high intracellular Cu levels were not detrimental for growth. These findings imply that this strain, which supposedly evolved in a low Cu environment, is unaffected by the accumulation of high intracellular Cu levels. Surprisingly, this strain was easily affected by Cu limitation when grown in low Fe conditions. These results suggest that *Synechococcus* WH7803, has a high demand for Cu, especially if experiencing Fe limitation. This is consistent with the deeper water column niche of WH7803 (Campbell and Carpenter 1987), presumably closer to the cuprocline, and the presence of genes encoding Cu/Zn superoxide dismutase (SOD, NCBI-GI: 147847826), FeSOD (NCBI-GI:147848617), and multi-Cu containing oxidases (MCO, NCBI-GI: 148239533) in its genome. Thus, when experiencing Fe limitation the Cu requirement of the WH7803 strain might increase as it switches from FeSOD to Cu/Zn SOD and increases its MCO activity to enhance Fe transport. The Cu

demand of the model oceanic *Synechococcus* strains (WH8102) might be much lower, as this strain lacks MCO and uses Ni SOD instead of Cu/ZnSOD (Palenik et al. 2003, Dupont et al. 2008). Therefore, the high Cu demand under Fe limiting conditions observed for our Sargasso Sea *Synechococcus* might not be a widespread physiological characteristic of oceanic *Synechococcus*.

The Cu quotas of the Sargasso Sea *Synechococcus* were up to one order of magnitude higher than those of the coastal strain (see Cu:C for both strains at pFe19\_pCu14 and pFe21\_pCu14). This suggests that differing trace metal conditions in coastal and open ocean environments might have mediated the retention and expression of genes (acquired via lateral gene transfer) encoding distinct trace metal transport and homeostasis mechanisms. These conclusions were first reached by genomic studies of the model oceanic (WH8102) and coastal (CC9311) *Synechococcus* (Palenik et al. 2003, 2006), demonstrating distinct genetic complements of metal-containing enzymes and transporters. The low Cu:C quotas we observed in the coastal *Synechococcus* under moderate Cu levels (pCu14), point towards efficient Cu detoxifying mechanisms, such as cellular Cu efflux (Croot et al. 2003), and/or the production and release of strong organic Cu ligands to lower the inorganic Cu concentration in seawater (Moffett and Brand, 1996).

Another important consideration is that apparent taxonomic patterns in trace metal quotas may depend upon the element used as a proxy for phytoplankton biomass when normalizing metal concentrations. To compare our Cu:C ratios to those presented in Ho et al. (2003), we converted their Cu:P to Cu:C using the cellular concentrations of C presented in Table 2.2 in Ho et al. (2003). The average carbon-normalized Cu quotas

(Cu:C) of Chlorophyceae and Prasinophyceae, which belong to the green plastid superfamily, are  $2.17 \pm 1.19$  and  $2.77 \pm 0.20$   $\mu\text{mol Cu} \cdot \text{mol}^{-1} \text{C}$ , respectively, while the Cu:C ratios of Prymnesiophyceae and Bacillariophyceae, which belong to the red plastid superfamily, are  $1.32 \pm 0.56$  and  $2.83 \pm 1.40$   $\mu\text{mol Cu} \cdot \text{mol}^{-1} \text{C}$ , respectively (Table 2.8). These Cu:C ratios do not support Ho et al.'s conclusion (2003) that systematic differences in trace metal quotas (including Cu) exist between the green algae and that of Prymnesiophyceae and Bacillariophyceae. In addition, the phylogenetic difference in Cu requirements (Cu:P) between the red and green plastid superfamilies described by Quigg et al. (2003) [ $0.512$  vs.  $0.194$  mmol Cu:P for the green and the red plastid superfamily, respectively (excluding the data for the green plastid dinoflagellate *Gymnodinium chlorophorum*)] is not observed if the Cu quotas are normalized to C [ $2.53$  vs.  $2.3$   $\mu\text{mol Cu} \cdot \text{mol}^{-1} \text{C}$  for the green and the red plastid superfamily, respectively, Table 2.8]. Thus, though phytoplankton trace metal concentrations are often normalized to cellular P concentrations, using P as a biomass proxy is not ideal, given its plasticity (Sterner and Elser 2002), and its tendency to adsorb to cell surfaces (Sanudo-Wilhelmy et al. 2004). Similar conclusions were reached by Twining et al. 2004. These combined results highlight the urgent need for a more consistent proxy for phytoplankton cellular biomass. Given the interaction between trace metal geochemical cycles and the global C cycle, we believe that using C as a proxy for phytoplankton biomass is most appropriate.

The replacement of Fe-containing catalysts with Cu-containing ones was hypothesized to be a means to survive in the very low Fe concentration waters of the open ocean. This was supported by the higher Cu quotas of oceanic diatoms relative to coastal diatoms observed in a previous study (Annett et al. 2008). We thus hypothesized that this oceanic-coastal trend might be observed in other phytoplankton taxa. However, our findings

revealed that the geographical origin of the phytoplankton had no effect on their Cu:C when all phytoplankton were treated as a group (regime effect,  $p = 0.200$ , Table 2.5).

Given the involvement of putative multi-Cu oxidases in the high-affinity Fe transport systems of marine diatoms (Peers et al. 2005, Wells et al. 2005, Maldonado et al. 2006), we also hypothesized that the Cu requirements of Fe-limited phytoplankton, across different taxa, may be higher than those of Fe-sufficient ones. However, only the Cu quotas of the coastal *Synechococcus*, and the coastal *Chrysochromulina* significantly increased  $\sim 2$ -5 times when Fe was limiting (Table 2.6, and Table 2.4), suggesting that the role for Cu in high-affinity Fe uptake system is not universal.

### 2.4.3 Steady-state Cu uptake rates

Under Fe/Cu sufficient conditions, the steady-state Cu uptake rates ( $\rho_{ss}\text{Cu}$ ) of the coastal *Synechococcus* ( $2.42 \times 10^{-20} \text{ mol Cu} \cdot \mu\text{m}^{-2} \cdot \text{d}^{-1}$ ) were similar to those previously measured ( $1.7 \times 10^{-20} \text{ mol Cu} \cdot \mu\text{m}^{-2} \cdot \text{d}^{-1}$ ; calculated from  $0.79 \times 10^{-21} \text{ mol Cu} \cdot \text{cell}^{-1} \cdot \text{d}^{-1}$ , at  $p\text{Cu}12.6$ ; Croot et al. 2003) for the Sargasso Sea *Synechococcus* (WH7803). Similarly, the  $\rho_{ss}\text{Cu}$  of the eukaryotic phytoplankton ranged from 0.22 to  $1.86 \times 10^{-20} \text{ mol Cu} \cdot \mu\text{m}^{-2} \cdot \text{d}^{-1}$  (Table 2.7), and were comparable to those previously published for marine diatoms ( $0.9$ - $5.62 \times 10^{-20} \text{ mol Cu} \cdot \mu\text{m}^{-2} \cdot \text{d}^{-1}$ , Annett et al. 2008). The order from the slowest to the fastest  $\rho_{ss}\text{Cu}$  of the eukaryotic phytoplankton was Dinophyceae, Prymnesiophyceae and Bacillariophyceae ( $0.49$ ,  $1.04$  and  $3.78 \times 10^{-20} \text{ mol Cu} \cdot \mu\text{m}^{-2} \cdot \text{d}^{-1}$ , respectively, Table 2.7), similar to the order of the Cu quotas under identical growth conditions (Fe and Cu sufficiency, see previous section). The  $\rho_{ss}\text{Cu}$  of the Bacillariophyceae were  $\sim 3.6$  and  $7.7$  times faster than those of Prymnesiophyceae and Dinophyceae under high Cu concentration, and 5 and 17 fold faster under low Cu concentration. The fastest rates of

Cu uptake by diatoms may be due to a higher density of Cu transporters at the cell surface or a slower Cu efflux (Croot et al. 2003).

The mixed-effect model also indicated that the  $\rho_{ss}\text{Cu}$  of the oceanic phytoplankton were significantly affected by the Cu concentration in the media while those of the coastal strains were not (Cu effect for oceanic group,  $p = 0.001$ ; for coastal group,  $p = 0.192$ ; Table 2.5). To further investigate these findings, the effects of varying Cu concentrations and Fe-limited growth rates on the Cu:C and  $\rho_{ss}\text{Cu}$  were also examined. Biodilution (Sunda and Huntsman 2000, Cullen et al. 2003) suggests that phytoplankton may accumulate higher intracellular metal concentrations (eg. Cd) under Fe-limitation because metal uptake rates are kept constant while growth rates are reduced. This biodilution effect can be investigated using the equation  $Q = \rho / \mu$ , where  $Q$  is the cellular metal quota ( $\text{mol Cu mol C}^{-1}$ ),  $\rho$  is the cellular uptake rate ( $\text{mol Cu mol C}^{-1} \text{ time}^{-1}$ ), and  $\mu$  is the specific growth rate ( $\text{time}^{-1}$ ). In our study, when Cu was replete (pCu 14), the average reduction in growth rate as a result of Fe-limitation was 25% for the oceanic species (Table 2.9). Therefore, the calculated, average increase in Cu:C quota due to biodilution would be 34% for these strains, assuming constant Cu uptake rates. Thus, the observed 27% increase in the oceanics' Cu:C ratios as a result of Fe-limitation can be entirely accounted for by biodilution (34% for 27%, Table 2.9). However, when Cu was low (pCu 15), the observed, average 72% increase in Cu:C for the Fe-limited oceanic species can not be fully accounted for by biodilution (expected increase in Cu:C  $\sim 45\%$  vs. observed increase in Cu:C  $\sim 72\%$ ). An additional increase in Cu uptake is needed ( $\sim 30\%$ ) to account for the total 72% increase observed in their Cu:C ratios. In support of this, we observed 28% faster Cu uptake rates ( $\rho_{ss}\text{Cu}$ ) under Fe limitation for the oceanic strains (Table 2.9). These results suggest that under Fe-limitation the slower growth rates and the

faster Cu uptake rates contribute almost equally to the increase in Cu:C observed for the oceanic phytoplankton grown at low Cu levels (pCu 15).

Table 2.9 The effects of Fe limitation on growth rate ( $\mu$ ), Cu:C ratios (both expected and observed), and steady-state Cu uptake rates ( $\rho_{ss}\text{Cu}$ ) in oceanic and coastal phytoplankton grown under replete (pCu 14) and low Cu (pCu 15) conditions. Calculation for expected Cu:C were based on the equation  $Q = \rho / \mu$  where  $Q$  is the cellular metal quota ( $\text{mol Cu} \cdot \text{mol C}^{-1}$ ),  $\rho$  is the cellular uptake rate ( $\text{mol Cu} \cdot \text{mol C}^{-1} \cdot \text{time}^{-1}$ ), and  $\mu$  is the specific growth rate ( $\text{time}^{-1}$ ), and assuming a constant cellular Cu uptake rate (see main text for details). Data used for calculation were from Table 2.3, 2.6 and 2.7. Please note that the  $\rho_{ss}\text{Cu}$  in Table 2.7 were converted from  $\text{mol Cu} \cdot \mu\text{m}^{-2} \cdot \text{d}^{-1}$  to  $\text{mol Cu} \cdot \text{mol C}^{-1} \cdot \text{d}^{-1}$  for this calculation using data from Table 2.3 and 2.6.

Change due to Fe limitation	Oceanic strains		Coastal strains	
	pCu = 14	pCu = 15	pCu = 14	pCu = 15
Average reduction of growth rates $= 1 - (\mu_{\text{pFe21}} / \mu_{\text{pFe19}})$	25%	31%	24%	25%
Expected average increase in Cu:C $= (\mu_{\text{pFe19}} / \mu_{\text{pFe21}}) - 1$	34%	45%	32%	34%
Observed average increase in Cu:C $= 1 - (Q_{\text{pFe21}} / Q_{\text{pFe19}})$	27%	72%	No change	No change
Observed change in $\rho_{ss}\text{Cu}$ $= 1 - (\rho_{ss}\text{Cu}_{\text{pFe21}} / \rho_{ss}\text{Cu}_{\text{pFe19}})$	No change	28% increase	23% reduction	38% reduction

Interestingly, and regardless of pCu level (pCu 14 and 15), the coastal strains exhibited identical Cu:C ratios for the Fe sufficient and Fe limited cultures (Table 2.9), even though the slower growth rates under Fe-limitation (24% or 25%, Table 2.9) predicted a biodilution-mediated increase in Cu:C (32 or 34%). This result suggests that the coastal strains in order to keep constant Cu quotas under Fe limitation are either a) effluxing Cu while keeping constant Cu uptake rates or b) acquiring Cu at a slower rate. Our results support the latter, with the coastal strains exhibiting a decrease in Cu uptake rates under Fe limitation of 23% and 38% for pCu of 14 and 15, respectively (Table 2.9). These results highlight the contrasting physiological strategies of coastal and oceanic strains to deal with varying concentrations of Cu and Fe in the ocean. They also suggest that different Cu homeostasis mechanisms exist in coastal and oceanic phytoplankton and that metal availability regulates differently the gene and/or protein expression of their Cu acquisition mechanisms. Future studies are needed to elucidate these unique Cu uptake and efflux strategies, at the gene and protein level.

The order of  $\rho_{ss}\text{Cu}$  for different eukaryotic phyla was also observed in the cellular Cu:C ratios (Dinophyceae < Prymnesiophyceae < Bacillariophyceae). Moreover, the average reduction in  $\rho_{ss}\text{Cu}$  and the cellular Cu:C ratios in response to a decrease in Cu availability is also similar. The average decrease in  $\rho_{ss}\text{Cu}$  and in cellular Cu:C is 5.3 and 4.5 fold, respectively, matching the reduction in the total Cu (5 fold decrease between Cu-sufficient and low-Cu treatment) but not in free  $\text{Cu}^{2+}$  concentration (10 fold decrease) in the media. This reduction is also consistent with other data from marine diatoms (4.2 vs. 4.1 fold, Annett et al. 2008). These results confirm previous conclusions that Cu acquisition is controlled by the concentration of organically complexed Cu instead of free  $\text{Cu}^{2+}$  (Hudson 1998, Quigg et al. 2006, Annett et al. 2008, Guo et al. 2010). In the study

of Hudson (1998) and Quigg et al. (2006), the observed Cu uptake rates in diverse marine phytoplankton were faster than the diffusive flux of inorganic Cu, indicating possible availability of organically complexed Cu. In our more recent study on Cu uptake kinetics (Guo et al. 2010), the short-term Cu uptake rates by diatoms, cultured in the presence of EDTA, also indicated Cu acquisition from organic Cu complexes. It has been demonstrated that cupric reductase activity exists at the cell surface of some marine phytoplankton (Jones et al. 1987). Thus, Cu dissociation from organic ligands mediated by cupric reductase may also be involved in Cu uptake by marine phytoplankton as observed in other eukaryotes (Hill et al. 1996, Puig et al. 2007). Hence, total Cu concentration in the sea may be a better indicator of Cu availability than free  $\text{Cu}^{2+}$ .

## 2.5 Conclusions

This study investigated the interaction between Fe and Cu nutrition in a diverse group of phytoplankton [comprising 12 species, from 4 phyla and 2 marine environments (coastal versus oceanic)] by examining growth rates, Cu:C quotas and steady-state Cu uptake rates under various Fe/Cu conditions. Our results highlight a complex physiological interaction between these two metals in marine phytoplankton. Nevertheless, the data point to some interesting trends. Despite the fact that the Cu:C ratios do not support our hypothesis of higher Cu requirements of oceanic species than coastal species, there are 5 independent lines of evidence supporting a more important role of Cu in the physiology of the oceanic than coastal phytoplankton. The mixed-effect model, which also includes the diatom data from Annett et al (2008), indicated that there was a significant Cu effect

on the growth rates and steady-state Cu uptake rates of the oceanic strains only. In addition, lowering the total Cu concentration in the media five fold decreased the Cu quotas and steady-state Cu uptake rates of the oceanic strains to a greater extent (5.5 and 5.4 fold, respectively) than those of the coastals (3.8 and 4.7 fold, respectively). Fe limitation had also only a significant effect on the Cu quotas of the oceanic strains, and a significant interaction between Cu and Fe was only found for the Cu: C ratios and steady-state Cu uptake rates of the oceanic strains. Thus, these combined findings suggest that oceanic phytoplankton are more sensitive to low Cu availability than coastal strains.

As expected, low Cu concentrations significantly reduced the steady-state Cu uptake rates and Cu:C quotas of most phytoplankton but these decreases matched the decline in total Cu concentration, and not the free  $\text{Cu}^{2+}$ , in the growth media. However, contrary to our predictions, in general, Fe limitation decreased the steady-state Cu uptake rates and Cu use efficiency of most phytoplankton. Thus, our hypothesis that Cu plays a role in the high-affinity Fe transport system of Fe limited phytoplankton is not supported by the data. The only Cu quotas that were significantly increased under Fe limitation were those of the coastal *Synechococcus*, the coastal *Chrysochromulina* strains (Table 2.6 and Table 2.4) and the oceanic diatom, *Thalassiosira oceanica* 1003 (Table 2.6). Thus, the hypothesized role of Cu in Fe transport may not be universal among Fe limited phytoplankton.

The phylogenetic trends were less evident than the oceanic-coastal trends suggesting that availability of Fe and Cu in the modern ocean (coastal vs. oceanic environment) are a strong determinant of the Cu stoichiometry of marine phytoplankton. The ten phytoplankton studied here often appear as common and dominant species in the sea and some are also harmful species (reviewed by Waterbury et al. 1986, Edvardsen and

Paasche 1998, Hamm 2000, Paasche 2001, Heil et al. 2005). The findings in this study are a first step towards understanding how the interaction between Fe and Cu availability in the ocean control marine phytoplankton composition and productivity.

## **Chapter 3**

### **Copper uptake kinetics of coastal and oceanic diatoms**

### 3.1 Introduction

Copper (Cu) is an essential micronutrient for phytoplankton and plays an important role as a cofactor of electron-transfer proteins, such as cytochrome oxidase in the respiratory chain reaction and superoxide dismutase in the detoxification of reactive oxygen species (reviewed by Raven et al. 1999, Merchant et al. 2006). Most recently, Cu has been shown to be involved in the high-affinity iron (Fe) transport system of coastal and oceanic diatoms (Maldonado et al. 2006), as previously shown in *Chlamydomonas* and yeast (Askwith et al. 1994, La Fontaine et al. 2002). In addition to these basic Cu demands of marine diatoms, it has been demonstrated that oceanic diatoms have higher Cu requirements than coastal strains, possibly due to the replacement of Fe-containing enzymes by Cu-containing equivalents (Annett et al. 2008). For example, in *Thalassiosira oceanica*, the Cu-containing enzyme plastocyanin—which is found in all higher plants, green algae and some blue-green algae—replaces the Fe-containing enzyme, cytochrome  $c_6$ , in photosynthesis (Peers & Price 2006). This replacement lowers Fe demand by 10%, and may partly explain the success of oceanic phytoplankton in open ocean waters, where Fe concentrations are too low to support the growth of coastal isolates (Peers & Price 2006). Conversely, Cu is considered toxic and can damage a cell when the intracellular Cu content is excessive (Rueter et al. 1979, Moffett et al. 1997, Sunda & Huntsman 1998c, Raven et al. 1999). Thus, the mechanisms of intracellular Cu homeostasis—controlling Cu uptake, intracellular distribution, utilization, and detoxification—have been the subject of considerable interest in yeast, higher plants, and freshwater microalgae (Clemens 2001, Puig & Thiele 2002, Merchant et al. 2006). As of yet, there is little information on the mechanisms of Cu internalization and homeostasis in marine phytoplankton.

As observed for other trace elements, the concentration of Cu in the sea tends to increase from open ocean to coastal waters (Boyle et al. 1981, Rutgers van der Loeff et al. 1997). Total dissolved Cu concentrations in non-polluted surface open ocean waters range from 0.5 to 6 nM, with an average concentration of 2 nM (Coale & Bruland 1988, Jickells & Burton 1988, Moffett 1995, Rutgers van der Loeff et al. 1997, Moffett & Dupont 2007). In comparison, Cu concentrations in coastal waters range from 2-150 nM (Sunda et al. 1990, Moffett et al. 1997, Buck et al. 2007) depending on varying degrees of contamination by anthropogenic Cu sources. In natural seawater, dissolved Cu species include free  $\text{Cu}^{2+}$  ions, inorganic complexes, and organic Cu complexes, though organic complexation dominates. Indeed, up to 99.8% of dissolved Cu is bound to the strong organic ligand class (L1) in the open ocean (Coale & Bruland 1988, 1990) and in coastal waters (Buck et al. 2007). In addition, changes in Cu speciation in coastal waters may be observed seasonally due to variations in phytoplankton community composition (Croot 2003) or regionally due to the absence of strong organic ligands (Moffett et al. 1997). Due to the difference in Cu concentrations in the open ocean and in coastal waters, Cu uptake mechanisms of phytoplankton inhabiting these contrasting environments may also vary.

Many studies have investigated Cu uptake kinetics and transport in yeast (reviewed by Puig and Theile 2002, Kim et al. 2008) and freshwater green algae (reviewed by Merchant et al. 2006). In yeast, high-affinity and low-affinity Cu transport systems have been identified (Dancis et al. 1994a, Hassett et al. 2000). The high-affinity system is energy dependent and specific for  $\text{Cu}^+$  over other metal ions (Lin & Kosman 1990, Dancis et al. 1994a); its  $K_m$  is  $\sim 4 \mu\text{M}$  dissolved Cu (DeRome & Gadd 1987, Lin & Kosman 1990, Dancis et al. 1994a). In contrast, *Chlamydomonas* only exhibits a high-

affinity Cu transport system, with an invariant  $K_m$  of 0.2  $\mu\text{M}$  dissolved Cu and a variable  $V_{\text{max}}$  depending on Cu availability during growth (Hill et al. 1996). These studies illustrate the variety of microbial Cu transport pathways and physiological responses to Cu availability.

In this study, we investigated the short-term Cu uptake kinetics of one oceanic diatom, *T. oceanica*, and one coastal diatom, *T. pseudonana*, grown under various non-toxic Fe and Cu levels. Our goal was to investigate the existence of a low- and a high-affinity Cu transport system in these organisms and determine what controls the substrate affinity and maximum transport velocity. Historically, the lack of suitable Cu radiotracers has posed a significant limitation to the study of Cu transport kinetics. Through a collaboration with the Canadian National Particle and Nuclear Physics Laboratory at Tri-University Meson Facility campus (TRIUMF) in Vancouver, BC, we have gained access to a regular supply of the short-lived  $^{64}\text{Cu}$  and  $^{67}\text{Cu}$  isotopes. The use of these isotopes in short-term uptake experiments allowed us to do extensive research on Cu uptake that would be very difficult to obtain with other methods.

## **3.2 Materials and methods**

### **3.2.1 Study organisms**

Two centric diatoms, *T. oceanica* (CCMP 1003) and *T. pseudonana* clone 3H (CCMP1335), isolated from oceanic and coastal environments, respectively, were used in this study. Cultures were obtained from the Bigelow Laboratory for Ocean Sciences,

West Boothbay Harbor, ME, USA. The mean cell diameters of *T. oceanica* and *T. pseudonana* grown under non-limiting trace metal conditions were ~ 6.5 and 4.6  $\mu\text{m}$ , respectively.

### **3.2.2 Media and culture manipulations**

Axenic diatoms were grown as semi-continuous batch cultures in the chemically well-defined artificial seawater medium AQUIL (Price et al. 1989) at  $19 \pm 1^\circ\text{C}$ . To eliminate circadian rhythms of phytoplankton when grown under a day-night light cycle, our cultures were grown under continuous illumination with cool-white fluorescent lights ( $150 \mu\text{mol} \cdot \text{quanta} \cdot \text{m}^{-2} \cdot \text{s}^{-1}$ , Sylvania, Mississauga, Canada), allowing us to monitor and execute experiments at any time of day.

Except for the addition of Fe and Cu, the AQUIL medium used in this study was identical in chemical composition to that described by Maldonado et al. (2006). Four culture media treatments were prepared for each species with various additions of Fe and/or Cu (Table 3.1). Sterile, trace metal clean techniques were used during all experiments and manipulations.

Table 3.1 Culture media with various Fe and Cu additions. The units of concentration were nM. Metals were added bound to 100  $\mu$ M EDTA. MINEQL + 4.61 (Environmental Research Software) was used to calculate free metal concentrations ( $pM = -\log [M^+]$ ). In these calculations we included the Cu contamination of our media (1 nM Cu, Maldonado et al. 2006).

	<i>T. oceanica</i>		<i>T. pseudonana</i>	
	[Fe] <sub>total</sub> (pFe)	[Cu] <sub>total</sub> (pCu)	[Fe] <sub>total</sub> (pFe)	[Cu] <sub>total</sub> (pCu)
Fe replete/Cu replete	1370 (19)	11.2 (14.1)	1370 (19)	11.2 (14.1)
Fe replete/Low Cu	1370 (19)	1.0 ( 15.1 )	1370 (19)	1.0 ( 15.1 )
Fe limited/Cu replete	1.28 (22)	11.2 (14.1)	12.5 (21)	11.2 (14.1)
Fe limited/Low Cu	1.28 (22)	2.96 (14.8)	12.5 (21)	1 ( 15.1 )

### 3.2.3 Determination of growth rates and cell sizes

Cells were acclimated to various Fe and/or Cu culture conditions in 28 mL polycarbonate tubes. In vivo fluorescence was measured daily with a Turner 10-AU Fluorometer (Turner Designs, Sunnyvale, CA, USA). The ln of fluorescence versus time was used to calculate growth rates ( $d^{-1}$ ). Cultures were considered acclimated when growth rates of five successive transfers varied by less than 15% (Brand et al. 1981). For the Cu uptake kinetic experiments, acclimated cultures in mid-exponential phase were transferred from 28 mL tubes to 2 L bottles. The growth rates of the diatoms in these bottles were monitored daily. Cell density and size ( $\mu$ m) were also determined for live samples using a Coulter Z2 Particle Count and Size Analyzer (Beckman Coulter Inc., Brea, CA, USA). Cell surface area ( $\mu$ m<sup>2</sup>) and volume ( $fL = 10^{-15}$  L) were calculated assuming a spherical cell shape.

### 3.2.4 Measurement of Cu uptake rates

For all experiments, 2L cultures of various Cu/Fe treatments were grown as indicated above. The non-radioactive Cu and a spike of the carrier-free tracer  $^{67}\text{Cu}$  ( $0.32 \text{ MBq L}^{-1}$ ) were buffered with  $100 \mu\text{M}$  EDTA in 125 mL chelexed synthetic ocean water (SOW) containing  $100 \mu\text{M}$  Si,  $10 \mu\text{M}$  P, and no  $\text{NO}_3^-$ , trace metals, or vitamins. Given that EDTA is often used as a ligand in phytoplankton culture media, EDTA was chosen for these experiments. The gamma-emitting radionuclide  $^{67}\text{Cu}$  ( $t_{1/2} = 62 \text{ h}$ ) was produced at TRIUMF. Different Cu concentrations were added depending on the experiments (see below). After the Cu and EDTA additions, the media had a pH of 8.1 and was allowed to equilibrate chemically for at least 12 hours before use. The next day, trace metal clean techniques were used to filter 250 mL aliquots of mid-log phase 2 L culture onto trace metal clean  $2 \mu\text{m}$  polycarbonate (Poretics, 24 hours acid-soaked) filters (47 mm) by gentle vacuum ( $<100 \text{ mm Hg}$ ) and washed with 10 mL chelexed SOW. Each filter was immediately resuspended in 125 mL of seawater containing the desired experimental ratio of  $^{67}\text{Cu}$  to non-radioactive Cu concentration/treatment. Though short-term Cu uptake by marine phytoplankton is not a light-dependent process (Gnassia-Barelli and Hardstedt-Romeo, 1982), the cells were incubated at room temperature and exposed to  $150 \mu\text{mol} \cdot \text{quanta} \cdot \text{m}^{-2} \cdot \text{s}^{-1}$  after the resuspension. The initial sampling time was 10 minutes after resuspension, followed by 15-30 minute sampling intervals. 25 mL aliquots of culture were removed during each sampling interval. Cells were vacuum filtered onto a  $2 \mu\text{m}$  25 mm polycarbonate membrane. The filtered cells were soaked for 5 minutes with 5 mL of 1 mM diethylenetriaminepentaacetic acid (DTPA) solution (dissolved in sterile SOW, pH adjusted to 8.14; Croot et al. 1999) to bind the extracellular adsorbed  $^{67}\text{Cu}$ , then washed with 5 mL SOW. The radioactive filters were placed in scintillation vials;

radioactivity was determined using a PerkinElmer 1480 WIZARD 3'' Gamma Counter (PerkinElmer Inc., Waltham, MA, USA). Duplicate initials (1 mL) of the uptake medium were also taken to determine the specific activity of  $^{67}\text{Cu}$  in the uptake media (MBq  $^{67}\text{Cu}/\text{Cu}$  concentration added). At the end of each  $^{67}\text{Cu}$  uptake experiment, a sample was fixed with Lugol's solution to determine cell density using the Coulter Z2 Particle Count after the  $^{67}\text{Cu}$  had decayed. The Cu uptake rates ( $\text{zmol} \cdot \mu\text{m}^{-2} \cdot \text{h}^{-1} = 10^{-21} \text{mol} \cdot \mu\text{m}^{-2} \cdot \text{h}^{-1}$ ) for each Cu concentration were determined by linear regressions of the accumulation of Cu as a function of time and were normalized to cell surface area.

To determine the optimal duration for the  $^{67}\text{Cu}$  uptake experiments, initial experiments were performed for up to 6 hours with Fe-replete *T. pseudonana* cultures. The results (data not shown) indicated that during the first two hours, cellular Cu increased linearly. Thus, the sampling time for Cu uptake experiments was limited to two hours.

### **3.2.5 Cu uptake kinetic parameters for cells grown under various Fe and/or Cu levels**

Sixteen (2, 10, 30, 60, 80, 100, 120, 150, 180, 240, 300, 500, 700, 1000, 1500, and 2000 nM; Figure 3.1) or eight (2, 30, 60, 120, 240, 500, 1000, and 2000 nM; Figure 3.2) Cu concentrations were used in the Cu uptake kinetic experiments. For each growth treatment, two independent cultures were grown. Rates of Cu uptake for all Cu concentrations tested were measured for both duplicate cultures, from which a mean Cu uptake rate ( $\text{zmol} \cdot \mu\text{m}^{-2} \cdot \text{h}^{-1}$ ) was calculated. These mean Cu uptake rates were used to calculate the  $V_{\text{max}}$  and  $K_{\text{m}}$  of each growth treatment, using the Michaelis–Menten equation (see Results) and the statistical program SigmaPlot 10.0 (Systat Software Inc. San Jose, CA, USA). The standard errors associated with the  $V_{\text{max}}$  and  $K_{\text{m}}$  parameters are

the standard errors from the best-fit values. A t-test (TDIST) was used to compare the effect of Cu or Fe on various treatments. The effects of Cu and Fe and its interaction (ANOVA) were investigated only for the low-affinity Cu transport system of *T. oceanica*, since this was the only transport system active in all Cu/Fe treatments.

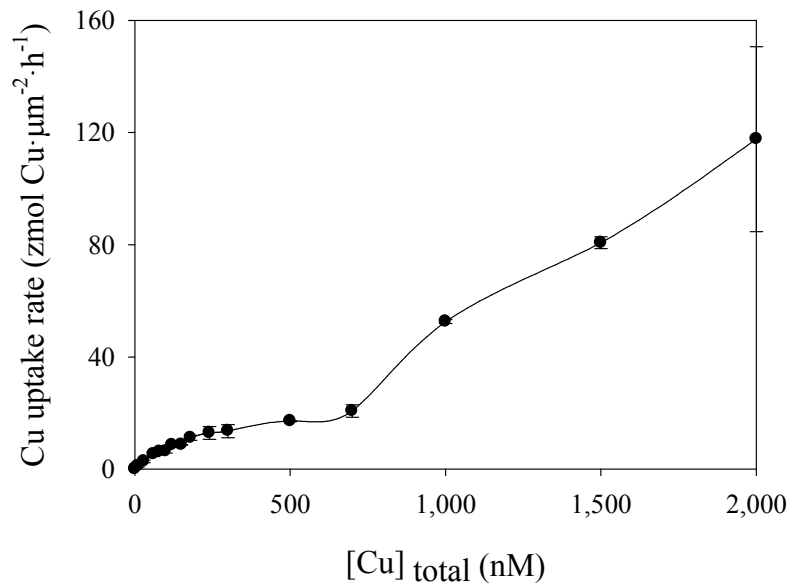


Figure 3.1 Kinetics of Cu uptake as a function of total Cu concentrations in Fe and Cu replete *T. pseudonana*. The rates of Cu uptake ( $\text{zmol} \cdot \mu\text{m}^{-2} \cdot \text{h}^{-1} = 10^{-21} \text{ mol} \cdot \mu\text{m}^{-2} \cdot \text{h}^{-1}$ ) were determined as described in Materials and Methods. The data points are the means of Cu uptake rates of duplicate cultures and the error bars represent the range. In these experiments, the EDTA concentration was kept constant at 100  $\mu\text{M}$  while the Cu concentrations were varied.

### 3.3 Results

#### 3.3.1 Cellular characteristics

*T. oceanica* and *T. pseudonana* were acclimated to different Fe and Cu concentrations (Table 3.1). Fe limitation significantly decreased (ANOVA,  $p < 0.001$ ) cell growth rate ( $d^{-1}$ ), surface area ( $\mu m^2$ ), and volumes (fL). In contrast, the effects of Cu availability were only obvious (ANOVA,  $p < 0.05$ ) on the cell surface area and volume of *T. oceanica* (Table 3.2), and showed a surprising increase with low Cu availability.

Table 3.2 Cellular characteristics (mean  $\pm$  SD) of live *T. oceanica* and *T. pseudonana* grown under different Fe and Cu levels. For specific Fe and Cu concentration and pMe in each medium, see Table 3.1 ( $d^{-1} = \text{day}^{-1}$ ;  $fL = \mu m^3 = 10^{-15} L$ ; n is the number of replicates).

	Treatment	Growth Rate ( $d^{-1}$ ) (n)	Cell surface area ( $\mu m^2$ )	Cell volume (fL)
<i>T. oceanica</i>	Fe replete/Cu replete	0.80 $\pm$ 0.09 (9)	85.62 $\pm$ 0.02	74.49 $\pm$ 0.03
	Fe replete/Low Cu	0.73 $\pm$ 0.10 (9)	139.31 $\pm$ 0.36	154.61 $\pm$ 0.59
	Fe limited/Cu replete	0.51 $\pm$ 0.10 (9)	59.37 $\pm$ 0.67	43.01 $\pm$ 0.73
	Fe limited/Low Cu	0.48 $\pm$ 0.08 (9)	70.60 $\pm$ 0.74	55.78 $\pm$ 0.88
<i>T. pseudonana</i>	Fe replete/Cu replete	1.79 $\pm$ 0.14 (8)	68.80 $\pm$ 1.30	53.67 $\pm$ 1.47
	Fe replete/Low Cu	1.75 $\pm$ 0.15 (5)	70.29 $\pm$ 0.00	55.41 $\pm$ 0.00
	Fe limited/Cu replete	0.82 $\pm$ 0.09 (9)	41.85 $\pm$ 0.40	25.46 $\pm$ 0.34
	Fe limited/Low Cu	0.73 $\pm$ 0.18 (5)	48.23 $\pm$ 1.30	31.50 $\pm$ 1.22

### 3.3.2 Kinetics of Cu transport

At Cu concentrations ranging from 2-500 nM, cellular Cu accumulation ( $\text{zmol } \mu\text{m}^{-2}$ ) in *T. oceanica* and *T. pseudonana* increased linearly as a function of time in the course of 2 hours (data not shown). Sixteen Cu concentrations (2, 10, 30, 60, 80, 100, 120, 150, 180, 240, 300, 500, 700, 1000, 1500, and 2000 nM) were first used in the Cu uptake kinetic experiments. For these initial experiments, *T. pseudonana* grown under Fe and Cu replete condition was used as a model. The Cu uptake rates ( $\text{zmol} \cdot \mu\text{m}^{-2} \cdot \text{h}^{-1}$ ) were a function of Cu concentrations and followed Michaelis-Menten uptake kinetics, approaching saturation at  $\sim 250$  nM Cu (Figure 3.1). Interestingly, the Cu uptake kinetics at these Cu concentrations clearly indicated that Cu uptake is biphasic (Figure 3.1). Considering the limitation of the radioactivity of  $^{67}\text{Cu}$  we can manipulate, in the rest of the Cu uptake kinetic experiments only eight Cu concentrations (2, 30, 60, 120, 240, 500, 1000, and 2000 nM) were chosen. Based on the statistical analysis, five out of eight treatments (graphs with inserts, Figure 3.2) also exhibited biphasic Michaelis-Menten kinetics of Cu uptake as a function of Cu concentration (Figure 3.2, Table 3.3). The first phase was observed at low Cu concentrations ( $\sim 0 - 500$  nM, see inserts) while the second phase was observed at higher Cu concentrations (up to 2000 nM). This biphasic uptake saturation kinetic pattern was assumed to reflect the simultaneous operation of a high-affinity and a low-affinity uptake system at low and high Cu concentrations, respectively (Knauer et al. 1997). Thus, a biphasic Cu uptake kinetic curve was fitted to our data using a Double Rectangular Hyperbola equation  $[V = V_{\text{max}1} [\text{Cu}]_{\text{total}} / ([\text{Cu}]_{\text{total}} + K_{\text{m}1}) + V_{\text{max}2} [\text{Cu}]_{\text{total}} / ([\text{Cu}]_{\text{total}} + K_{\text{m}2})]$  (Nissen 1991) (Table 3.3), where  $V$  is the total Cu uptake rate ( $\text{zmol Cu} \cdot \mu\text{m}^{-2} \cdot \text{h}^{-1}$ ),  $V_{\text{max}1}$  and  $V_{\text{max}2}$  are the maximum uptake rates of the two uptake systems,

[Cu]<sub>total</sub> is the total copper concentration, and  $K_{m1}$  and  $K_{m2}$  are the half-saturation constants of the two uptake systems. According to these analyses (Table 3.3), the  $K_m$  values were 50-, 870- and 21-fold lower for the high-affinity Cu transport system compared to the low-affinity Cu transport system in Fe/Cu replete, Fe replete/low Cu *T. oceanica* and Fe limited/low Cu *T. pseudonana*, respectively. For these same cultures, the  $V_{max}$  values were also lower by 3.3-, 183- and 13-fold, respectively, for the high-affinity Cu transport system. Fe/Cu replete and Fe-replete/low Cu *T. pseudonana*, also exhibited two Cu transport systems. However, the low-affinity uptake system did not saturate and as a result, the data could not be fitted by the Double Rectangular Hyperbola equation. In addition, the  $K_m$  of the high and low transport systems were identical in some cases (i.e. Fe limited/Cu replete and Fe limited/low Cu of *T. oceanica* and Fe limited/Cu replete *T. pseudonana*), so we assumed that only one transport system was active. Given the high  $K_m$  values (~ 1000 nM), we classified these Cu transport systems as low-affinity.

Figure 3.2 (next page) Michaelis-Menten kinetics of Cu uptake as a function of total Cu concentrations in *T. oceanica* and *T. pseudonana* cultured under different Cu and Fe levels (see Table 3.1). The rates of Cu uptake ( $\text{zmol} \cdot \mu\text{m}^{-2} \cdot \text{h}^{-1} = 10^{-21} \text{ mol} \cdot \mu\text{m}^{-2} \cdot \text{h}^{-1}$ ) were determined as described in Materials and Methods. The data points are the means of Cu uptake rates of duplicate cultures, curves are the line of best fit for the Double Rectangular Hyperbola equation. In these experiments, the EDTA concentration was kept constant at 100  $\mu\text{M}$  while the Cu concentrations were varied.

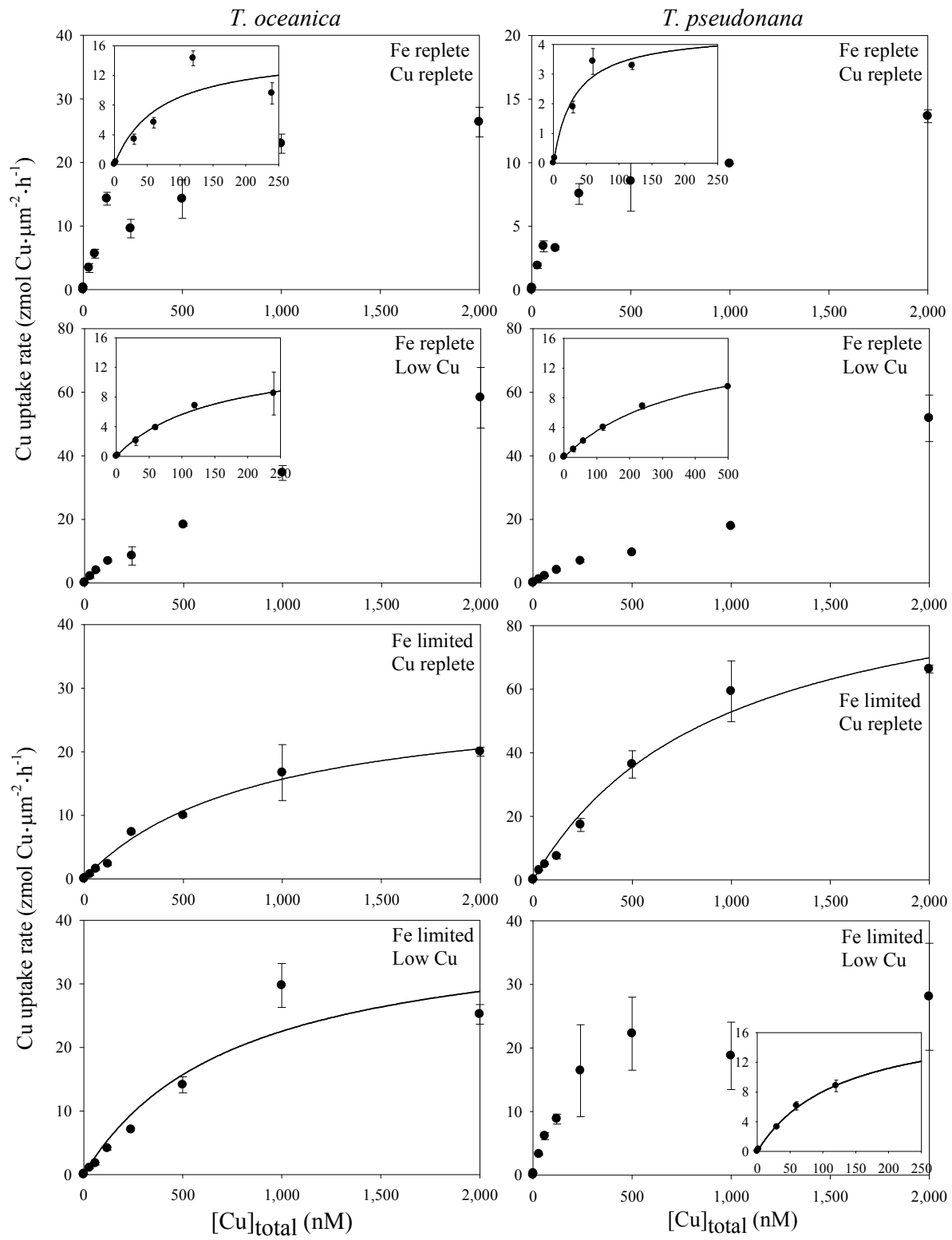


Table 3.3 Kinetic parameters of the high- and low-affinity Cu transport system in *T. oceanica* and *T. pseudonana* grown under various Fe and Cu levels. The  $K_m$  and  $V_{max}$  values ( $\pm$  standard error of best-fit value) were calculated for the mean Cu uptake rates of duplicate independent cultures measured at Cu concentrations ranging from 0 to 2000 nM. The high- and low-affinity uptake system parameters were calculated using the double Michaelis-Menten equation [ $V = V_{max1} [Cu]_{total} / ([Cu]_{total} + K_{m1}) + V_{max2} [Cu]_{total} / ([Cu]_{total} + K_{m2})$ ].  $R^2$  is the regression coefficient of the Michaelis-Menten equation fit to the data. For specific Fe and Cu concentration and pMe in each medium, see Table 3.1.

		Low-affinity		High-affinity			
Treatment		$K_m$ (nM)	$V_{max}$ ( $z\text{mol Cu} \cdot \mu\text{m}^{-2} \cdot \text{h}^{-1}$ )	$K_m$ (nM)	$V_{max}$ ( $z\text{mol Cu} \cdot \mu\text{m}^{-2} \cdot \text{h}^{-1}$ )	Cu range (nM)	$R^2$
<i>T. oceanica</i>	Fe replete/Cu replete	2410 $\pm$ 8335	36 $\pm$ 48	48 $\pm$ 110	11 $\pm$ 13	0-2000	0.9422
	Fe replete/Low Cu	6336 $\pm$ 2253	238 $\pm$ 63	7.3 $\pm$ 32	1.3 $\pm$ 1.1	0-2000	0.9985
	Fe limited/Cu replete	879 $\pm$ 156	29 $\pm$ 2.4			0-2000	0.9901
	Fe limited/Low Cu	771 $\pm$ 383	40 $\pm$ 8.9			0-2000	0.9252
<i>T. pseudonana</i>	Fe replete/Cu replete	NA, did not saturate at 2000 nM		188 $\pm$ 48	12 $\pm$ 1.1	0-1000	0.9710
	Fe replete/Low Cu	NA, did not saturate at 1000 and 2000 nM		373 $\pm$ 41	17 $\pm$ 1.0	0-500	0.9977
	Fe limited/Cu replete	923 $\pm$ 222	101 $\pm$ 11			0-2000	0.9828
	Fe limited/Low Cu	1117 $\pm$ 525	63 $\pm$ 4.9	52 $\pm$ 129	4.8 $\pm$ 7.8	0-2000	0.9971

### 3.3.3 Low-affinity Cu uptake kinetics

*T. oceanica* and *T. pseudonana* had significantly different low-affinity Cu uptake kinetics under Fe replete conditions, but similar kinetics under Fe limitation (Figure 3.2, Table 3.3). When Fe was sufficient, Cu uptake by *T. pseudonana* did not saturate. In contrast, Fe sufficient *T. oceanica* exhibited saturating uptake kinetics. When Fe was limiting, both *T. oceanica* and *T. pseudonana* had similar  $K_m$ , ( $\sim 1\mu\text{M}$ ) and  $V_{\max}$  (30 & 100  $\text{z mol Cu} \cdot \mu\text{m}^{-2} \cdot \text{h}^{-1}$ , respectively). These results indicate that the low-affinity Cu transport system of *T. oceanica* and *T. pseudonana* had different responses to Fe availability. Statistical analyses ( $p < 0.05$ , ANOVA and TDIST) indicate that Cu availability in the growth media had no significant effect on the  $K_m$  of the low-affinity Cu transport system in *T. oceanica* and *T. pseudonana* (Table 3.4). Meanwhile, low Cu availability had a significant effect on the  $V_{\max}$  of low-affinity Cu uptake by *T. oceanica* ( $p = 0.012$ , ANOVA, Table 3.4) when Fe availability was high (6.5-fold faster for low Cu cultures), and by *T. pseudonana* ( $p = 0.007$ , TDIST, Table 3.4) when Fe was limiting (2-fold slower for cultures grown under low Cu concentration). Fe limitation significantly affected only the  $V_{\max}$  of low-affinity Cu transport in *T. oceanica* grown under low Cu availability ( $p = 0.015$ , ANOVA, Table 3.4), where the  $V_{\max}$  of Fe limited culture was 6-fold slower than that of the Fe replete cultures. Fe also had a significant effect on the low-affinity Cu transport system in *T. pseudonana* (Table 3.3), although we were unable to obtain robust fits to the data to compare the  $K_m$  and  $V_{\max}$  values statistically. The Cu uptake in Fe replete *T. pseudonana* was not saturated at 1000 or 2000 nM Cu compared to Fe limited treatments.

### 3.3.4 High-affinity Cu uptake kinetics

*T. oceanica* and *T. pseudonana* had different  $K_m$  and  $V_{\max}$  kinetics for the high-affinity Cu transport system depending on the Fe and Cu availability (Figure 3.2, Table 3.3). When Fe and Cu were sufficient, both of these diatoms had similar  $K_m$  ( $\sim 50\text{-}200\text{ nM}$ ) and  $V_{\max}$  ( $\sim 10\text{-}12\text{ z mol} \cdot \mu\text{m}^{-2} \cdot \text{h}^{-1}$ ). For cultures grown under low Cu, *T. oceanica* had a

lower half-saturation constant (51-fold lower  $K_m$ ,  $p < 0.0001$ , TDIST) and a slower maximum rate of Cu uptake (13-fold lower  $V_{max}$ ,  $p < 0.0001$ , TDIST) than *T. pseudonana*. Moreover, when Fe was limiting, the high-affinity Cu transport system seemed to disappear in *T. oceanica* and in Cu replete *T. pseudonana*. Within the error of the estimates (Table 3.4), Cu availability had no significant effect on the  $K_m$  and  $V_{max}$  of high-affinity Cu transport system in *T. oceanica*. However, low Cu significantly increased  $K_m$  and  $V_{max}$  ( $p = 0.010$  and  $0.005$ ) in Fe replete *T. pseudonana* (Fe replete/low Cu vs. Fe replete/Cu replete, Table 3.4). Fe limitation had significant effects on the high-affinity Cu uptake kinetics of both species (Table 3.4). When Fe concentration was low, the high-affinity Cu transport system in *T. oceanica* was down-regulated (turned off). Similarly, Fe limitation turned off the high-affinity transport system of *T. pseudonana* when Cu was replete. In contrast, Fe-limitation up-regulated the high-affinity of *T. pseudonana* when Cu was low by decreasing its  $K_m$  by  $\sim 7$ -fold ( $p=0.031$ , Table 3.4).

Table 3.4 Effects (p-value, TDIST and two-way ANOVA) of Cu availability, Fe availability and the interaction between Fe and Cu availability on  $K_m$  and  $V_{max}$  of the low- and high-affinity Cu transport system in *T. oceanica* and *T. pseudonana*. For specific Fe and Cu concentration and pMe in each medium, see Table 3.1.

	Species	Treatment	Kinetic parameter	Metal effect	p-value	Statistics
High-affinity	<i>T. pseudonana</i>	Fe replete/Cu replete	$K_m$	Cu	0.010	TDIST
		vs. Fe replete/Low Cu	$V_{max}$	Cu	0.005	
		Fe replete/Low Cu	$K_m$	Fe	< 0.0001	TDIST
		vs. Fe limited/Low Cu				
Low-affinity	<i>T. pseudonana</i>	Fe limited/Cu replete	$V_{max}$	Cu	0.007	TDIST
		vs. Fe limited/Low Cu				
	<i>T. oceanica</i>	All treatments	$V_{max}$	Fe	0.015	Two-way
				Cu	0.012	ANOVA
				Fe&Cu	0.023	

## 3.4 Discussion

### 3.4.1 Cu uptake kinetics of phytoplankton

The Michaelis-Menten kinetics of Cu uptake by the centric diatoms *T. oceanica* and *T. pseudonana* seem to follow biphasic kinetics when cells are exposed to total Cu concentrations ranging from 2 to 2000 nM. Biphasic uptake kinetics are usually ascribed to the presence of two uptake systems, a high- and a low-affinity uptake system operating simultaneously (Epstein et al. 1963, Komor & Tanner 1975). These uptake kinetics have been reported in many organisms for various substrates, including sugar transport in the green alga *Chlorella* (Komor & Tanner 1975), nitrate uptake by marine phytoplankton (Collos et al. 1997), glucose transport by fungi (Schneide & Wiley 1971), and Cu and phosphate uptake by higher plants (Austenfeld & Veltrup 1983, Perez-Llorens & Niell 1995). For Cu transport, two uptake systems have been found in the freshwater green alga, *Scenedesmus subspicatus* (Knauer et al. 1997), where the  $K_m$  of the low-affinity and high-affinity Cu transport systems are 2.82 pM and 0.07 pM of free  $\text{Cu}^{2+}$ , respectively. In the present study, the  $K_m$  of the low- and high-affinity Cu transport system for *T. oceanica* grown under Fe/Cu sufficient conditions are 2410 nM and 48 nM total Cu, respectively, thus differing by 50-fold. If these  $K_m$  values expressed as total Cu concentrations, are converted to free  $\text{Cu}^{2+}$  concentrations (using the side reaction coefficient and conditional thermodynamic constant of CuEDTA reported in Sunda et al. 2005), the resulting  $K_m$  are 1.84 pM and 0.04 pM, respectively. These  $K_m$  values are very similar to those values of *S. subspicatus*. The  $K_m$  value of the high-affinity Cu transport system in *T. pseudonana* is also low, 188 nM (0.14 pM expressed in free  $\text{Cu}^{2+}$ ), but 3.5- and 2-fold higher than the  $K_m$  of *T. oceanica* and *S. subspicatus*, respectively. The Cu transport kinetics of the diatoms in this study are also different from that of the green algae *C. reinhardtii* (Hill et al. 1996). In *C. reinhardtii*, only one temperature-dependent Cu transport system has been found, with a  $K_m$  of ~210 nM total Cu (Hill et al. 1996). Furthermore, Michaelis-Menten Cu uptake kinetics have been determined for a limited set of marine phytoplankton by Croot et al. (2003). A similar Cu transport pathway exists

in a cyanobacterium and a dinoflagellate. The  $K_m$  of the cyanobacteria *Synechococcus* sp. DC2 and the dinoflagellate *Amphidinium carterae* were  $\sim 15.5$  pM and  $39.8$  pM free  $\text{Cu}^{2+}$ , respectively. These high  $K_m$  values are characteristic of low-affinity Cu transport systems. However, it is important to note that Croot et al. (2003) did not conduct the Cu uptake experiments with cultures grown at the low Cu concentration used in our study and that of Knauer (1997). Assuming that the  $K_m$  reported by Croot et al. (2003) are those of a low-affinity Cu transport system, the low-affinity Cu transport system of our diatom *T. oceanica* has higher affinity for Cu (8- or 22-fold lower  $K_m$ ) than those of *Synechococcus* and *Amphidinium*.

The  $V_{\max}$  of low- and high-affinity Cu transport systems are also normally different. In general, the low  $K_m$  of a high-affinity transport system results in a slower  $V_{\max}$  (Raymont 1980, Kajikawa et al. 1997, Persson et al. 2000). In *S. subspicatus*, the  $V_{\max}$  of high-affinity Cu transport system is 28-fold lower than that of the low-affinity Cu transport system (Knauer et al. 1997). In the diatoms *T. oceanica* and *T. pseudonana*, the mean difference between  $V_{\max}$  of the high-affinity and low-affinity transport system is  $\sim 90$ -fold, but range from 3- to 182-fold.

Quigg et al. (2006) measured the short-term Cu accumulation rate by *T. pseudonana* in natural sea water (Sandy Hook seawater) with  $28$  pM Cu'. Their Cu uptake rate,  $546$   $\text{zmol Cu} \cdot \text{um}^{-2} \cdot \text{h}^{-1}$  ( $9.1$   $\text{zmol Cu} \cdot \text{um}^{-2} \cdot \text{min}^{-1}$ , Quigg et al. 2006), is higher than that reported here ( $13.7$   $\text{zmol Cu} \cdot \text{um}^{-2} \cdot \text{h}^{-1}$ ) for Fe/Cu replete *T. pseudonana* at  $2000$  nM total Cu (with  $25$  pM Cu'). This 40-fold difference may be due to a disparity in intracellular Fe and Cu concentrations between the *T. pseudonana* cultures and/or the sampling time for the determination of Cu uptake rates. In Quigg et al. (2006) study, *T. pseudonana* was acclimated in Aquil medium with  $84$  nM dissolved Fe, whereas we used  $1370$  nM dissolved Fe for the Fe replete culture and  $12.5$  nM for the Fe limited ones. In addition, while our sampling time was 2 hours, that of Quigg et al. was only 20 minutes. Indeed, if we calculate Cu uptake rates for only the first time point (15 minutes), our Cu uptake rate of the Fe limited/Cu replete *T. pseudonana* ( $537$   $\text{zmol Cu} \cdot \text{um}^{-2} \cdot \text{h}^{-1}$ , measured at  $2000$

nM total Cu, or 25 pM Cu') is almost identical to that measured by Quigg et al. (546 zmol Cu ·  $\mu\text{m}^{-2}$  · h<sup>-1</sup>).

### 3.4.2 *T. oceanica* versus *T. pseudonana* Cu uptake kinetics.

Though the data presented here suggest that *T. oceanica* and *T. pseudonana* have both a low and a high-affinity Cu transport system, there were distinct differences between these two species. For example, the low-affinity transport systems for *T. oceanica* and *T. pseudonana* grown under Fe/Cu replete conditions were very different: while that of *T. oceanica* saturated at ~ 2000 nM, that of *T. pseudonana* showed no saturation at that Cu concentration. These results suggest that under Fe/Cu replete conditions, *T. pseudonana*, the coastal isolate, has more efficient intracellular Cu homeostasis mechanisms than *T. oceanica*. These mechanisms may include Cu efflux and/or intracellular metal-binding peptides. Indeed, some freshwater and marine phytoplankton have been documented to efflux internalized Cu (Verma and Singh 1991, Knauer et al. 1997, Pandey et al. 1997, Croot et al. 2003). Cu storage by phytochelatins has been observed in marine phytoplankton (Ahner et al. 1994, 1997, 2002, Morelli and Scarano 2004).

The low-affinity Cu uptake systems of *T. oceanica* and *T. pseudonana* were similar ( $K_m \sim 1\mu\text{M}$ , and  $V_{\text{max}} 30\text{-}100 \text{ zmol Cu} \cdot \mu\text{m}^{-2} \cdot \text{h}^{-1}$ ) only when cells were Fe limited. Interestingly, Fe limitation down-regulated (or turned off) the high-affinity Cu transport system in both diatoms. In the case of *T. oceanica*, the high-affinity Cu transport system seemed to be turned off by Fe limitation in both Cu growth conditions (Cu replete and low Cu), while that of *T. pseudonana* was turned off by Fe-limitation only under Cu replete conditions. In contrast, Fe-limited *T. pseudonana* grown with low Cu up-regulated its high-affinity Cu transport system. These changes may reflect the need to take up extra Cu when Fe is low due to the up-regulation of multi-copper oxidase (MCO) in the high-affinity Fe transport system. Therefore, Fe nutrition controls Cu uptake differently in *T. pseudonana* and *T. oceanica*. In addition, when Fe sufficient cells were subjected to low Cu levels, the high-affinity Cu transport system of *T. oceanica* had significantly lower  $K_m$

(51-fold,  $p < 0.0001$ , TDIST) and  $V_{\max}$  (13-fold,  $p < 0.0001$ , TDIST) than that of *T. pseudonana*. Thus, the high-affinity Cu transport system of Fe replete *T. oceanica* is more efficient under low Cu than that of *T. pseudonana*. This potentially reflects the lower Cu concentrations in the open ocean and the evolution of a diatom in a chronically low Fe environment, where intracellular Cu may have partially relieved Fe use in some key biochemical pathways.

### 3.4.3 Strong Cu and Fe effects on Cu Uptake Kinetics

Cu and Fe availabilities in growth media have a strong effect on the Cu uptake kinetics of *T. oceanica* and *T. pseudonana*, and an interaction between Fe and Cu exists in these diatoms. However, the results obtained here indicate that Cu uptake kinetics are complex, and suggest that Cu transport is regulated dynamically by both Fe and Cu. At present, we are unable to explain all the interactions between Cu and Fe nutrition on Cu transport. Thus, we have restricted this discussion to the most significant results.

Cu availability had significant effects on the  $V_{\max}$  of low-affinity Cu uptake in *T. oceanica* ( $p = 0.012$ , two-way ANOVA, Table 3.4) and *T. pseudonana* ( $p = 0.007$ , TDIST, Table 3.4), and these effects were different depending on Fe availability ( $p = 0.023$ , two-way ANOVA, Table 3.4). When Fe is sufficient, the  $V_{\max}$  of low-affinity Cu transporter in *T. oceanica* is up-regulated under low Cu (6.5-fold higher for low Cu cultures,  $p = 0.021$ , TDIST). Similar up-regulation of the low-affinity Cu transport system has been observed in *C. reinhardtii* (Hill et al. 1996), where the  $V_{\max}$  in Cu-deficient cells ( $169 \pm 9 \text{ amol} \cdot \text{cell}^{-1} \cdot \text{h}^{-1}$ ) is 20-fold faster than that of Cu sufficient cells ( $8.16 \pm 0.6 \text{ amol} \cdot \text{cell}^{-1} \cdot \text{h}^{-1}$ ). Thus, in *C. reinhardtii*, the same Cu transport system operates in Cu replete and Cu deficient cells, but more Cu transporters are expressed under Cu deficient conditions (Hill et al. 1996). In a similar manner, Fe limited *T. oceanica* may be expressing a higher density of low-affinity Cu transporters when Cu is low. In contrast to this findings, low Cu in Fe limited *T. pseudonana* elicited slower  $V_{\max}$  ( $p = 0.007$ , TDIST, Table 3.4). As for the effects of Fe availability on Cu uptake kinetics, it has been discussed in the session

discussing *T. oceanica* versus *T. pseudonana*.

#### 3.4.4 High-affinity and low-affinity Cu transporters in eukaryotes

In the yeast *S. cerevisiae*, Cu transport is mediated by a high- and a low-affinity uptake system depending on Cu availability. In the high-affinity transport system, Cu is reduced from  $\text{Cu}^{2+}$  to  $\text{Cu}^+$  by plasma membrane reductases, including highly specific cupric reductases (Hassett & Kosman 1995) and FRE1, which also functions in Fe transport (Georgatsou et al. 1997). After Cu is reduced,  $\text{Cu}^+$  is taken up by Cu transport proteins (Ctr1p and Ctr3p) which are localized in the plasma membrane (Dancis et al. 1994b, Labbe et al. 1997, Pena et al. 2000). The expression of these proteins is regulated by intracellular Cu deficiency. In phytoplankton, it has been demonstrated that cupric reductase activity exists at the cell surface (Jones et al. 1987, Hill et al. 1996). Recently, homologs (*Tp*FRE1-3) to these reductases of the high-affinity Cu and Fe transport system in yeast (FRE1 AND FRE2) were identified in the genome of the diatom *T. pseudonana* (Kustka et al. 2007). These reductases thus may also have a cupric reductase function in the high-affinity Cu transport system in *T. pseudonana*. CTR, a Cu permease, is deemed to be a canonical member of a high-affinity Cu transport family of proteins in eukaryotic organisms (Dancis et al. 1994a, Dancis et al. 1994b, Kampfenkel et al. 1995, Lee et al. 2000, Zhou & Thiele 2001, Sancenon et al. 2003, Zhou et al. 2003). A putative CTR has also been found in the genome of *T. pseudonana* (*Thaps3/chr\_11a:66327-68695*, see <http://genome.jgi-psf.org/Thaps3/Thaps3.home.html>). This transporter may be the high-affinity Cu uptake transporter of marine diatoms.

Potential transporters in the low-affinity Cu transport system include FET4 (also a low-affinity  $\text{Fe}^{2+}$  permease) and SMF1 in yeast (Dix et al. 1997, Liu et al. 1997, Hassett et al. 2000). In phytoplankton, P-type ATPase  $\text{Cu}^{2+}$  transporters are found in the thylakoid membrane and in the plasma membrane of the freshwater *Synechococcus* species PCC7942 (Kanamaru et al. 1994; Phung et al. 1994). Cu-transporting ATPases exist in the genome of the marine diatom *T. pseudonana* (*thaps1\_ua\_kg.chr\_16a000004*, see

<http://genome.jgi-psf.org/Thaps3/Thaps3.home.html>), and the *Synechococcus* WH8102 (Palenik et al. 2003). These P-type ATPases may regulate low-affinity Cu transport in marine phytoplankton. The low-affinity Cu transporters may also involve members of the NRAMP (Natural Resistance-Associated Macrophage Protein) and the ZIP/IRT (Zinc IRT-like Protein/Fe-Regulated Transporter) families due to their wide selectivity for cations ( $\text{Cu}^{2+}$ ,  $\text{Cd}^{2+}$ ,  $\text{Fe}^{2+}$ ,  $\text{Mn}^{2+}$ , and  $\text{Zn}^{2+}$ ) (Gunshin et al. 1997, Grotz et al. 1998, Korshunova et al. 1999, Ramesh et al. 2003)). Indeed, physiological studies of marine phytoplankton have indicated that high availability of  $\text{Cu}^{2+}$  inhibits cellular Mn and Zn uptake in the diatom *T. pseudonana* (Sunda & Huntsman 1983, 1996), supporting a common transporter for Cu, Mn and Zn. We thus propose that in marine diatoms, different, non-specific metal transporters may work together as low-affinity Cu transporters.

### 3.4.5 Oceanographic implications

Using diatoms as model organisms, this study presents the first evidence of the co-occurrence of a high- and a low-affinity Cu transport system in marine phytoplankton. One of our principle observations from this work is that the characteristics of these Cu transport systems are different in the coastal and the oceanic diatom investigated here, potentially reflecting the evolutionary adaptation of species to different trace metal regimes. The open ocean isolate, *T. oceanica*, has the highest affinity for Cu transport of any phytoplankton tested to date, which is consistent with the very low Cu concentrations in offshore oceanic waters. In contrast, the coastal strain, *T. pseudonana*, was able to tolerate relatively higher Cu concentrations that are typical for coastal waters. Moreover, the Cu uptake systems in the two diatom species are differentially controlled by Cu and/or Fe nutrition. For example, while Fe replete *T. oceanica* lowered the  $K_m$  and  $V_{max}$  of its high-affinity Cu transport system under low Cu conditions, such a response is not observed in *T. pseudonana*. Another disparity between these two strains is their ability to increase the number of Cu transporters at the cell surface ( $V_{max}$ ) in response to low Cu. As observed in other phytoplankton (Hill et al. 1996), *T. oceanica* increased the  $V_{max}$  of

the low-affinity Cu transport system in response to low Cu, while *T. pseudonana* decreased its  $V_{\max}$ . However, the responses of Cu uptake kinetics to different Fe and/or Cu conditions are complex, providing more support for the dynamic interaction between Fe and Cu in diatoms physiology and highlighting the need for further study.

The Cu uptake rates determined here using CuEDTA, a non-photolabile organic Cu complex (Natarajan and Endicott 1973), question our present understanding of what controls Cu transport in marine phytoplankton. The free ion model (Hudson 2005) assumes that only inorganic metal species are labile and utilized directly by phytoplankton, while organically bound metals are essentially unavailable. However, using CuEDTA as a model organic Cu complex, our results suggest that the flux of inorganic Cu to the cell surface ( $J_D$ ) is insufficient to account for the Cu uptake rates we measured ( $\rho\text{Cu}$ ). When both diatoms were grown in Fe/Cu replete conditions, the observed Cu uptake rates, at 6 different Cu concentrations ranging from 2 to 500 nM, exceeded the corresponding calculated maximum diffusion rates of inorganic Cu by factors of 1.5 to 15.1 (Table 3.5). The mean ratio of  $\rho\text{Cu}: J_D$  ratio was 7.2 and 3.3 for *T. oceanica* and *T. pseudonana*, respectively. For only *T. pseudonana*, at the 2 highest Cu concentrations (1000 and 2000 nM), the diffusive flux of inorganic Cu fully accounted for the Cu uptake rates measured. Faster rates of Cu uptake relative to the diffusive flux of inorganic Cu to the cell surface has also been observed in recent studies (Quigg et al. 2006, Annett et al. 2008). These results suggest that diatoms might be able to access Cu bound within organic Cu complexes. Thus, Cu uptake may not be always controlled by the free  $\text{Cu}^{2+}$  or the  $\text{Cu}'$  concentration, but instead by total Cu concentration. Further study is needed to investigate this Cu uptake mechanism. Reductive release of Cu from organically bound  $\text{Cu}^{2+}$  complexes by cell surface cupric reductases may be one mechanism of Cu uptake in marine diatoms (Semeniuk et al. 2009). In addition, at identical  $\text{Cu}'$  concentrations, the ratios of Cu uptake to maximum diffusive fluxes of inorganic Cu were 1.4 to 5 times higher in *T. oceanica* than in *T. pseudonana*. *T. oceanica* may thus have higher Cu(II) reductive ability or a higher affinity  $\text{Cu}^+$  transporters, which is supported by the lower  $K_m$  of the high-affinity transport system of

*T. oceanica* (48 nM) relative to *T. pseudonana* (188 nM).

Our field investigations in Station Papa in the Subarctic Pacific in September of 2006 and May 2008 provide further evidence of the availability of organic Cu to indigenous phytoplankton. At an in situ Cu concentration of 2 nM, we measured  $\rho\text{Cu}$  of 2.3 & 5.8  $\mu\text{mol Cu} \cdot \text{mol C}^{-1} \cdot \text{h}^{-1}$ , respectively (Semeniuk et al. 2009 and D. Semeniuk & M. Maldonado unpublished). Assuming that the mean phytoplankton size is  $\sim 3 \mu\text{m}$  in radius and that 0.4% of total Cu is inorganic Cu (Donat and Bruland, 1995), we calculate a diffusive flux of Cu on the order of  $0.5 \mu\text{mol Cu} \cdot \text{mol C}^{-1} \cdot \text{h}^{-1}$ . The rates of Cu uptake by indigenous phytoplankton are thus 5-10 times faster than the inorganic Cu diffusive flux, indicating that Cu uptake in the open ocean might be controlled by the total Cu concentration. Given the  $K_m$ s of the low- and high- affinity Cu transport system for our oceanic isolate (2410 nM and 48 nM, respectively), indigenous phytoplankton most likely have an active high-affinity Cu transport system in the open ocean, where total Cu concentration is  $\sim 2 \text{ nM}$  (Coale & Bruland 1988, Jickells & Burton 1988, Moffett 1995, Rutgers van der Loeff et al. 1997, Moffett & Dupont 2007). Our study raises fundamental questions about Cu availability in the world oceans. It also highlights the effects that phytoplankton Cu acquisition mechanisms, which potentially involve cupric reductases, may have on the distribution and speciation of Cu in seawater. The link between Fe and Cu nutrition is also evident, but further studies are needed to fully elucidate the complex interaction between these two metals in phytoplankton physiology.

Table 3.5 Measured Cu uptake rates (pCu) by *T. oceanica* and *T. pseudonana* grown in Fe/Cu replete media, maximum diffusive rate of dissolved inorganic Cu (Cu') from the bulk solution to the surface of the diatom cell ( $J_D$ ), and the ratio of pCu:  $J_D$ . The measured Cu uptake rates reported here are the average linear uptake rates ( $\pm$  range) of the two independent cultures. The maximum diffusive rate of Cu' was calculated using the equation  $J_D = 4\pi rD[\text{Cu}']$ , where r (cm) is the cell radius and D ( $2.16 \times 10^{-2} \text{ cm}^2 \cdot \text{h}^{-1}$  at 20°C) is the diffusion coefficient of dissolved inorganic Cu (Hudson and Morel 1993). The concentration of free  $\text{Cu}^{2+}$  (pCu) was calculated using the program MINEQL + 4.61 (Environmental Research Software). The concentration of Cu' was calculated from the inorganic side reaction coefficient ( $\alpha_{\text{Cu}} = [\text{Cu}']/[\text{Cu}^{2+}] = 16.1$ , Sunda et al. 2005).

[Cu] <sub>total</sub> (nM)	[Cu'] (pM)	pCu	Measured Cu uptake rate (pCu) (zmol Cu · cell <sup>-1</sup> · h <sup>-1</sup> )		Max Cu' diffusion rate ( $J_D$ ) (zmol Cu · cell <sup>-1</sup> · h <sup>-1</sup> )		Ratio (pCu: $J_D$ )	
			<i>T. oceanica</i>	<i>T. pseudonana</i>	<i>T. oceanica</i>	<i>T. pseudonana</i>	<i>T. oceanica</i>	<i>T. pseudonana</i>
			2	0.02	14.8	26 ± 8	11 ± 0.5	1.7
30	0.4	13.6	291 ± 59	130 ± 13	26	23	11.1	5.6
60	0.7	13.3	482 ± 60	235 ± 29	52	47	9.2	5.0
120	1.5	13.0	1224 ± 84	225 ± 8	105	94	11.7	2.4
240	2.9	12.7	820 ± 123	518 ± 55	209	188	3.9	2.8
500	6.2	12.4	1220 ± 260	587 ± 161	436	391	2.8	1.5
1000	12	12.1	1965 ± 127	681 ± 1	872	781	2.3	0.9
2000	25	11.8	2256 ± 199	939 ± 34	1743	1563	1.3	0.6

## **Chapter 4**

**Sequence analysis and gene expression of potential components of copper transport and homeostasis in *Thalassiosira pseudonana* grown under low copper and iron availability**

## 4.1 Introduction

The redox metal copper (Cu) is an essential micronutrient for phytoplankton. It plays a key role in numerous metabolic pathways, such as respiration (cytochrome *c* oxidase, Merchant et al. 2006), photosynthesis (plastocyanin, Ho and Krogmann 1984, Nosenko et al. 2006, Peers and Price 2006), oxidative stress (Cu/Zn superoxide dismutases, Chadd et al. 1996), organic nitrogen assimilation (amine oxidases, Palenik et al. 1988-1989), as well as Fe acquisition (multicopper ferroxidases, La Fontaine et al. 2002). Most recently, in the green alga *Chlamydomonas*, Cu deficiency has been shown to affect the composition of chloroplast membrane lipids, thus, inhibiting the integrity and function of photosystem II (Castruita et al. 2011). However, at very high concentrations, Cu can cause oxidative damage to lipids, proteins and DNA, as free Cu ions can participate in redox reactions to yield hydroxyl radicals (Halliwell and Gutteridge 1984). Thus, cells have to develop both Cu acquisition and homeostasis mechanisms to control intracellular Cu concentrations (Eide 1998, Puig and Thiele 2002, Merchant et al. 2006, Kim et al. 2008).

Numerous culture studies have investigated the toxic effects of high Cu levels on the physiology of marine phytoplankton (Brand et al. 1986, Cid et al. 1995, Moffett and Brand, 1996, Davis et al. 2006). Conversely, growth reduction caused by Cu deficiency ( $pCu=15$ ) has been demonstrated in marine phytoplankton from various taxa (Peers et al. 2005, Annett et al. 2008, Guo et al. in press). Marine Cu concentrations, ranging from a low of 0.5-6 nM in open oceans (Jickells and Burton 1988, Coale and Bruland 1990, Moffett 1995, Rutgers van der Loeff et al. 1997, Moffett and Dupont 2007) to a high of 2-150 nM in coastal waters (Sunda et al. 1990, Moffett et al. 1997, Buck et al. 2007) may thus be growth limiting or toxic for phytoplankton in open or coastal waters, respectively (Rueter et al. 1979, Moffett et al. 1997, Sunda and Huntsman 1998a, Raven et al. 1999, Peers et al. 2005, Moffett and Dupont 2007, Guo et al. in press). This suggests that the mechanisms of Cu assimilation and homeostasis in coastal and oceanic phytoplankton may be very different. Our recent physiological study on Cu transport in marine diatoms

indicated the presence of two Cu uptake systems (a high-affinity and a low affinity), as well as distinct Cu uptake kinetics for a coastal (*T. pseudonana*) and an oceanic diatom (*T. oceanica*, Guo et al. 2010). However, the specific genes and proteins involved in these Cu transport systems are still unknown. Similarly, Cu homeostasis mechanisms have not yet been identified in these organisms.

In contrast, the components and mechanisms of Cu acquisition and intracellular distribution by the yeast *Saccharomyces cerevisiae* have been well studied (Puig and Thiele 2002). Using sequence homology to these yeast counterparts, most homologs in plants, freshwater microalgae and other organisms have been identified (Eide 1998, Puig and Thiele 2002, Merchant et al. 2006, Puig et al. 2007). In these organisms, Cu acquisition depends on a high-affinity Cu uptake system at the plasma membrane (Puig and Thiele 2002, Sancenon et al. 2003, 2004, Page et al. 2009). This system is comprised of Cu reductases and conserved Cu<sup>+</sup> transporters, which belong to the CTR family, including 2 CTR transporters (CTR1 and CTR3) in yeast, 2 homologs (COPT1 and 2) in *Arabidopsis* (Sancenon et al. 2003, 2004) and 3 homologs (COPT1, CTR1 and 2) in *Chlamydomonas* (Page et al. 2009).

In addition to the CTR family transporters, some non-specific metal transporters may also have a function in Cu transport. The NRAMP (natural resistance-associated macrophage protein) and ZIP/IRT (zinc IRT-like protein/Fe-regulated transporter) families are thought to transport primarily Fe and Zn in yeast and plants (Guerinot 2000, Curie and Briat 2003, Hell and Stephan 2003), but many studies have indicated that these transporters may also play a role in Cu uptake due to the wide selectivity for cations (Cu<sup>2+</sup>, Cd<sup>2+</sup>, Fe<sup>2+</sup>, Mn<sup>2+</sup>, and Zn<sup>2+</sup>) (Gunshin et al. 1997, Grotz et al. 1998, Korshunova et al. 1999, Ramesh et al. 2003). Indeed, high availability of ionic Cu<sup>2+</sup> inhibits Mn and Zn uptake rates in *Chlamydomonas* sp. and *T. pseudonana* (Sunda and Huntsman 1983, 1988a, 1988b).

Once the Cu is taken up, Cu is distributed to specific targets by Cu chaperones and intracellular Cu transporters. In yeast, Cu is delivered by chaperone ATX1 to the Golgi

apparatus, by COX17 to cytochrome c oxidase in the mitochondria and by CCS to Cu/Zn SOD in the cytosol (Puig and Thiele 2002). Some homologs of these Cu chaperones have been identified in *Arabidopsis* and *Chlamydomonas* (Wintz and Vulpe 2002, Merchant et al. 2006). In addition, in *Arabidopsis*, Cu is delivered to plastocyanin and Cu/Zn SOD in the chloroplast by the Cu-transporting P-type ATPases PAA1 and PAA2 (Abdel-Ghany et al. 2005).

The recently sequenced diatom *T. pseudonana* is a valuable model for marine phytoplankton studies (Armbrust et al. 2004), allowing the identification of potential components of Cu assimilation and homeostasis. In this study, we searched the genome of *T. pseudonana* for candidate genes involved in Cu assimilation and intracellular distribution using known homologs in fungi, green algae, plants and animals. We identified 11 genes, including putative Cu and Zn transporters and Cu chaperones, and tested their transcriptional expression in *T. pseudonana* cultures acclimated to different Fe and Cu levels. Considering the physiological link between Cu and Fe, we also tested the transcriptional regulation of genes encoding various components of the Fe transport system in *T. pseudonana* (Kustka et al. 2007).

## **4.2 Materials and methods**

### **4.2.1 Candidate genes and sequence analysis**

Sixteen genes potentially involved in Cu transport and homeostasis in *Thalassiosira pseudonana* were tested for gene expression patterns under different Fe and Cu culture conditions. Among these, 11 genes were identified in the *T. pseudonana* genome (JGI; <http://genome.jgi-psf.org/thaps3/thaps3.download.html>) by blastp searches using homologous genes from other organisms. They included members of the CTR family, Cu-translating P-type ATPase, Cu chaperones and genes of the ZIP family. Five genes

including ferric reductases (*TpFRE1*, *TpFRE2*), the Fe permease (*TpFTR1*), the multi-copper oxidase (*TpFET3*) and the *TpNRAMP* were directly obtained from Kustka et al. (2007). The conserved motifs of candidate genes were analyzed by comparing their predicted protein sequences with homologues from other organisms. Multiple alignments were performed with Clustal W 1.8. The putative transmembrane domains (TM) were predicted by TMHMM v. 2.0 (<http://www.cbs.dtu.dk/services/TMHMM/>) and TMPred ([http://www.ch.embnet.org/software/TMPRED\\_form.html](http://www.ch.embnet.org/software/TMPRED_form.html)).

#### 4.2.2 Algal culturing

Diatom *Thalassiosira pseudonana* clone 3H (CCMP1335) was obtained from the Provasoli-Guillard Center for Culture of Marine Phytoplankton (West Boothbay Harbor, ME, USA). Cells were grown axenically using semi-continuous batch culturing and the chemically well-defined artificial seawater medium AQUIL (Price et al. 1989). The cultures were grown in 28 mL polycarbonate tubes and were maintained at  $19 \pm 1^\circ\text{C}$  and a continuous light intensity of  $150 \mu\text{mol quanta} \cdot \text{m}^{-2} \cdot \text{s}^{-1}$ , provided with cool-white fluorescent lights. These continuous light conditions allow an unconstrained sampling schedule. Four culture media treatments were prepared with various additions of Fe and/or Cu, including Fe and Cu replete (Control), Fe replete/low Cu (-Cu), low Fe/ Cu replete (-Fe), and low Fe and low Cu (-Cu/-Fe) treatment (Table 4.1). Except for the addition of Fe and Cu, the AQUIL medium used in this study was prepared and was identical in chemical composition to that described by Maldonado et al. (2006). All cultures were acclimated to these four media for about a year. The growth rates ( $\text{d}^{-1}$ ) of the cultures were monitored daily using in vivo Chl fluorescence measurements with a Turner Designs AU-10 Fluorometer (Sunnyvale, CA, USA). Cell density ( $\text{cells mL}^{-1}$ ) and cell size ( $\mu\text{m}$ ) were determined using a Coulter Z2 Particle Count and Size Analyzer. Sterile trace metal-clean techniques were used during all experiments and manipulations.

For gene expression under steady-state growth conditions, triplicate cultures of acclimated cells were prepared using 250 mL of media for control and low Cu treatment,

or 500 mL of media for low Fe and low Cu/Fe treatment. Approximately  $1 \times 10^8$  cells, in late exponential phase, were collected for RNA extraction. For the rapid Cu resupply experiments, cells acclimated to Fe replete/low Cu condition were grown in triplicate 4 L polycarbonate bottles. The Cu addition was prepared as a CuEDTA complex ([Cu]:[EDTA] = 1:2) one day before dilution into the cultures, and was added to our mid-exponential phase cultures at a final concentration of 500 nM (pCu=12.4). Cells were sampled for RNA isolation immediately prior to the Cu addition and at 1, 3, 6 and 12 hours after the Cu was added.

Table 4.1 Growth rate ( $d^{-1}$ ) and cell diameter ( $\mu m$ ) of *T. pseudonana* grown under different Fe and Cu concentrations. All values ( $\pm$ SD) are the average of three biological replicates. The base level of Cu in the low Cu media (no Cu was added) was 1 nM due to contamination. Contamination level for Fe was also about 1 nM, and both were used in calculating the free metal concentration (pMe =  $-\log [Me^{n+}]$ ).

Treatments	Fe & Cu Replete (Control)	Fe replete/Low Cu (-Cu)	Low Fe/Cu replete (-Fe)	Low Fe/Low Cu (-Cu/-Fe)
[Cu <sub>total</sub> ] (nM)	11.2	1	11.2	1
[Cu <sup>2+</sup> ] (pCu)	13.9	15.1	13.9	15.1
[Fe <sub>total</sub> ] (nM)	1370	1370	12.5	12.5
[Fe <sup>3+</sup> ] (pFe)	19	19	21	21
Growth rate ( $d^{-1}$ )	1.73 $\pm$ 0.11	1.80 $\pm$ 0.11	1.03 $\pm$ 0.03	0.87 $\pm$ 0.03
Cell diameter ( $\mu m$ )	5.06 $\pm$ 0.02	4.84 $\pm$ 0.07	3.88 $\pm$ 0.00	4.04 $\pm$ 0.04

### 4.2.3 RNA extraction and quantitative real-time PCR

Algal cells were harvested on 47 mm polycarbonate filters of various porosities, according to their cell size (3  $\mu\text{m}$  for the control and low Cu treatments and 2  $\mu\text{m}$  for the low Fe and low Cu/Fe treatments, Table 4.1), flash-frozen in liquid nitrogen, and stored at  $-80\text{ }^{\circ}\text{C}$  until RNA extraction. Cell lysis and total RNA isolation were performed using the RNAqueous<sup>TM</sup> kit (Ambion, Austin, TX, USA) followed by DNase treatment for 1 hour using TURBO-DNA-free kit (Ambion). The purity of total RNA was tested by reverse transcript (RT) reactions to make sure that there was no genome DNA contamination. Then, purified total RNA was quantified spectrophotometrically and 400 ng were reverse transcribed into first-strand cDNAs in 20  $\mu\text{L}$  reaction using Superscript II (Invitrogen, Carlsbad, CA, USA). For quantitative real-time PCR (qRT-PCR), gene-specific primers with amplicon sizes in the range of 90–190 bp were designed (see Supplemental Table 4.1) using the genomic sequence data for *T. pseudonana* or those reported in Kustka et al (2007). cDNA was then amplified by RT-PCR using those gene-specific primers and iQ<sup>TM</sup> SYBR Green Supermix (Bio-Rad, Hercules, CA, USA). Each 20  $\mu\text{L}$  PCR reaction contained  $0.3\text{ }\mu\text{mol L}^{-1}$  each of forward and reverse primers, and 2 ng transcribed RNA. Quantitative RT-PCR was performed using the iQ5 real-time system (Bio-Rad Laboratories, Hercules, CA, USA) with the thermocycle conditions as follows:  $95\text{ }^{\circ}\text{C}$  for 3 min, 40 cycles of  $95\text{ }^{\circ}\text{C}$  for 15 s,  $60\text{ }^{\circ}\text{C}$  for 30s, and  $72\text{ }^{\circ}\text{C}$  for 30 s; and melt-curve analysis starting at  $55\text{ }^{\circ}\text{C}$  for 10 s with  $0.3\text{ }^{\circ}\text{C}$  steps for 133 cycles. The transcript abundance was determined by the  $2^{-\Delta\Delta C_T}$  method (Livak and Schmittgen, 2001) from technical duplicates of each biological triplicate. The  $\Delta C_T$  values were calculated after normalizing to an endogenous reference gene (*TpActin*, Kustka et al. 2007) and the  $\Delta\Delta C_T$  values were calculated relative to the RNA sample from cells grown in Fe and Cu replete medium. The relative gene expression data were presented as the fold change in mRNA abundance. Melting curves with single peaks for each primer indicated the presence of a unique final product, and the unique product was also confirmed by gel electrophoresis and gene sequence from one reaction.

#### **4.2.4 Statistical analysis**

For steady-state experiments, two-way ANOVA (SigmaStat 3.5) and ANOVA Tukey analysis (Graphpad Prism 5) were used to analyze the differences between treatment means of relative gene expression values within each gene. For the rapid Cu resupply experiments, a t-test was used to compare the relative gene expression values obtained at  $t=0$  hours (no Cu addition) with the relative gene expression value obtained at  $t = 1, 3, 6$  and 12 hours, respectively.

### **4.3 Results**

#### **4.3.1 Effects of long-term acclimation to low Fe and/or low Cu on growth rate and cell size**

In agreement with our previous results (Guo et al. 2010; Zhu et al. 2010), low Cu had no effect on the growth rate or cell diameter. As expected, long-term Fe starvation had a significant effect ( $p < 0.001$ , two-way ANOVA) on the growth rate (41% reduction) and cell size of *T. pseudonana* (Table 4.1). However, there were significant interactions between low Fe and low Cu with respect to both growth ( $p = 0.03$ ) and cell size ( $p < 0.001$ ). A significant growth rate reduction (15%) due to low Cu was only observed when Fe was also limiting.

#### **4.3.2 Putative CTR Cu transporters and their gene expression**

CTR Cu transporters are identified by certain conserved motifs that have been shown experimentally to be involved in Cu binding in yeast or other organisms (Puig and Thiele 2002, Sancenon et al. 2003, 2004, Page et al. 2009). To identify putative Cu transporters in the *T. pseudonana* genome, three CTR genes (CTR1-3) of *Saccharomyces cerevisiae*, four Cu transport genes (CTR1-3 and COPT1) of *Chlamydomonas reinhardtii* and five

COPT genes (COPT 1-5) of *Arabidopsis thaliana* were used as queries in blastp searches against the JGI database (<http://genome.jgi-psf.org/Thaps3/Thaps3.home.html>). Due to the low similarity and high divergence of most proteins between taxa, blasts with both the whole sequence and the characteristic functional motif of CTR genes (Figure 4.1b) were performed. Two CTR-like genes were identified, and named *TpCTR|24275* and *TpCTR|9391* (24275 and 9391 are the protein ID numbers of each gene in the *T. pseudonana* genome). The sequences were confirmed by RT-PCR and were identical to the gene models except for a small deletion (8 amino acids) in *TpCTR|24275*. The protein sequences of the CTR-like genes (*TpCTR|24275* and *TpCTR|9391*) contain three transmembrane domains (TM1-3, Figure 4.1a) which are key structural features of the CTR family (Puig et al. 2002). The MxxxM motif at the end of TM2 domain, which is critical for Cu uptake (Puig et al. 2002), and the GxxxG motif in the middle of TM3 domain formed the CTR-signature motif MxxxM-x<sub>12</sub>-GxxxG (De Feo et al., 2007) in these *TpCTR*-like genes (Figure 4.1b).

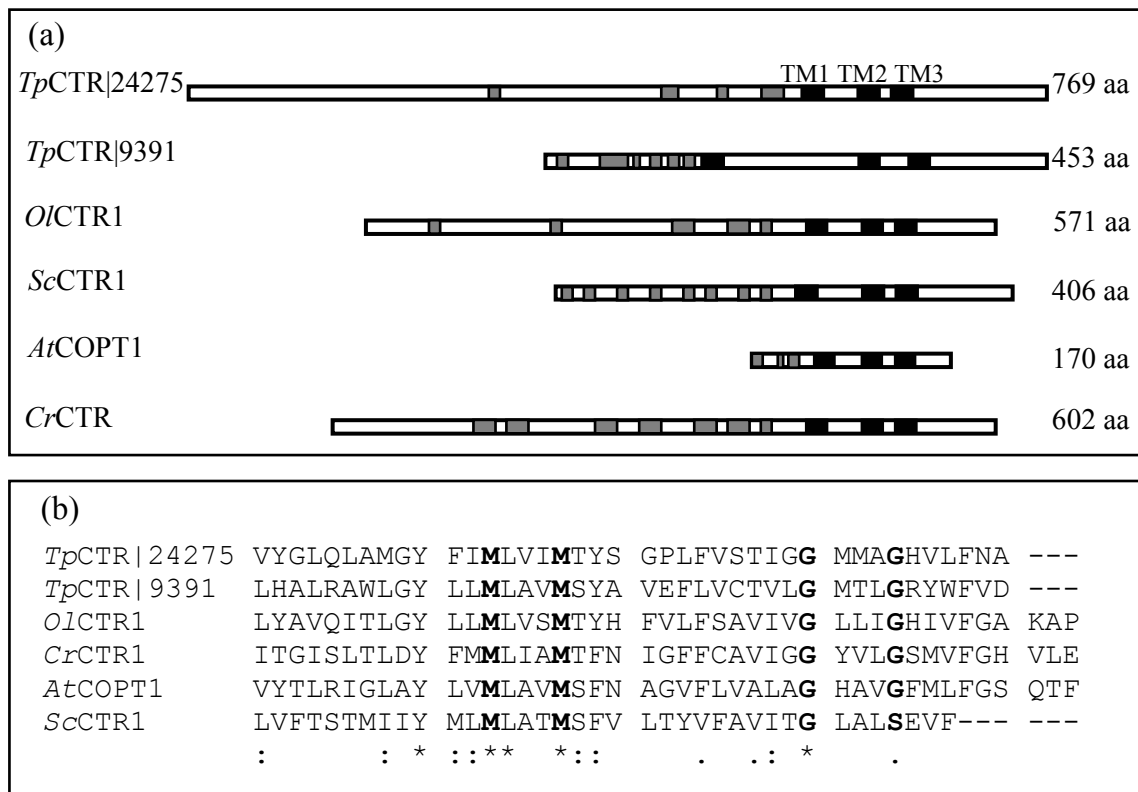


Figure 4.1 Structural model and conserved motifs of the CTR proteins of *S. cerevisiae* (*ScCTR1*), *A. thaliana* (*AtCOPT1*), *C. reinhardtii* (*ChCTR1*), *O. lucimarinus* (*OlCTR1*) and putative CTRs of *T. pseudonana* (*TpCTR* and *TpCTR/S*). The structural model and amino acid sequences are represented from the amino terminus (left) to carboxyl terminus (right). (a) Structural model for the Cu transport proteins. Three putative transmembrane domains (TM1-3) for each protein are indicated in black boxes. Putative Cu binding motifs are indicated in gray boxes. The sizes of each protein in amino acids are shown on the right. (b) Amino acid sequences of the conserved CTR motif in TM2 and 3, which is arranged as MxxxMx<sub>12</sub>GxxxG. Asterisks, colons and periods represent identical, strongly similar and weakly similar residues, respectively.

Aside from this conserved motif, the N-terminal parts of CTR proteins differ a great deal between organisms, although they all have metal-binding motifs containing Cys, Met and His. It was not possible to align the protein sequences of the two *T. pseudonana* CTR-like proteins with those of *S. cerevisiae* (ScCTR1, gi|1345859), *A. thaliana* (AtCOPT1, gi|15237802), or *C. reinhardtii* (CrCTR1, jgi|196101). A search of the NCBI database with *TpCTR|24275* retrieved homologs from *Phaeodactylum tricornutum*, *Ostreococcus lucimarinus*, *Micromonas pusilla* and *Perkinsus marinus*, but not from *Chlamydomonas*. This may be significant in view of the suggestion that diatoms acquired a significant number of genes by lateral gene transfer from members of the Mamiellales (Prasinophyceae) to which *Ostreococcus* and *Micromonas* belong (Moustafa et al. 2009). An alignment of these sequences showed that they shared a number of putative conserved Cu-binding residues and motifs, including HxH, Cx<sub>6/7</sub>CxxxC, HxxxC and Cx<sub>5/8</sub>MxM (Figure 4.2). These motifs are different from those of yeast in which Met-rich motifs (MxxM and/or MxM) are typical. They are more similar to those of *Chlamydomonas*, in which several Cys- and Met-containing motifs CxxMxxMxxCx<sub>5/6</sub>C occur (Page et al. 2009). The relative affinity of Cys, Met and His for Cu<sup>+</sup> is pH dependent. For example, for yeast grown at ~ pH 4.5 (in an oxic environment and in micromolar Cu concentrations) the Cu<sup>+</sup> binding amino acids Cys and Met are preferred over His, while when grown at pH 7.4, Cys and His are preferred over Met (Rubino et al. 2011). Diatom *T. pseudonana* was grown in nanomolar levels of Cu and high pH (8.14), thus Cys- and His-rich motifs would be more effective to bind Cu. The Cys- and His-containing motifs in the N-terminal domains of these putative CTR genes in *T. pseudonana* suggest evolutionary selection to acquire Cu from a high pH environment (Rubino et al. 2011). In the cytoplasmic C-terminus, *TpCTR|24275* contains a conserved motif CC (Figure 4.2) which functions in Cu binding and transferring Cu to cytosolic Cu chaperones in yeast (Xiao and Wadd 2002).

Figure 4.2 (next page) Alignment of putative *T. pseudonana* CTR (*TpCTR*|24275) with other organisms, including *Fragilariopsis cylindrus* (*FcCTR*, JGI protein ID: 233228), *Phaeodactylum tricornutum* (*PtCTR*, JGI protein ID: 47805), *Perkinsus marinus* (NCBI: gi|294867495), *Ostreococcus lucimarinus* (*OICTR1*, JGI protein ID: 31321) and *Micromonas pusilla* (*MpCTR*, JGI protein ID: 55157). Bars above the sequence indicate the predicted transmembrane domains (TM1-3). Columns of conserved residues are shaded. Conserved potential Cu-binding residues in the N-terminal and C-terminal domains are indicated by letters C, H and M. Asterisks, colons and periods represent identical, strongly similar and weakly similar residues, respectively

TpCTR|24275 -LRAITKQALSSQKPPPTGAGAFESVVGSHPKLQCLITLDDGVEKATATAATVGFDTWBAHPLDLP-RPFSQGGVAY--NKEELRINVAQVVDLFRKGLVERNGVRSSEG---  
 PcCTR|233228 YSRERRIALDGLASSLDHPE--FLKLDQTH---ELILSSGTTFRKATATVGLD---EPLSLY-WGLERNGVIL--ARVDSLRDVAIVVIVPSSADITLILGASPKKNSIT  
 PtCTR|47805 -LRERRIADGQCCASDABELPQSVGLAD---TSLLEDGLITRSTATATV---GTPLALWVCELEKADPHTT--AMVPSLRINVAQVNSHFWASADRLR--RQSSALMSE  
 Pn|294867495 HSEKQ-----EIPED-----  
 OlCTR1|31321 TYASRRRPLDAPFANRPRRSGRGTGSRSGM---KHDGAVSITRSLAKE-----ELK-MLVQDQGGEMMRGDLDFRIGALNNSHDLRSLDAAPH---  
 MpCTR|55157 GYANRVEALEVYARQALDA---PFRRAQMD--ETHGGRGAPTRVVAHESA-----MLP-SARDAPEDATI--DALESFAADNAAKAMPFLDAVLG---  
 Consensus

TpCTR|24275 ---VRAKIDSGRERERDILGGANDLEHVVVAKPSSSDGATATGP-----TIDVETDRRPLRPLV-PPAKKH-----GSDMVEKSPFLQNDGQSESDAFCRR  
 PcCTR|233228 TITLLDEDRCKEYVSTITVYQAILERHSHVYVYNGEKEDDCKAKHETA<sub>yy</sub>---NIVAMDATDAGPLVPLV-PAADQDNDG-----KIRSEDTSPYVHCRDQ---TDIRALPD  
 PtCTR|47805 LAPIDQMIH---KYSLEAEVYASTHLRERERKQDQKQAPRQSRASIM---VLDVETDRQVPLRPLV-PPAKKH-----NERTFASRRESVLIR---KIDRAVPL  
 Pn|294867495 -----TLLTLEK---KQELVIVRPPGKGLLYYEDGILTMQVPLNIH---KIDVYVHESKES---S---  
 OlCTR1|31321 -----NGRGGFVEREARQMSQEPQVYAPVWVSPAREIIEEILD---VEKHAATDQVAAVMT-PALLRS-----EIPGTCGRNPLFIEDIEPVAE  
 MpCTR|55157 -----YVNGGFPRANVYSEK--EHPVWVANDRSALVAGDREAS<sub>yy</sub>---POLRGGKGGTVMSEAVMT-PALMVE-----ELEEAGSSSDAPKANSKIDVSEKPLR  
 Consensus

TpCTR|24275 FSE-VVNLGKAGQMLN---GQEKQKHTH---LAKSHHRL-----QIARFRANVGMHLRFA---GTQSRRLGHVNSDRLNDVTFPCMGKQVHDEERH  
 PcCTR|233228 GHTAIVNLGKAGQMLN---LPSSESSSSTVYVSKQAPLVAADREVRM<sub>yy</sub>---GMEQQQQK---SICFRANVGMHLRFA<sub>yy</sub>---SHISRRRLREHDCRNCINVTDFCMMICMFKPGQ  
 PtCTR|47805 FSE-VVNLGKAGQMLK---NYSLE---LFAHSHHRL-----PQSRFRANVGMHLRFA---SPRHRRLQVITDQVCAHINFYCMNGLRDEAKQK  
 Pn|294867495 ---VVNLGKAGQMLN---HLSVYK---L---PAAVPL-----KITRFRANVGMHLRFA---LPSRRL---AEEK-NAGLIDQMMVQ---A  
 OlCTR1|31321 IAG-VVNLGKAGQMLN---GLFAMLSL---EKVSHHRL-----TGRFRANVGMHLRFA---VTSRRRLR---LIDK-DAGKLYCMICMFKPATA---A  
 MpCTR|55157 IFA-VVNLGKAGQMLDLPDGGEDRSESEK---LAVDTHREK---DQGAASDGTFRANVGMHLRFA---SITRRLR---LLES-RAGHYVCMICMFKPAGQK  
 Consensus

TpCTR|24275 MLNRRKESLYCLLQSLVESRGSIAEAELEPKH---SYTRSLQKESSEEDIMNARVEPFYVVAEAFRANYMPQMBQK---VGGTSMVMDGRFMM---GKAVDLPFNVLE  
 PcCTR|233228 ELINDKESLYCLLQSLVAKRQV-ISAARPCIE---EHWKQVSGHIVVSPANINV7---KPSGVVYD---FC---WGTVMVNSPQMGK---STVILLPFRNVLE  
 PtCTR|47805 QGINDKESLYCLLQSLVAKRRAKQVPEQIEDGVVGLAVNEDVYVSPAPVAVVQELALNPTTGE-----EELFC---VGGTSMVMDGRFMM---GKAVDLPFNVLE  
 Pn|294867495 NYCDKEMEPVAVVAV---VAKIRND---JHKTQVNSALEPAK---GNGGSPVETPD-PNAPC---TSTVNSDGRVAFSP-TKCVLLPFSNVLE  
 OlCTR1|31321 CAITSSASHAVQDIN---LQNDWYAA---LNRGTDAAAGD---GEMITA-----PTGMCITRIADVMDGKPLMGKASGQKMLLRFNSLR  
 MpCTR|55157 ---SPEVAVNSG---GLMVDQK---SECHKVYKQTVVAVDYK---SNDGGG---SGELNKKIATSMVMDGR-LGMKREDGCVTRKELKLE  
 Consensus

TpCTR|24275 IRRRRLSNTSELPRMLDSVLMRSTY--ELRPMRRL-----IDRNLVAGDQAMFSCMLVDFYQHGRSTLSSMAGHLLPNAKLSVVMWLKRN  
 PcCTR|233228 SEMNPLAVVPLCALHLKPYQQRVWVAYMSATYQL-----PAPALVWQDLEAYLLMLLHIVRFLVLMVILGLVSHILNAPDAI---WPIHE  
 PtCTR|47805 FRRRRLSNTSELPRMLDSVLMRSTY--ELRPMRRL-----FRRSRYVGLQALPTSPMLVWVYSCILRMVNLGLMPCHVSNAPVIL---NPKK-  
 Pn|294867495 IRRRRLSNTSELPRMLDSVLMRSTY--ELRPMRRL-----IYSLRACLESSELDNMLAVWVYSCILRCLCAQLVCHVRSNVRV  
 OlCTR1|31321 FRRRRLSNTSELPRMLDSVLMRSTY--ELRPMRRL-----AYAVMPLMGLVYGLLMVNSYVTEPFLRSTVDELTLRHLRSPAPV---ADDT-  
 MpCTR|55157 IRRRRLSNTSELPRMLDSVLMRSTY--ELRPMRRL-----IYSLRACLESSELDNMLAVWVYSCILRCLCAQLVCHVRSNVRV---GRAT-  
 Consensus

TpCTR|24275 IQSENREKALGCK-----CIEVYQSTQK--VTELGSHQVPSHMLLEDRCSEDDIEDVVS---VPSGTFPK---STL  
 PcCTR|233228 EINHLEIDNLDENS-----IDNDSVMDR--VVALFAGKPSNSNG---SMLINENNRK<sub>yy</sub>---HIVVPEKSTPK---QQM  
 PtCTR|47805 ---QTNREKELCK-----GKRF-----EILTPELAKCK---VPSSTPK---DILL  
 Pn|294867495 ---RIGNREKCK-----EITVSNVSTSEETERYHETSPKPLVRFID---CCOTPFYTK  
 OlCTR1|31321 -----TQCSFASPSDKQDCGCAPTHVADNPLPSCVAAVAESKSG<sub>yy</sub>---GSSALRASVTL  
 MpCTR|55157 -----GGARCAARV-----GTVEGSDKSGS---RAGDAPSERSGDGGG---DGGDAMTRFMMK---EPLKGRSRSEKPNFR  
 Consensus

The protein sequence of *TpCTR|9391* does not share these N-terminal motifs with *TpCTR|24275*, but is more similar to that of COPT1 in the green alga *Chlamydomonas* (Page et al. 2009) and the vascular plant *Arabidopsis* (Kampfenkel et al. 1995) in which the N-terminal domain contains His and Met-rich Cu binding motifs, including the large motifs Mx<sub>3</sub>Mx<sub>3</sub>HxMHxMxHx<sub>2</sub>MHHxMxHxMxH, Hx<sub>2</sub>HxMxMM, and MxMx<sub>3</sub>H. In addition, two Met-containing motifs (MxxM) and one Cys and His-containing motif (Cx<sub>4</sub>Hx<sub>5</sub>H) are also present in the N-terminal domain. All these structures and motifs suggest that these two proteins are suitable candidates for CTR-like Cu transporters.

Under long-term low Fe and/or low Cu conditions, the relative gene expression of these two CTR-like genes (*TpCTR|24275* and *TpCTR|9391*) increased significantly (~2 fold,  $p < 0.05$ ) when Fe was limiting, but there was no effect of low Cu (1.0 nM as opposed to 11.1 nM) (Figure 4.3). However, when 500 nM excess Cu was resupplied to cultures that were only Cu limited, the relative expression of both genes dropped about 2.5-fold within 1 hour and increased very little over the next few hours (Figure 4.4). This is the behaviour expected for a gene encoding a high-affinity Cu transporter. Note that this level of Cu is not toxic to *T. pseudonana* (Davis et al. 2006) even though it is much higher than levels used for the “replete” cultures. The cellular Cu concentration increased linearly for 5 h following the Cu addition, while the growth rate and maximum photosynthetic quantum yields (Fv/Fm) were unchanged up to 12 h after Cu addition (data not shown).

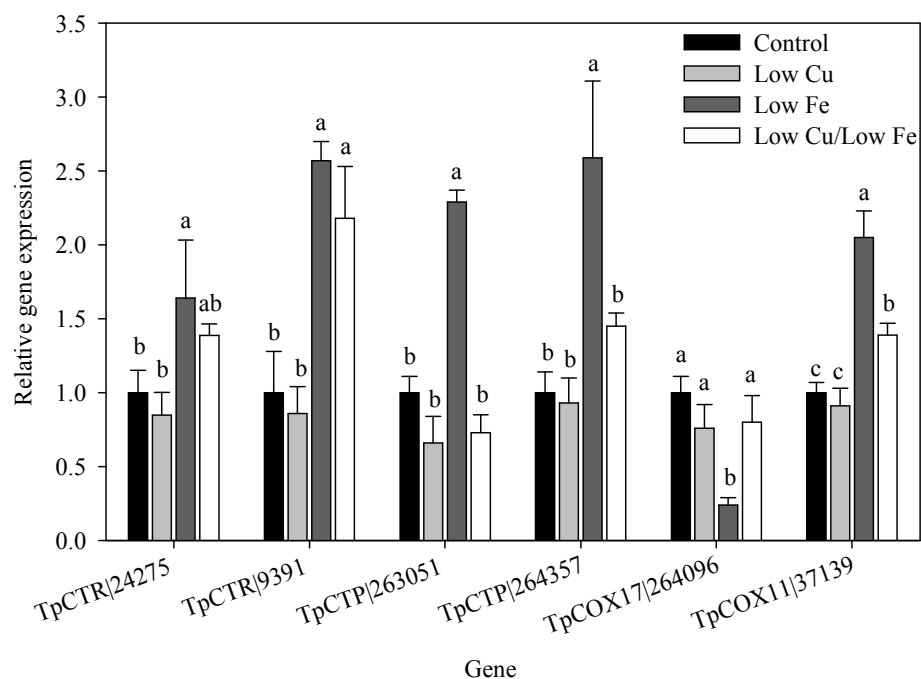


Figure 4.3 Steady-state relative gene expression of putative Cu transporters and Cu chaperones in *T. pseudonana* under different Fe and Cu levels. Each bar represents the mean value ( $\pm$  standard deviation) of three independent cultures. Within each gene, the four treatments were compared statistically (ANOVA Tukey test); the same letters above bars indicate treatments that were not statistically different ( $p < 0.05$ ). For statistical analysis by two-way ANOVA see Table 4.2.

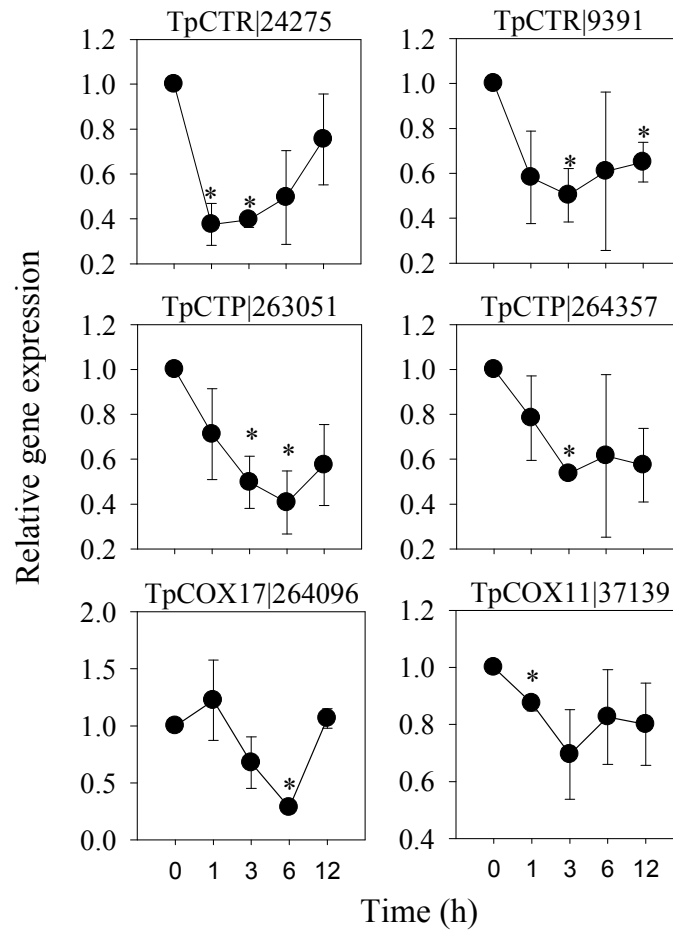


Figure 4.4 Relative gene expression of putative Cu transporters and Cu chaperones in low Cu acclimated *T. pseudonana* supplied with excessive Cu (500 nM). Each point represents the mean value ( $\pm$  standard deviation) of three independent cultures. Within each gene, each point was compared statistically with the control (0 hours) (t-test); the stars above points indicate statistically different ( $p < 0.05$ ).

### 4.3.3 Putative Cu-transporting P-type ATPases and their gene expression

The well-studied Cu-transporting p-type ATPases of *S. cerevisiae*, *A. thaliana* and *Synechococcus elongatus* are unified by the possession of a number of conserved motifs that always occur in the same order (Figure 4.5, Lutsenko and Kaplan 1995, Solioz and Vulpe, 1996). Genes *S. cerevisiae* CCC2 (gi|6320475), *A. thaliana* PAA1 (gi|42573157) and *Synechococcus elongatus* PACS (gi|435125) were used as the queries to find the homologous genes in *T. pseudonana*. Two putative Cu-transporting P-type ATPases were identified and named *TpCTP|263051* and *TpCTP|264357*. *TpCTP|263051* has eight predicted transmembrane domains, as well as the phosphatase (TGE), ion-transduction (CPC), phosphorylation (DKTGTIT) and ATP binding (GDGVNDS) motifs, all in the same order (Solioz and Vulpe 1996, Abdel-Ghany et al. 2005). *TpCTP|264357* does not have the phosphatase domain and has only one of the four transmembrane domains that precede it. In addition, *TpCTP|263051* contains two short consensus metal binding motifs (GMTCSSC and GLTCATC) in the N-terminal region (Figure 4.5a). These motifs are similar to the motif (GMTCxxC) of known Cu-transporting P-type ATPases in other organisms (Fu et al. 1995, Shikanai et al. 2003).

Compared to *TpCTP|263051*, *TpCTP|264357* is shorter and has no consensus metal binding motifs (GMTCxxC) in the N-terminal region (Figure 4.5a). However, at the overall sequence level, the *TpCTP|264357* gene is most similar to the best characterized Cu-transporting P-type ATPase RAN1 of *Arabidopsis* (model%: 100, hit%: 65, score: 1220, %id: 44, data are not shown) which is required for loading Cu onto the ethylene receptor in a late secretory compartment (Hirayama et al. 1999, Woeste and Kieber 2000).

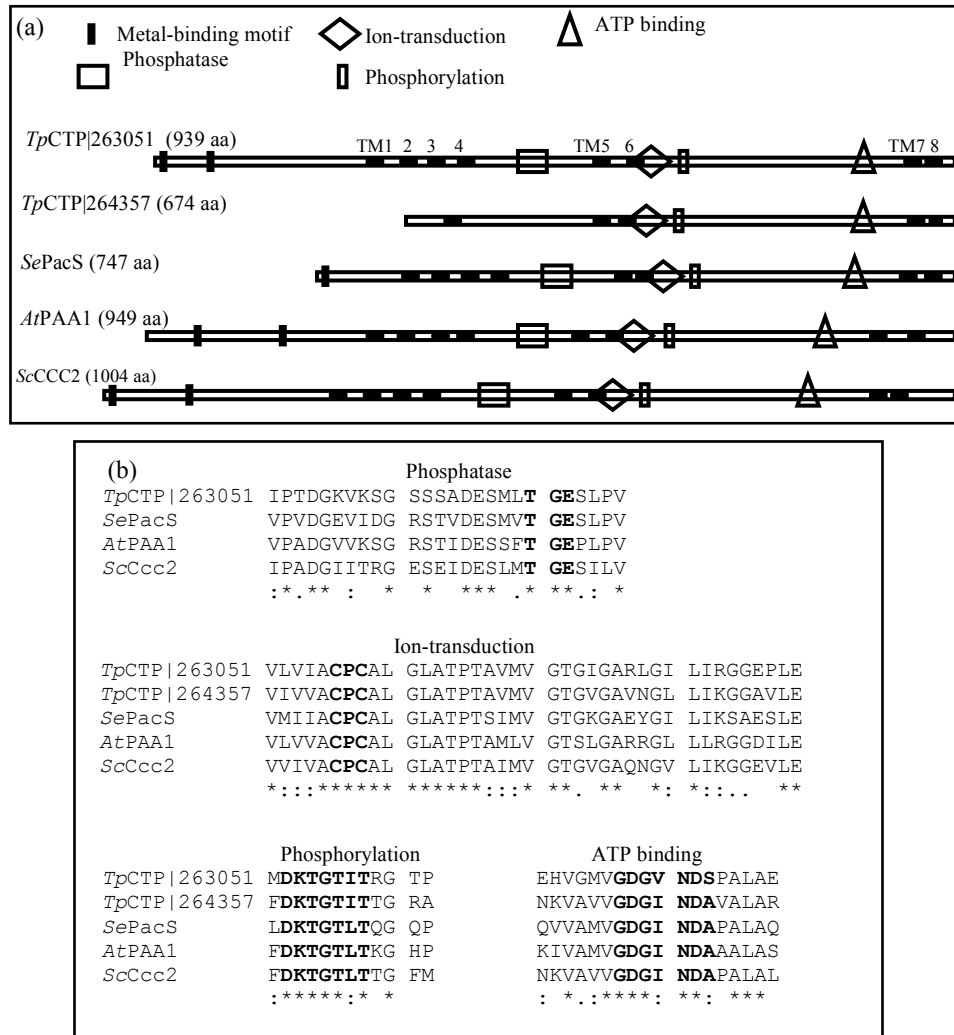


Figure 4.5 Structural models and conserved motifs of Cu-transporting p-type ATPase of *S. cerevisiae* (*ScCcc2*), *A. thaliana* (*AtPAA1*), *Synechococcus elongatus* (*SePacS*) and putative *TpCTP*|263051 and *TpCTP*|264357 of *T. pseudonana*. (a) Structural model for the Cu-transporting p-type ATPase. All proteins except for *TpCTP*|264357 contain metal-binding motifs and eight putative transmembrane domains (TM1-8) shown in black. They also contain four functional conserved motifs, including phosphatase, ion-transduction, phosphorylation and ATP binding motifs, except *TpCTP*|264357 has no phosphatase motif. (b) Amino acid sequence alignment of four functional conserved domains in which functional residues are indicated in bold. Asterisks, colons and periods represent identical, strongly similar and weakly similar residues, respectively.

Under long-term low Fe and/or low Cu conditions, there was a significant interaction between low Fe and low Cu availability on the relative gene expression of these two putative Cu-transporting P-type ATPases. Low Cu had no effect when Fe was replete, but significantly counteracted the increased expression seen when the cells were Fe limited (Figure 4.3, Table 4.2). However, after the Cu-limited cultures (but Fe replete) were given a Cu addition of 500 nM, the transcript levels of these two genes dropped significantly below control levels and remained low for the next 12 h (Figure 4.4).

Table 4.2 Statistic results (two-way ANOVA) of low Fe effect, low Cu effect, and the Fe and Cu interaction on transcript abundance of putative genes involved in Cu and Fe acquisition under long-term low Fe and/or low Cu conditions. Only significant effects are listed ( $p < 0.05$ ). Negative and positive effects are indicated with (-) and (+) symbol, respectively. Fe×Cu represents a significant interaction between the metal levels.

Gene	Effect	Gene	Effect
Cu transporters		High-affinity Fe transport components	
<i>TpCTR</i>  24275	Fe (-)	<i>TpFRE1</i>	Fe (-), Cu (+), Fe×Cu
<i>TpCTR</i>  9391	Fe (-)	<i>TpFRE2</i>	Fe (-), Cu (+), Fe×Cu
<i>TpCTP</i>  263051	Fe (-), Cu (+), Fe×Cu	<i>TpFET3</i>	Fe (-), Cu (+)
<i>TpCTP</i>  264357	Fe (-), Cu (+), Fe×Cu	<i>TpFTR1</i>	Fe (-)
Cu chaperones		Zn transporters	
<i>TpCOX11</i>  37139	Fe (-), Cu (+), Fe×Cu	<i>TpZIP</i>  32375	Fe (-), Cu (+)
<i>TpCOX17</i>  264096	Fe (+), Fe×Cu	<i>TpZIP</i>  268980	Fe (+), Cu (+), Fe×Cu
NRAMP		<i>TpZIP</i>  22351	Cu (+)
<i>TpNRAMP</i>	Fe (-)	<i>TpZIP</i>  263800	Cu (-)
		<i>TpZIP</i>  11826	Fe (-), Cu (+), Fe×Cu

#### 4.3.4 Putative Cu chaperones

Copper chaperones deliver Cu to various Cu-binding proteins in the cell. In *S. cerevisiae* and *A. thaliana*, CCS1 delivers Cu to Cu/Zn SOD, ATX1 delivers Cu to the multicopper oxidase on the Golgi membrane and COX17 delivers Cu to the mitochondrion for cytochrome oxidase (Glerum et al. 1996, Wintz and Vulpe 2002). No homologs of ATX1 and CCS1 were found in *T. pseudonana*, but a putative COX17 was identified (*Tp*COX17|264096). Using a text search, another putative Cu chaperone, a homolog of COX11 which is required for cytochrome c oxidase assembly in mitochondria (Tzagoloff et al. 1993), was identified (*Tp*COX11|37139).

COX17 is a 69-amino acid protein in yeast and contains an important functional motif CCxC and a conserved twin Cx<sub>9</sub>C motif that forms a helical hairpin (Heaton et al. 2000, Banci et al. 2008). These conserved motifs were identified in *Tp*COX17|264096 (Figure 4.6a) when it was aligned with its homologues from *S. cerevisiae* (gi|6325125), *A. thaliana* (gi|15217755), *C. reinhardtii* (gi|159484378 ) and *O. lucimarinus* (gi|144578972). The *Tp*COX11|37139 is also highly related to its homologs from other organisms (Figure 4.6b), and contains the essential Cu-binding motif CFCF (Carr et al. 2002).

The relative gene expression of putative chaperone *Tp*COX17|264096 was down-regulated by long-term low Fe, but this reduction was only observed when Cu was sufficient (Figure 4.3, Table 4.2). In contrast, the *Tp*COX11|37139 was up-regulated (1.5-3 fold) by low Fe (Figure 4.3, Table 4.2). Low Cu only down-regulated the gene *Tp*COX11|37139, but only when Fe was also limiting (Figure 4.3). In the Cu-resupply experiment, the relative expression of *Tp*COX17|264096 and *Tp*COX11|37139 was down-regulated significantly (1.5-2.5 fold) 6 hours and 1 hour, respectively, after the Cu addition (Figure 4.4).

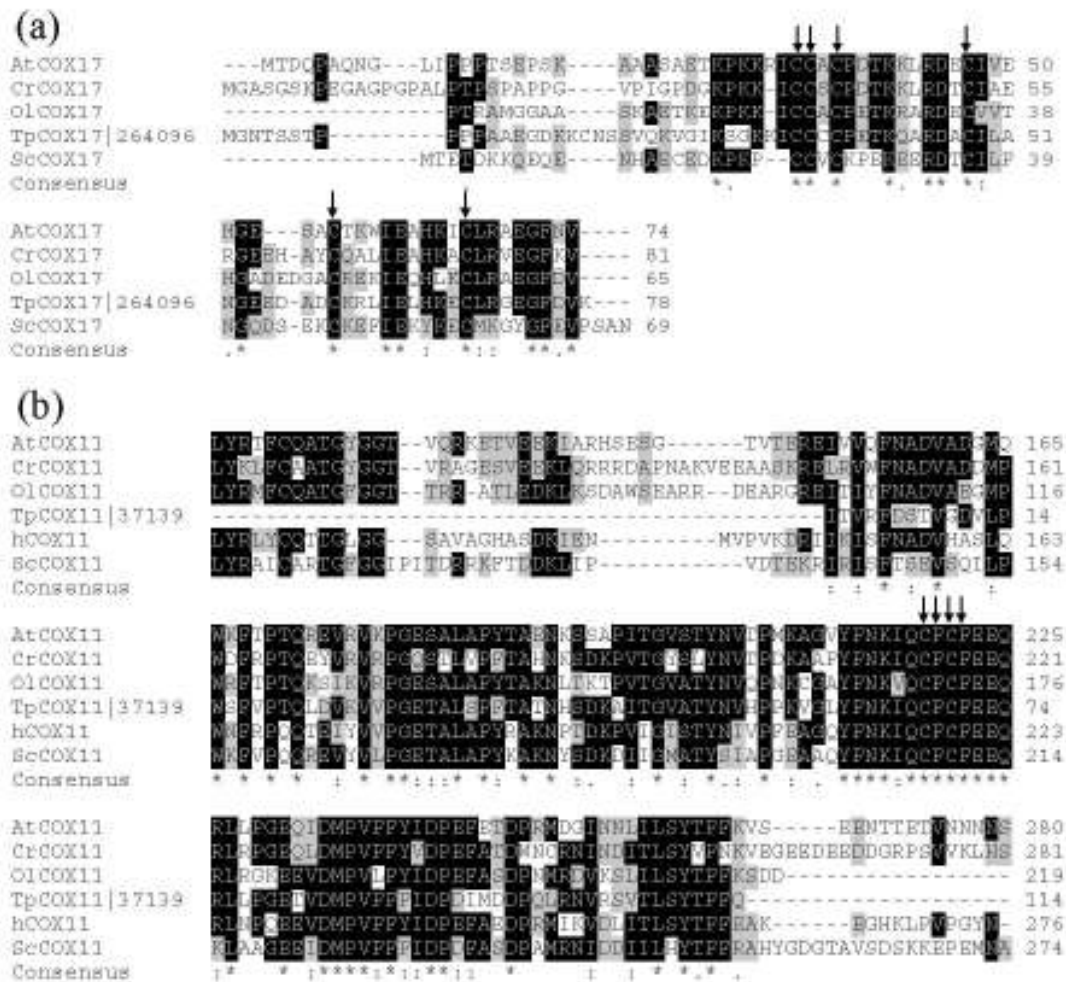


Figure 4.6 Alignment of putative *TpCOX17|264096* (a) and *TpCOX11|37139* (b) from *T. pseudonana* with other known or putative homologous from *S. cerevisiae* (*Sc*), *A. thaliana* (*At*), *C. reinhardtii* (*Ch*), and *O. lucimarinus* (*Ol*). Columns of conserved residues are shaded. Residues found to be essential for function of COX17 and COX11 are indicated with arrows. Asterisks, colons and periods represent identical, strongly similar and weakly similar residues, respectively.

### 4.3.5 Putative ZIP transporters

The ZIP proteins are a large family of  $Zn^{2+}$  and  $Fe^{2+}$  transporters related to the originally characterized ZRT and IRT transporters (Gaither and Eide 2001, Eide 2006, Hanikenne et al. 2008). They are classified into four subfamilies (Guerinot 2000, Gaither and Eide 2001). To search for ZIP homologs in the *T. pseudonana* genome, we used as queries 19 ZIP genes which are members of these four subfamilies. No homologs were found using as queries genes belonging to the subfamily I. Only one gene (*TpZIP|11826*) was found using as queries genes belonging to the subfamily II (*CrZIP6* and *HsZIP1-2*). In contrast, using genes of the *gufA* subfamily (*CrIRT1-2*, *CrZRT4* and *CrZIP2*) as queries five homologs were found, including *TpZIP|32375*, *TpZIP|268980*, *TpZIP|22351*, *TpZIP|268192* and *TpZIP|263800*. In addition, homologs of these five putative *T. pseudonana* ZIPs were found in *O. lucimarinus* genome by blastp search (protein ID are 86026, 42358, 12811 and 27890).

Most ZIP proteins contain eight predicted transmembrane domains (TM1-8) with extracytoplasmic amino- and carboxy-terminal ends (Guerinot 2000). There is a long cytoplasmic loop which is called the “variable region” between TM3 and TM4. The sequences of this loop are not conserved but contain histidine residues which are often involved in metal binding (Gaither and Eide, 2001). In TM4 and TM5, highly conserved histidine residue and adjacent polar or charged amino acids (e.g. serine and glutamic acid) are essential for the functioning of ZIP proteins (Rogers et al. 2000, Gaither and Eide, 2001). These features are also present in the putative *T. pseudonana* ZIPs. Four of the ZIP-like proteins were compared with three *Chlamydomonas* and one *Ostreococcus* protein (*CrIRT1*, *CrIRT2*, *CrZRT4* and *OIZIP|12811*, Figure 4.7). Gene *TpZIP|268192* was omitted because it is 93% identical to *TpZIP|32375* at the nucleotide level. These four putative diatom ZIPs contain 6-8 predicted transmembrane domains, and a long cytoplasmic loop with histidine residues between TM3 and TM4 (not shown). The highly conserved amino acid His in TM4, and His and Glu in TM5 are also present, but the amino acid adjacent to His in TM4 is Asn instead of Ser, except for *TpZIP|268980*

(Figure 4.7). The sequence of *TpZIP|11826* is closely related to subfamily II ZIPs from human (*HsZIP1-2*) and green algae (*CrZIP6*) (Figure 4.8). The alignment shows that the transmembrane domains are more conserved than loops, and *TpZIP|11826* contains His in TM4 and TM5 and Ser in TM4 that are conserved among most family members (Gaither and Eide, 2000, 2001). All these features suggest that these five genes in *T. pseudonana* might be Zn transporters belonging to the ZIP family.

Long-term low Fe and/or low Cu affected differently the relative expression of these five ZIP-like genes (Figure 4.9). Three putative ZIPs were affected by low Fe availability: two of them (*TpZIP|32375* and *TpZIP|11826*) were up-regulated, while one (*TpZIP|268980*) was down-regulated (Figure 4.9). Low Cu down-regulated three putative ZIPs; one of them (*TpZIP|268980*) was affected by low Cu or low Fe to the same extent, while two of them (*TpZIP|11826* and *TpZIP|22351*) were affected by low Cu only under Fe deficient conditions. In contrast, under low Fe conditions, low Cu increased the transcript abundance of *TpZIP|263800* relative to those with high Cu (Figure 4.9). In the Cu resupply experiments, only *TpZIP|32375* increased significantly within 12 hours after Cu addition (Figure 4.10).





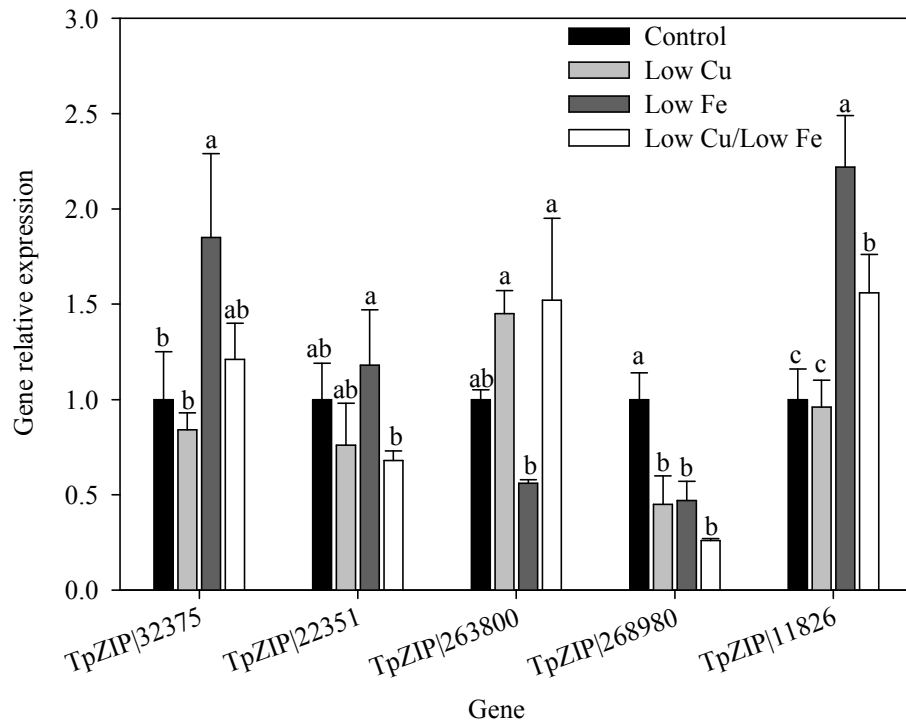


Figure 4.9 Steady-state relative gene expression of putative ZIP-like transporters in *T. pseudonana* under different Fe and/or Cu availability. Each bar represents the mean value ( $\pm$ standard deviation) of three independent cultures. Within each gene, the four treatments were compared statistically (ANOVA Tukey test); the same letters above bars indicate treatments that were not statistically different ( $p < 0.05$ ). Statistical analysis of effect of Fe, Cu and their interactions (Fe $\times$ Cu) on gene expressions by two-way ANOVA see Table 4.2.

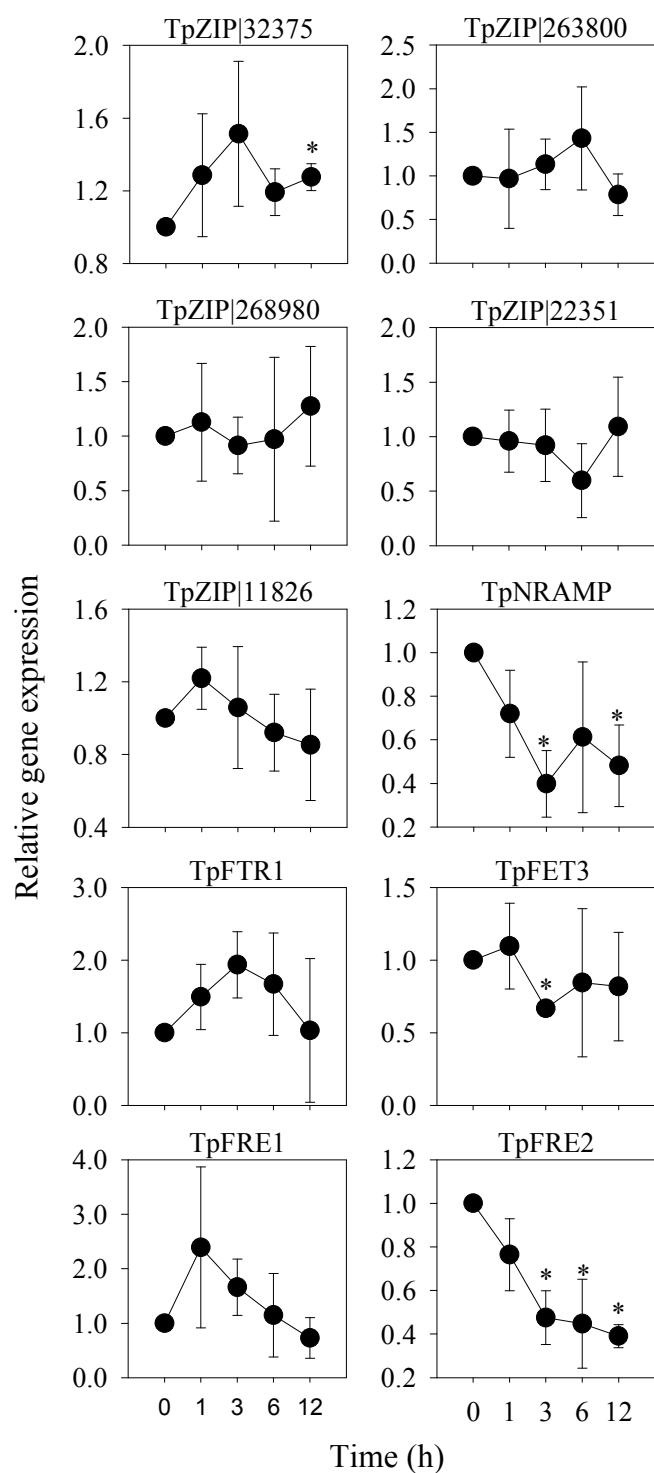


Figure 4.10 The relative gene expression of putative ZIP-like transporters and putative components of Fe transport system in low Cu acclimated *T. pseudonana* supplied with excessive Cu (500 nM). Each point represents the mean value ( $\pm$ standard deviation) of three independent cultures. Within each gene, each point was compared statistically with the control (0 hours) (t-test); the stars above points indicate statistically different ( $p < 0.05$ ).

#### 4.3.6 Relative gene expression of components of Fe uptake system

Components of the high-affinity Fe transporter system in *T. pseudonana* consist of Fe reductases (*TpFRE1* and *TpFRE2*), the Fe transporter (*TpFTR*), and the membrane-bound multi-copper ferroxidase (*TpFET3*). The effect of Fe availability on these components has been well studied by Kustka et al. (2007), though the effects of Cu or the interaction between Cu and Fe nutrition has not been explored. We therefore tested these genes using our low Fe, low Cu, and both low Fe and Cu cultures. Under long-term low Fe and/or low Cu, the transcript abundance of the putative high-affinity Fe transporter *TpFTR* and the putative divalent metal transporter *TpNRAMP* were only affected by Fe availability. Moreover, the degree of up-regulation of these genes in response to Fe limiting concentrations was the highest (35 and 135 fold, respectively, versus 1.6-20 fold for all other 14 genes) among the 16 genes tested in this study. The relative gene expression of the Fe reductases encoding genes *TpFRE1* and *TpFRE2* were up-regulated (5-20 fold) by low Fe regardless of the Cu levels (Figure 4.7a). However, as observed for some of the Cu chaperone genes, co-limitation by Fe and Cu elicited a less pronounced up-regulation of *TpFRE2* than Fe limitation alone (Figure 4.11).

Similar Fe effects were also observed in the expression of the gene *TpFET3*, but the degree of up-regulation was only 1.5 - 2 fold. In contrast, low Cu availability down-regulated the expression of *TpFET3* under both Fe levels, and down-regulated the two Fe reductases under Fe deficient condition (Figure 4.11, Table 4.2). In the Cu re-supply experiments under Fe sufficient condition, the Cu addition down-regulated (2 fold) the relative gene expression of *TpFRE2* after 3 hours and kept this level throughout the rest of the experiment (Fig 10), while it did not affect the gene expression of *TpFRE1*. The transcript level of *TpNRAMP* and *TpFET3* also dropped 3 hours after the Cu addition.

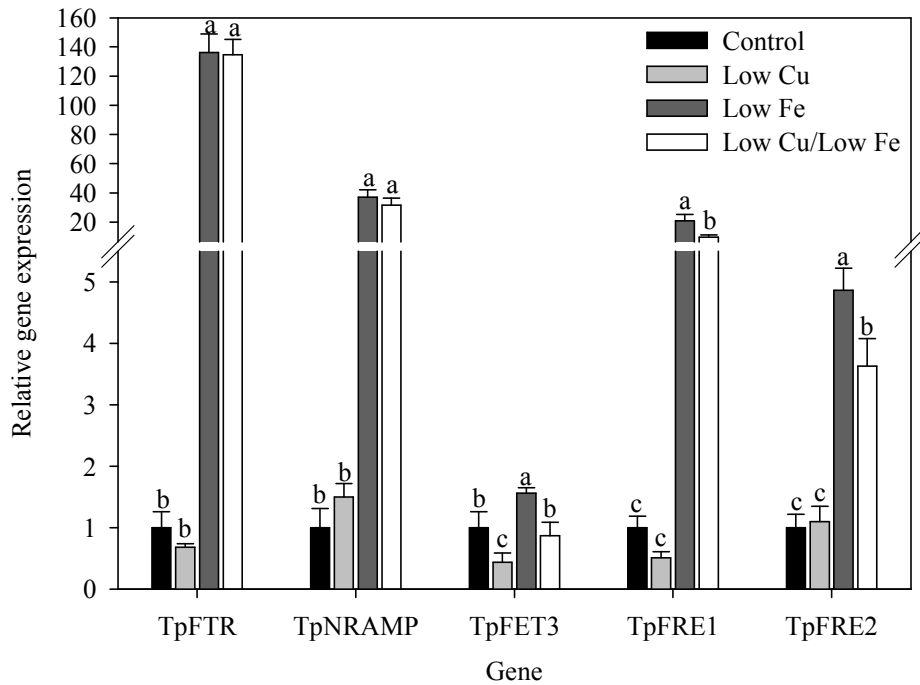


Figure 4.11 Steady-state relative gene expression of putative components for Fe transport in *T. pseudonana* under different Fe and Cu availability. Each bar represents the mean value ( $\pm$ standard deviation) of three independent cultures. Within each gene, the four treatments were compared statistically (ANOVA Tukey test); the same letters above bars indicate treatments that were not statistically different ( $p < 0.05$ ). Statistical analysis of effect of Fe, Cu and their interactions (Fe $\times$ Cu) on gene expressions by two-way ANOVA see Table 4.2.

## 4.4 Discussion

Candidate genes for Cu chaperones, as well as Cu and Zn transporters were identified using transmembrane domains, conserved Cu or Zn binding motifs and the right order of motifs in known homologs in fungi, green algae, plants and animals. The effects of long-term low Fe and Cu levels on the relative expression of these genes were also tested. In general, the effects of low Cu on gene expression were more subtle (1.5-2.5 fold), but still statistically significant, than those of low Fe (1.5- 135 fold). We attribute this result to the significantly slower growth rates achieved by our Fe limited cultures (41% reduction relative to the controls) than our low Cu treatments (0 and 15% reduction in low Cu/high Fe and low Cu/low Fe treatments, respectively). This is due to the trace metal contamination in our cultures (~ 1nM Fe and Cu) relative to the cellular demand of *T. pseudonana* for Fe ( $14 \pm 0.1 \mu\text{mol Fe:mol C}$ , Maldonado and Price 1996) and Cu ( $1.88 \pm 0.8 \mu\text{mol Cu:mol C}$ , Annett et al. 2008). Interestingly, low Fe and Cu availabilities had opposite effects (Table 4.2, Figure 4.3, 4.8 and 4.11). Most of these genes (12 genes) were up-regulated and 2 genes were down-regulated by low Fe. In contrast, no Cu effect was observed when Fe was replete except for TpZIP|268980 and TpFET3, but 8 genes were down-regulated and 2 genes were up-regulated by low Cu under Fe deficient conditions. These data suggest a link between Cu and Fe metabolism, as well as a possible interaction among Zn, Cu and/or Fe transport and homeostasis.

### 4.4.1 Potential components of Cu acquisition system in *T. pseudonana*

In yeast, Cu acquisition includes a low-affinity and a high-affinity Cu uptake system (Puig and Thiele 2002). The high-affinity system is more active in Cu deficient cells, and is comprised of cell surface  $\text{Cu}^{2+}$  reductases and  $\text{Cu}^+$  permease-CTR family transporters (Rees and Thiele, 2004). In this study, we identified two CTR-like Cu transporters TpCTR|24275 and TpCTR|9391. Although the size of these two CTR-like genes is different from other known CTR transporters and the sequence similarity with other homologues is low, these putative CTR-genes have the conserved CTR Cu-binding

motifs and transmembrane domains (see results). In addition, the expression of these two genes was down-regulated by an increase in Cu from 1 to 500nM (Figure 4.4), as observed in other organisms (Dancis et al. 1994, Sancenon et al. 2003, 2004, Page et al. 2009); thus these genes are likely to be an integral part of Cu transport in *T. pseudonana*. However, the down-regulation of the expression of these genes in the short-term Cu resupply experiments is not consistent with the results observed in the steady-state experiments, in which low Cu had no effect on their expression. This difference may be explained by the Cu concentrations in the steady-state experiments (1 nM and 11.2 nM for Cu deplete and replete medium, respectively) versus the Cu resupply experiments (from 1 nM to 500 nM Cu). According to our Cu uptake kinetics study, two Cu uptake systems exist in *T. pseudonana* (Guo et al. 2010). The  $K_m$  of the high-affinity Cu transport system ranges from 52-373 nM, depending on the growth conditions. Thus, given that the Cu concentrations in the steady state experiments were below the  $K_m$ , no significant changes in the relative gene expression of these two CTR-like genes might be expected. This conclusion is also supported by the similarity between the steady-state Cu uptake rates ( $\rho_{ss}Cu$ ) of *T. pseudonana* under 2 and 11.2 nM Cu conditions ( $3.48 \pm 0.52$  versus  $2.92 \pm 0.29$  and  $1.78 \pm 0.73$  versus  $2.51 \pm 0.73 \times 10^{-20}$  mol Cu  $\mu m^{-2} d^{-1}$  under sufficient and deficient Fe condition, respectively) as found in Annett et al. (2008). Given the gene expression, physiological Cu uptake data, and functional structure of these two CTR-like genes, we propose that they encode high-affinity Cu transporters in *T. pseudonana*. To verify this function, functional complementation experiments in loss-of-function yeast mutants are needed.

In the high-affinity Cu transport system in yeast, Cu is reduced from  $Cu^{2+}$  to  $Cu^+$  by plasma membrane Fe reductases (*ScFRE1-2*) before import into the cell (Hassett and Kosman 1995, Georgatsou et al. 1997). In the green alga *Chlamydomonas*, both  $Cu^{2+}$  and  $Fe^{3+}$  are reduced by the same reductase (Weger, 1999). In *Arabidopsis*, the Fe reductases *AtFRO2* and *AtFRO3* exhibit Cu reductase activity under Fe deficiency (Yi and Gueriot 1996; Robinson *et al.* 1999). In addition, Cu and Fe reductase activities in the plasma membrane of pea root are also increased under both Fe and Cu depletion (Welch et al.

1993, Cohen et al. 1997). Thus, plasmalemma bound ferric reductases often reduce  $\text{Cu}^{2+}$ . The putative Fe reductases in *T. pseudonana* (*TpFRE1* and *TpFRE2*) are homologs to the yeast *ScFRE* (Kustka et al. 2007), but only *TpFRE2* was down-regulated by Cu addition in the Cu resupply experiment (Figure 4.10). This suggests that *TpFRE2* may function as a Cu reductase in the high-affinity Cu transport system in *T. pseudonana*.

#### **4.4.2 Intracellular Cu transporters and Cu chaperones in *T. pseudonana***

Two putative Cu-transporting P-type ATPases (*TpCTP|263051* and *TpCTP|264357*) were identified in the *T. pseudonana* genome. Their involvement in Cu homeostasis is suggested by their down-regulation after Cu addition in the Cu resupply experiment (Figure 4.8). The Cu-transporting P-type ATPases normally transport Cu within the cell (Lutsenko and Petris, 2003, Abdel-Ghany et al. 2005). In yeast, the Cu-transporting P-type ATPase *ScCCC2* resides in the trans-Golgi network and delivers Cu to the multi-Cu ferroxidase *Fet3p*. The homologs of *ScCCC2* in *Arabidopsis* are *AtRAN1* and *AtHMA5*. The *AtRAN1* encoded protein is believed to be localized in the ER and delivers Cu to the Cu-binding ethylene receptors (Rodriguez et al. 1999, Chen et al. 2002), whereas *AtHMA5* is believed to be in the plasma membrane or in a late secretory compartment (Pilon et al. 2006). In plants Cu is delivered to plastocyanin and Cu/Zn superoxide dismutase by two additional Cu-transporting P-type ATPases, *AtPAA1* and *AtPAA2*, which transport Cu across the plastid envelope and thylakoids, respectively (Abdel-Ghany et al. 2005). However, the genes encoding plastocyanin and Cu/Zn superoxide dismutase are not found in the *T. pseudonana* genome, thus Cu might not be needed for these proteins. In addition, no signal peptides were found in these Cu-transporting P-type ATPases, which means that they are either cytoplasmic or mitochondrial. Thus, these two putative Cu-transporting P-type ATPases in *T. pseudonana* may function to deliver Cu intracellularly to various compartments for the synthesis of Cu containing proteins.

In the mitochondria, cytochrome c oxidase and its Cu cofactor are critical for cellular survival. The Cu chaperone *COX17* delivers Cu to the mitochondrial inter-membrane

space (Harrison et al. 1999). Another Cu chaperone, COX11, is a membrane-bound mitochondrial Cu<sup>+</sup>-binding protein in yeast (Carr et al. 2002) and may receive Cu from COX17 and assemble Cu into cytochrome c oxidase (Carr et al. 2002). The relative expression of putative *TpCOX17*|264096 and *TpCOX11*|37139 was down-regulated by the 500 nM Cu addition (Figure 4.4), but was unaffected by acclimation to low Cu levels, compared to Cu and Fe replete levels (Figure 4.3). Copper redistribution was observed previously in *Chlamydomonas*, in which Cu was reallocated from plastocyanin to cytochrome oxidase under Cu deficient condition (Merchant 2006). Copper redistribution may also occur in *T. pseudonana* by changing the expression of these Cu-transporting P-type ATPases and Cu chaperones.

#### **4.4.3 Transcriptional activation of Fe transport-related genes in response to Cu deficiency**

The gene expression of putative Fe permeases (*TpFTR*), Fe reductases (*TpFRE1* and *TpFRE2*), multi-Cu ferroxidases (*TpFET3*) and *TpNRAMPs* was up-regulated under Fe deficient conditions (Figure 4.11), indicating the activation of the high-affinity Fe uptake system. These results are consistent with those of Kustka et al. (2007) with *TpFET3* as an exception. In Kustka et al. study (2007), Fe deficiency did not change the transcript abundance of *TpFET3*, while in our study, low Fe increased its abundance by 1.5 and 2-fold when Cu was sufficient and deficient, respectively. However, this change is marginal compared to the results of Maldonado et al. (2006) in which a 60-fold increase was observed. We are unable to explain this discrepancy, as similar concentrations of free Cu are found in our culture media.

The gene expression of some of these Fe transport-related genes was regulated by Cu availability. *TpFET3*, *TpFRE1* and *TpFRE2* were down-regulated by long-term low Cu (Figure 4.11), and *TpFET3*, *TpFRE2*, and *TpNRAMP* were down-regulated by short-term Cu addition (Figure 4.10), suggesting that Cu may also be involved in Fe homeostasis. As found in our study, Cu deficiency did not affect the expression of the Fe permease

(FTR) in *Chlamydomonas* (La Fontaine et al. 2002). Meanwhile, the effect of Cu deficiency on the transcript abundance of *TpFET3* (two-fold down-regulation) was opposite to that (~2 to 3-fold up-regulation) of *CrFOX* (the homolog of FET3 in *Chlamydomonas*, La Fontaine et al. 2002). However, in accordance with our results, the protein abundance of *CrFOX* was about 10-fold lower in Cu deficient cells (La Fontaine et al. 2002), suggesting that the multi-Cu ferroxidase abundance was controlled by Cu levels at the post-transcriptional level (La Fontaine et al. 2002). This might also be the case for *TpFET3*.

#### **4.4.4 Copper and Fe deficiency induce changes in Zn transporters**

Some members of ZIP family in yeast and plant are involved in Cu uptake (Grotz et al. 1998, Waters and Eide, 2002, Wintz et al. 2003). In yeast, *ScFET4* is involved in low-affinity Cu transport (Hassett et al. 2000), and is a Zn and Fe transport protein (Waters and Eide, 2002). In the plant *Arabidopsis*, *AtZIP2* and *AtZIP4* may function in Cu uptake due to their complementation of the yeast *CTR1* mutant, which is defective in high-affinity Cu uptake (Wintz et al. 2003). In our study, the ZIP-like gene *TpZIP|263800* was up-regulated by Cu deficiency when Fe was also low, suggesting that it is involved in Cu uptake under low Fe condition.

The putative ZIPs *TpZIP|32375* and *TpZIP|11826* were up-regulated by Fe deficiency, while *TpZIP|268980* was down-regulated. Zinc homeostasis changes induced by Fe deficiency were observed in *Arabidopsis* (Buckhout et al. 2009). More specifically, the transcript abundance of one Zn plasma membrane efflux carrier and two Zn vacuolar influx carriers was up-regulated by Fe deficiency, while Zn plasma membrane influx carrier was down-regulated (Buckhout et al. 2009). The regulation induced by Fe was defined as a secondary effect (Yang et al. 2010), where Zn uptake and efflux capacity has to be adjusted when the Zn uptake exceeded nutritional cellular requirement. The increase in Zn uptake was mediated by the up-regulation of a low affinity divalent transporter (*AtIRT*) under Fe deficiency (Korshunova et al. 1999, Buckhout et al. 2009,

Yang et al. 2010). In the oceanic diatom *T. oceanica*, it has been suggested that  $\text{Fe}^{2+}$  may enter the cell through a putative divalent metal transporter under Fe deficiency (Lane et al. 2008). In *T. pseudonana*, cellular internalization of  $\text{Fe}^{2+}$  by divalent metal ion transporters (ie. NRAMP) has been suspected, though it was hypothesized that such transporters might instead participate in mobilizing Fe out of intracellular vacuoles (Kustka et al. 2007). At present the function of these Fe regulated ZIP genes in *T. pseudonana* is unknown. If these genes encode for Zn transporters similar to those in *Arabidopsis*, the putative *TpZIP|32375* and *TpZIP|11826* may mediate cellular Zn efflux at the plasma membrane or vacuolar Zn influx, while *TpZIP|268980* may function as a Zn uptake transporter at the cell surface.

In this study, we identified genes encoding the putative CTR-like Cu transporters, Zn transporters, and Cu chaperons in the diatom *T. pseudonana*. We also postulate that genes showing differential expression in response to different Cu concentrations are most likely to be involved in Cu homeostasis. In addition, a possible strong link between Cu and Fe metabolism was observed. Although these putative genes are proved to be good candidates for Cu transporters and chaperones on the basis of sequence analysis and gene expression, there are still many unresolved questions. The position and functions of the putative CTR transporters and P-type Cu transport ATPases are not known, and how these proteins are regulated at the post-translational level remains to be investigated. Performing yeast complementation experiments, using fluorescent metal binding dyes to determine Cu distribution within cells, and using proteomic approaches to study specific responses to Cu and/or Fe deficiency in *T. pseudonana* may help our understanding of the roles that each transporter and chaperone is playing in Cu homeostasis.

## Chapter 5

**Functional complementation of *Saccharomyces cerevisiae ctr1Δctr3Δ* double-mutant (MPY17) by expression of *Thalassiosira pseudonana* CTRs**

## 5.1 Introduction

Cu transporters (CTR) are important components of cellular Cu homeostasis (Puig and Thiele, 2002, Merchant et al. 2006, Puig et al. 2007). They control Cu uptake from the environment, as well as Cu sequestration and distribution inside the cell. In eukaryotes, most CTR family members are documented to be canonical Cu permeases (Puig and Thiele 2002, Page et al. 2009, Puig et al. 2007). They were first found in the yeast *Saccharomyces cerevisiae*, a model organism for investigating Cu transport mechanisms. Cu transporters in *S. cerevisiae* include *ScCTR1* and 3, which are high-affinity Cu transporters in the plasma membrane, and *ScCTR2*, whose sequence is similar to *CTR1* but functions as a low-affinity Cu transporter in the vacuole membrane (Kampfenkel et al., 1995). Later, more CTR homologs were indentified in animals, plants, fungi and green algae by functional complementation of a high-affinity Cu transport deficient *S. cerevisiae* mutant (Labbe et al. 1999, Zhou and Gitschier, 1997, 2001, Lee et al. 2000, Sancenon et al. 2003, Page et al. 2009). Two CTR proteins were indentified in humans, including *hCTR1* and *hCTR2* (Zhou and Gischier 1997). Protein *hCTR1* is the homolog of *ScCTR1* and is localized to the plasma membrane. Protein *hCTR2* is similar to *hCTR1*, and is localized to the plasma membrane and in late endosomes and lysosomes, but its function is currently unknown. In the plant *Arabidopsis*, six CTR members are known as COPT 1-6 (Sancenon et al. 2003, Puig et al. 2007). Among these, COPT1 and COPT2 are believed to be Cu transporters localized to the plasma membrane, as they are able to fully rescue the growth of the high-affinity Cu transport deficient yeast *ctr1Δ* mutant. In contrast, COPT3 and COPT5 may function in intracellular Cu transport, as these two partially rescue the growth of the *ctr1Δ ctr3Δ* yeast mutant (Sancenon et al. 2003, Puig et al. 2007). The functions of COPT4 and COPT6 are still unknown (Puig et al. 2007). Four CTR homologs (*ChCTR1-3* and *ChCOPT1*) were indentified in the green algae *Chlamydomonas*. *ChCTR1* and *ChCTR2* are established as the Cu assimilatory transporters and localized to the plasma membrane, while *ChCTR3* may be a soluble protein. To date CTR proteins have been identified and characterized in many organisms,

including the fission yeast *Schizosaccharomyces pombe* (*SpCTR4*, *SpCTR5* and *SpCTR6*, Zhou and Thiele 2001, Bellemare et al. 2002, Beaudoin et al. 2006), the rice *Oryza sativa* (*OsCOPT1* and *OsCOPT5*, Yuan et al. 2010), the fruit fly *Drosophila melanogaster* (*DmCTR1A*, B and C, Zhou et al. 2003), the mouse *Mus musculus* (*mCTR1*, Lee et al. 2000), the lizard *Podarcis sicula* (*PsCTR1*, Riggio et al. 2002), and the bony fish *Danio rerio* (*DrCTR1*, Mackenzie et al. 2004).

Although the size and the amino acid sequences of CTR proteins vary among family members, most CTR family proteins have structurally conserved domains and Cu-binding motifs (Dumay et al. 2006, DeFeo et al. 2007). CTRs have three transmembrane (TM1-3) domains (Dumay et al. 2006), an extracellular N-terminus and an extracellular short loop between TM2 and TM3 (Figure 5.1a). The second transmembrane domain (TM2) contains a conserved MxxxM motif which is important for Cu uptake (Puig et al. 2002), while TM3 contains a conserved GxxxG motif that is required for the trimeric assembly of CTR molecules (Aller et al. 2006). These two motifs formed the CTR-signature motif MxxxM-x<sub>12</sub>-GxxxG (Figure 5.1 and 5.2) (De Feo et al., 2007). The extracellular N-terminus contains Met and/or Cys-riched Cu-binding motifs. Most CTR members contain Met-riched motifs in N-terminus (MxM and/or MxxM, Dumay et al. 2006). These motifs are repeated eight times in *ScCTR1* (Dancis et al. 1994b), twice in *hCTR1* (Zhou and Gischier 1997) and *mCTR1* (Lee et al. 2000), and five times in *SpCTR4* (Labbe and Thiele 1999). In *ScCTR3*, these motifs are absent, and instead, an abundance of cysteine residues exist throughout the protein and within its putative transmembrane domains (11 Cys of 241 total residues, Koch et al. 1997). In the green algae *Chlamydomonas*, Cys and Met-containing motifs exist in the N-terminus; the most common form is a novel Cys-Met motif (CxxMxxMxxC-x<sub>5/6</sub>-C Page et al. 2009). In the intracellular C-terminus of CTR proteins, some functionally important charged amino acids, cysteine and histidine, exist (Peñas et al. 2005). These conserved characteristics and functions of CTR proteins in animal, plant, green algal and fungal genomes suggest that CTRs perform a common and essential role in eukaryotes. In addition, genetic, biochemical and electron microscopy analyses have suggested that CTR proteins

assemble as a homotrimer and form a pore in the membrane (Figure 5.1b, Nose et al. 2006, Dancis et al. 1994a, Pena et al. 2000, Aller and Unger 2006). With Cu accumulation experiments, CTRs have also been suggested to be highly specific for  $\text{Cu}^+$  (Eisses and Kaplan 2002, Lee et al. 2002, Page et al. 2009).

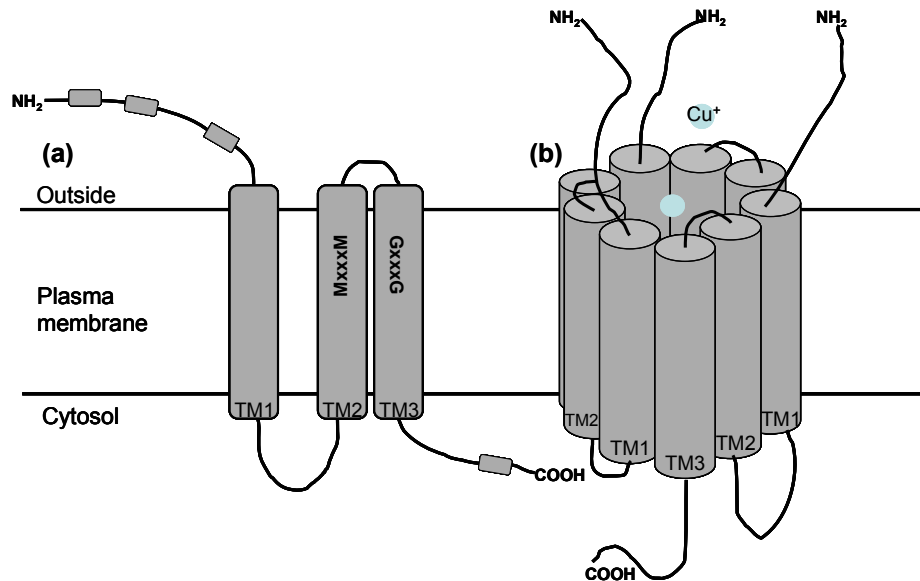


Figure 5.1 Membrane topological structure model (a) and homo-trimer structure (b) of CTR family proteins. Extracellular Met-enriched motifs and intracellular Cys/His motifs are indicated by small gray boxes (Redrawn from Kim et al. 2008).



The Cu affinity, half-saturation constant ( $K_m$ ), of CTR proteins is  $\sim 1-5 \mu\text{M}$  in yeasts, humans and plants (Lin and Kosman 1990, Dancis et al. 1994a, Kampfenkel et al. 1995, Zhou and Gitschier 1997, Eisses and Kaplan 2002, Lee et al. 2002, ) and  $0.2 \mu\text{M}$  in *Chlamydomonas* (Hill et al. 1996). The activity of these CTR proteins can be regulated by Cu concentration at the transcriptional and post-transcriptional levels. However, the patterns of regulation of CTR proteins by Cu are not universal. For example, in yeast, *Arabidopsis* and *Chlamydomonas*, the transcription of CTR proteins is activated when Cu is deficient and repressed when Cu is sufficient (Dancis et al. 1994a., Labbe et al. 1997, Page et al. 2009, Yamaguchi-Iwai et al. 1997, Zhou and Thiele 2001, Sancenon et al. 2004). In contrast, such regulation is not found in mammals (Lee et al. 2000, Tennant et al. 2002). At the post-transcriptional level, for *ScCTR1* and *hCTR1*, endocytosis is induced by low Cu ( $0.1-1 \mu\text{M}$ ), while degradation at the plasma membrane is induced by high Cu ( $10 \mu\text{M}$  or more for *ScCTR1* and  $100\mu\text{M}$  for *hCTR1*, Ooi et al. 1996. Petris et al. 2003). Such Cu-induced degradation of the CTR proteins would downregulate or prevent excessive Cu uptake when Cu level is elevated (Petris et al. 2003).

The function of the CTR family proteins and their multi-level regulation have been well studied in many organisms, but not in marine phytoplankton. Our results of Cu uptake kinetics in the marine diatom *T. pseudonana* suggest that a high-affinity Cu transport system does exist, with a  $K_m$  of  $\sim 0.2 \mu\text{M}$ . We have also identified two putative CTR homologs in the genome of this diatom (*TpCTR|24275* and *TpCTR|9391*; Chapter 4), using blast searches and the characteristic functional motif of known CTR genes. *TpCTR*s contain three transmembrane domains (TM1-3, Figure 4.1a of Chapter 4) and the CTR-signature motif  $\text{MxxxM-x}_{12}\text{-GxxxG}$ . The N-terminus of *TpCTR* proteins includes metal-binding motifs containing Cys, Met and His, although these motifs are different from those of CTR proteins of *S. cerevisiae* (*ScCTR1*, gi|1345859) and *A. thaliana* (*AtCOPT1*, gi|15237802). However, an alignment of *TpCTR|24275* with homologs from *Phaeodactylum tricornutum*, *Ostreococcus lucimarinus*, *Micromonas pusilla* and *Perkinsus marinus* indicates that it shares a number of putative conserved Cu-binding residues and motifs, including HxH,  $\text{Cx}_{6/7}\text{CxxxC}$ , HxxxC and  $\text{Cx}_{5/8}\text{MxM}$  (Figure

4.2 of Chapter 4). Indeed, these are most similar to the Cys-and Met-containing motifs of *Chlamydomonas* (CrCTR1, jgi|196101). In addition, except for two Met-containing motifs (MxxM) and one Cys and His-containing motif (Cx<sub>4</sub>Hx<sub>5</sub>H), the N-terminal motifs of *TpCTR|9391* are most similar to that of COPT1 in the green alga *Chlamydomonas* (Page et al. 2009) and the vascular plant *Arabidopsis* (Kampfenkel et al. 1995), which contain His and Met-riched Cu binding motifs (Mx<sub>3</sub>Mx<sub>3</sub>HxMHxMxHx<sub>2</sub>MHHxMxHxMxH, Hx<sub>2</sub>HxMxMM, and MxMx<sub>3</sub>H). This combined evidence points to these two putative genes (*TpCTR|24275* and *TpCTR|9391*) as the candidates genes of CTR transporters in *T. pseudonana*. Moreover, the transcription levels of these two genes were down-regulated under excess 500 nM Cu addition. Given the gene expression, physiological Cu uptake data, and functional structure of these two CTR-like genes, we hypothesized that these two putative CTR-like genes encode the high-affinity Cu transporters in *T. pseudonana*. In order to test their function, we assessed the ability of *TpCTR|24275* and *TpCTR|9391* to complement the inability of *S. cerevisiae* mutant MPY17 to grow on non-fermentable carbon sources due to their high-affinity Cu transport deficiency.

## 5.2 Materials and Methods

### 5.2.1 Organisms and growth conditions

*Thalassiosira pseudonana* clone 3H (CCMP1335) was acclimated to Fe replete/low Cu conditions (pFe19\_pCu15.1) under continuous light at 150  $\mu\text{mol photons m}^{-2} \text{ s}^{-1}$  at 19 $\pm$ 1 °C. The growth medium was sterile, artificial seawater AQUIL (Price et al. 1988/1989). The medium was prepared and had identical chemical composition as that described in Maldonado et al. (2006). The yeast strain used in this study was MPY17 (genotype *MATa gall trp1-1 his3 $\Delta$ 200 ura3-52 ctr1::ura3::Kn<sup>r</sup> ctr3::TRP1 his3 lys2-801 CUP1'*) (Peña et al. 1998). Yeast cells were kindly provided by Dr. Thiele (Duke

University) and were maintained on YPD plates (1% yeast extract, 2% bactopectone and 2% dextrose). Synthetic complete plates lacking uracil (SC-ura) were used for the selection of yeast transformants. YPEG medium (1% yeast extract, 2% bactopectone, 2% ethanol and 3% glycerol) was used to test the growth of the yeast transformants with target CTR genes.

### **5.2.2 Cloning of putative CTR-like genes in *T. pseudonana***

Total RNA was isolated from *T. pseudonana* using the RNAqueous™ kit (Ambion, Austin, TX, USA) followed by DNase treatment for 1 hour using TURBO-DNA-free kit (Ambion). cDNAs were then synthesized using Superscript II (Invitrogen, Carlsbad, CA, USA). To clone the putative CTR-like genes, PCR reaction was carried out using the cDNA as a template with the primers *TpCTR|24275* -F (TAATGAAAACGACCGTGC TGACA), *TpCTR|24275*-R (CCTTACAAAGTGAAGTACAGCA), *TpCTR|9391*-F (CTATGAGTGAATCCACGTCATCA) and *TpCTR|9391*-R (AATCACGGATCCTCC GGTGGCAT). *Pfu* DNA polymerase (Invitrogen) was used in the PCR reactions following the manufacture's instruction. The PCR products were then analyzed by electrophoresis and purified using the QIAquick PCR Purification Kit ( Qiagen) for the cloning.

The purified PCR products were inserted into TOPO® TA cloning vector pCR®2.1 (Invitrogen) and then transformed into One Shot® TOP10 Chemically Competent *Escherichia coli* cells (Invitrogen). The transformants were cultured and selected on LB agar plates with 50 µg/mL kanamycin overnight at 37°C. Five to ten colonies were picked for each gene and grown overnight at 37°C in 5 mL LB media with ampicillin. The recombinant vectors were then isolated using the QIAprep Spin Miniprep Kit (Qiagen) and sequenced (Macrogen, USA) to confirm the DNA sequence of the target genes.



### 5.3 Results and Discussion

Compared to the negative control cells (yeast mutant MPY17), transformed yeast cells with plasmid p416GPD or with plasmid p416GPD and target genes were able to grow on SC-ura plates (Figure 5.3), indicating that the transformation was successful and that the plasmid was expressed in the yeast. However, the transformants with plasmid and putative *T. pseudonana* CTR-like genes (*TpCTR|24275* and *TpCTR|9391*) were unable to grow on YPEG plates, which contained the non-fermentable carbon sources ethanol and glycerol (in Figure 5.1). The basic principle of the functional complementation experiments is that yeast growth depends on the uptake of the substrate of the transporter of interest. The functional complementation analysis in this study was performed in the yeast strain MPY17 which is a *S. cerevisiae* double-mutant, lacking the high affinity Cu transport genes CTR1 and CTR3 (Pena et al. 1998). A consequence of the high affinity Cu uptake defect is the absence of functional cytochrome c oxidases which are essential for the proper functioning of the mitochondrial respiratory electron transport chain. Thus, this yeast mutant can not grow on YPEG plates because it lacks functional cellular respiration. However, the mutation can be complemented by the expression of CTR-type Cu transporters from other organisms, including CTR genes from humans, mice, fission yeasts and plants (Zhou and Gitschier, 1997, Zhou and Thiele 2001, Lee et al. 2000, Sancenon et al. 2003). Our two putative CTR genes did not complement yeast  $\Delta ctr1 ctr3$  mutant MPY17, indicating that these two genes can't function as high-affinity Cu transporters in this mutant.

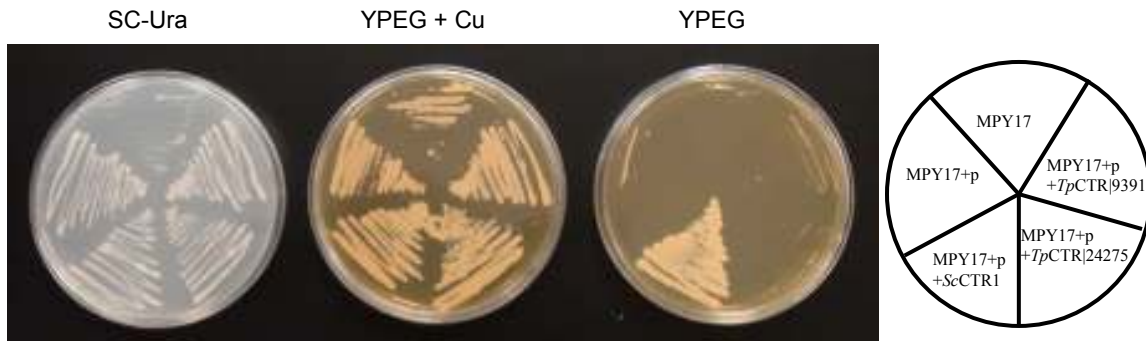


Figure 5.3 Non-functional complementation of the yeast mutant MPY17, which is deficient in high affinity Cu transport, by putative *T. pseudonana* CTR-like genes *TpCTR|24275* and *TpCTR|9391*. MPY17 cells and transformed MPY17 cells with vector p416GPD were negative controls. Transformed MPY17 cells with vector p416GPD and yeast CTR1 (*ScCTR1*) were positive control. Yeast cells were grown for 2 days on glucose SC-ura select plates, ethanol/glycerol (YPEG) plates and Cu-enriched ethanol/glycerol (YPEG + 100  $\mu$ M CuSO<sub>4</sub>) plates.

The expression of these genes in yeast mutant cells includes two levels: the transcript and the protein level. In order to test the expression of our target CTR genes in the yeast mutant at the transcription level, we amplified the putative *TpCTR|24275* and *TpCTR|9391* from the transformed yeast cells. The length of ORFs of *TpCTR|24275* and *TpCTR|9391* are 2310 and 1032 bp, respectively. Both putative CTR genes can be amplified from the cDNA of transformed yeast cells (Figure 5.4), suggesting that the plasmid construction and yeast transformation were successful, and indicating that both putative CTR-like genes were expressed at the transcript level. We therefore propose some possible explanations for our functional complementation results. One possibility is that these two *T. pseudonana* CTR-like genes (*TpCTR|24275* and *TpCTR|9391*) are Cu transporters but are not localized to the plasma membrane. They may be localized to the tonoplasts to maintain Cu homeostasis in the cytosol, like gene *ScCTR2*, a low-affinity Cu transporter on the tonoplast of yeast cells (Kampfenkel et al., 1995). Another possibility is that these two CTR proteins are localized in the plasma membrane, but do not function as high-affinity Cu transporters. Alternatively, these proteins may function as high-affinity Cu transporters on the plasma membrane, but they can't work independently, as they might need other components to form a heteromeric protein complex to perform the Cu transport function. The heteromeric CTR protein complex has been observed in *S. pombe* and rice *Oryza sativa* (Zhou and Thiele 2001, Loannoni et al. 2010, Yuan et al. 2011).

In general, it is suggested that *S. cerevisiae* CTR1, CTR3, and human CTR1 are homotriplexes (Figure 5.1). They work independently as high-affinity Cu transporters and appear to be functionally redundant (Knight et al. 1996, Pena et al. 2000). In addition, Cu transporters can be heteromeric protein complexes. The Cu transport complex containing at least two distinct partners was first found in *S. pombe*, in which CTR4 and CTR5 form a dual partner complex (Zhou and Thiele 2001, Loannoni et al. 2010). The co-expression of both subunits is required for their function as a Cu transporter: when CTR5 is absent, the heterologous expression of only CTR4 in Cu-transport defect *S. cerevisiae* mutant can't complement the yeast Cu uptake. Meanwhile, the presence of both CTR4 and

CTR5 determines their proper localization to the plasma membrane; otherwise, each protein is confined to an intracellular compartment (Zhou and Thiele 2001). This kind of heteromeric protein complex was also identified in rice *O. sativa* which contains 7 COPT proteins (COPT1-7). The Cu-transport defect phenotype of yeast *S. cerevisiae* mutant can be complemented by co-expression of proteins COPT1, COPT5 and protein XA13 (Yuan et al. 2010), and co-expression of COPT2, COPT3, or COPT4 with COPT6, respectively (Yuan et al. 2011). Thus, further complementation experiments of the co-expression of *T. pseudonana* putative CTR genes may be needed to test their function as a high-affinity Cu transporter. Meanwhile, determination of their cellular location and their expression at the protein level in *T. pseudonana*, grown under different Cu levels will be helpful to elucidate their functions.

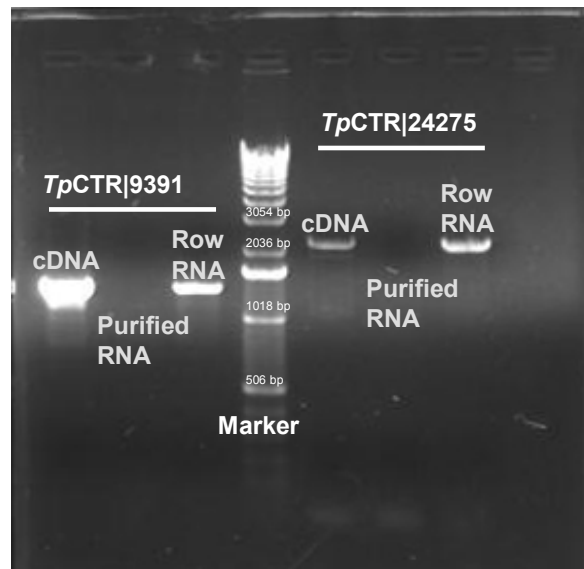


Figure 5.4 PCR products of putative CTR-like genes *TpCTR|24275* and *TpCTR|9391* from cDNA of transformed yeast cells. Row RNA (RNA+DNA) and purified RNA are positive and negative controls, respectively.

## **Chapter 6**

### **General conclusion**

## 6.1 Summary of major findings and contributions

To date, most investigations on Cu and marine phytoplankton have focused on Cu toxicity. Laboratory and field studies have shown that high dissolved Cu(II) concentrations in some coastal areas inhibit the growth of certain phytoplankton taxa (Brand et al. 1986) and thus affect phytoplankton community composition (Sunda et al. 1981; Moffett et al. 1997). In turn, marine phytoplankton may influence the speciation of dissolved Cu by releasing strong Cu-binding organic ligands in response to Cu toxicity (Moffett and Brand 1996; Croot et al. 2000; Vasconcelos and Leal 2001). For example, some studies indicated that phytoplankton, including *E. huxleyi*, *T. pseudonana*, and *Dunaliella sp.*, could produce glutathione and other thiol-containing compounds in response to Cu additions (Leal et al. 1999, Ahner et al. 2002, Dupont and Ahner 2005). Furthermore, metabolic and transcriptional responses to Cu toxicity have also been investigated in some marine diatoms and cyanobacteria (Reinfelder et al. 2000, Davis et al. 2006, Stuart et al. 2009). However, less is known about the physiological roles of Cu in marine phytoplankton, and the mechanism of Cu assimilation at physiological and molecular (gene and protein) levels.

Copper is an important redox active transition metal, acting as a cofactor in many enzymes that scavenge reactive oxygen species or catalyze redox reactions. In addition to the well known role of Cu in respiration for most organisms (cytochrome oxidase, Stryer 1988), earlier studies on marine phytoplankton also showed that Cu is involved in the detoxification of superoxide radicals (i.e., Cu-containing superoxide dismutases; Chadd et al. 1996), and the breakdown of organic N sources (Palenik et al. 1988, 1989). The importance of Cu for phytoplankton metabolism has been emphasized in recent years, especially for phytoplankton in the open ocean and those experiencing Fe limitation. For example, a recent study has shown that Cu is essential for photosynthesis in the oceanic diatom, *T. oceanica*, which uses the Cu-containing electron carrier, plastocyanin, instead of the most widely used Fe containing cytochrome  $c_6$  (Peers and Price 2006). The replacement of Fe with Cu allows *T. oceanica* to lower its Fe requirement, and thus grow

more efficiently in the low Fe waters that it inhabits. Copper is also important for some phytoplankton when experiencing Fe limitation, as their high affinity Fe transport system requires Cu for the proper functioning of Cu-containing ferric oxidases.

The micronutrient iron limits primary productivity in 30% of the global ocean. In these regions, phytoplankton may have a higher demand for Cu in order to acquire Fe more efficiently, using their high affinity Fe transport system. In addition, the concentrations of Fe are significantly lower in the open ocean than in coastal waters. The replacement of Fe with Cu in oceanic phytoplankton might allow them to survive in waters with low Fe. In light of these findings, increased attention has focused on the role of Cu as a micronutrient for phytoplankton growth. When I started my PhD research, some of the unanswered questions regarding Cu nutrition included: a) what are the mechanisms of Cu acquisition and homeostasis in marine phytoplankton? b) is the replacement of Fe with Cu in some metabolic pathways a common survival strategy of oceanic phytoplankton inhabiting low Fe waters? c) does Fe limitation increase the demand for Cu in phytoplankton from a variety of phyla? d) are high affinity Cu organic ligands produced under Cu limitation? e) are phytoplankton able to access Cu within these organic complexes or do they rely exclusively on dissolved inorganic Cu? f) how do Fe and Cu availability interact in controlling intracellular Cu demand, Cu uptake kinetics, Cu transport rates and the expression of genes encoding for Cu transport proteins or Cu chaperones?

The overall goal of my dissertation was to elucidate the Cu requirements of various phytoplankton taxa, as well as to determine mechanisms of Cu acquisition and homeostasis in model species. To accomplish this goal, I used a multidisciplinary approach, complementing physiological and molecular research. Given the interaction between Fe and Cu nutrition observed in four previous phytoplankton studies (Peers et al. 2005, Well et al. 2005, Maldonado et al. 2006, Annett et al. 2008), I also studied how both Fe and/or Cu availability (at optimal and limiting levels) control these mechanisms. Using short-lived Cu radioisotopes, the Cu requirements and steady-state Cu transport

rates ( $\rho_{ss}\text{Cu}$ ) of multiple phytoplankton genera, as well as Cu uptake kinetics of two marine centric diatoms, an oceanic (*T. oceanica*) and a coastal isolate (*T. pseudonana*) were investigated. Furthermore, putative genes encoding the potential components of Cu transport and homeostasis in the model coastal diatom *T. pseudonana* were identified, and their expression responses to different Fe and/or Cu conditions were investigated. Finally, the function of putative Cu transporters (CTR) in *T. pseudonana* was examined with functional complementation experiments using a yeast mutant deficient in high affinity Cu transport.

In chapter 2, I studied the interactive effects of Fe and Cu availability on the growth rates, intracellular Cu levels (Cu quotas) and steady-state Cu transport rates ( $\rho_{ss}\text{Cu}$ ) of 12 phytoplankton [from four phyla and two marine habitats (coastal and oceanic)]. My results demonstrate that low Cu has a significant effect on the growth rates and  $\rho_{ss}\text{Cu}$  of the oceanic phytoplankton strains, but not the coastals. Distinct trends in Cu quotas were observed for phytoplankton from various phyla, however, these patterns were dependent upon the element used as a proxy for phytoplankton biomass (P vs. C). My results highlight an urgent need for a more consistent proxy for phytoplankton biomass. Given the interaction between trace metal geochemical cycles and the global C cycle, I believe that C is the most appropriate phytoplankton biomass proxy. Contrary to my original hypothesis, the Cu quotas (Cu:C) of all the oceanic strains were not higher than those of the respective coastal strains. However, there were multiple lines of evidence supporting a more important role of Cu in the physiology of the oceanic phytoplankton. Yet, only some phytoplankton had significantly higher Cu:C ratios when Fe was limited, suggesting that the role of Cu in the high-affinity Fe transport system is not universal. My study on Cu requirements uses diverse and ecologically relevant phytoplankton species and thus provides a better understanding of how the interaction between Fe and Cu availability in the sea controls marine phytoplankton composition and productivity.

In chapter 3, I was the first to establish biphasic Cu uptake rates as a function of Cu concentrations in marine phytoplankton, using two diatoms as model organisms (one

coastal and one oceanic). The results suggest the existence of a high and a low affinity Cu transport system in marine phytoplankton. Furthermore, the high and the low Cu transport systems have different kinetics in the coastal and the oceanic diatom, potentially reflecting the evolutionary adaptation of these organisms to their respective trace metal regimes. Specifically, *T. oceanica* has the highest affinity Cu transport system ( $K_m = 7.3$  nM Cu) of any phytoplankton studied to date, in agreement with the lower Cu concentrations found in the open ocean relative to those in coastal waters. The kinetics of Cu uptake in *T. oceanica* and *T. pseudonana* were affected differently by Fe and/or Cu availability suggesting that Cu transport is regulated dynamically, in a complex manner, by both Fe and Cu. My calculated rates of Cu uptake by indigenous phytoplankton in this thesis suggest that field communities will have an active high-affinity Cu transport system in open ocean waters where the total Cu concentrations are  $\leq 2$ nM.

In chapter 4, I identified and characterized the genes encoding the potential components of Cu acquisition and homeostasis mechanisms using the coastal diatom *T. pseudonana* as a model organism. The candidate genes were identified using transmembrane domains, conserved Cu binding motifs and the right order of motifs in homologues in other eukaryotic organisms. The expressions of these genes under various Fe and Cu culture conditions were also investigated. Among the genes identified, I found genes encoding the putative low (ZIP-like) and high affinity (CTR-like) Cu transport proteins. My results suggest a significant role for Fe in controlling the expression of Cu-related genes, as well as a complex interaction between Cu and Fe response networks in this diatom. These data provide fundamental molecular information to further study the mechanisms of Cu acquisition and homeostasis in marine phytoplankton.

## 6.2 Conclusions and findings for specific dissertation hypotheses

### 6.2.1 Oceanic phytoplankton have a higher Cu demand for growth than coastal strains

Though Fe availability limits primary productivity in 30% of the global ocean, phytoplankton growth rates in these regions are moderate, averaging  $\sim 0.3 \text{ d}^{-1}$  (Welschmeyer et al. 1991). Estimates of phytoplankton Fe demand rate in these regions are well above the calculated Fe supply rate. Thus, in order for phytoplankton to support such growth rates, they must have evolved either a lower cellular Fe demand and/or unique mechanisms for Fe uptake and storage (Sunda and Huntsman 1995a, Maldonado and Price 1996, Marchetti et al. 2009). Recent studies have shown that to save on Fe, some oceanic diatoms replace photosynthetic Fe containing enzymes with Cu containing ones (Peers and Price 2006), and/or use Cu/Zn SOD instead of FeSOD to detoxify oxygen radicals. Thus, I hypothesized that oceanic phytoplankton, from various phyla, might have higher Cu requirements as a result of replacing Fe containing enzymes with Cu containing ones. This hypothesis was tested by measuring growth rates and Cu quotas in diverse phytoplankton grown under various Cu and Fe conditions (Chapter 2). Lowering Cu levels had a significant effect on the growth rates of the oceanic phytoplankton compare to those of the coastal, indicating that Cu has a more important physiological role in oceanic phytoplankton. In addition, the effect of low Cu on the growth rates of oceanic phytoplankton was dependant on Fe availability and phylum. For example, low Cu significantly reduced the growth rate of only 2 strains, the oceanic *Synechococcus* and the oceanic *Phaeocystis* (Prymnesiophyceae), but only when Fe was also low (pFe21 and pFe 22, respectively). These results suggest that the oceanic *Phaeocystis* and the Sargasso Sea *Synechococcus* also require higher Cu concentrations for growth when Fe is low, as observed previously in marine diatoms (Peers et al. 2005, Maldonado et al. 2006, Annett et al. 2008, Semeniuk et al. 2009). Although the Cu:C

were not significantly higher in oceanic strains, there are still five independent lines of evidence supporting a more important role of Cu in the physiology of oceanic phytoplankton. The mixed-effect model statistics indicated a significant Cu effect on the growth rates and steady-state Cu transport rates of the oceanic strains, but not the coastal strains. In addition, lowering the Cu concentration in the media decreased the Cu quotas and steady-state Cu transport rates of the oceanic strains to a greater extent (5.5 and 5.4 fold, respectively) than those of the coastals (3.8 and 4.7 fold, respectively). Iron limitation only had a significant effect on the Cu quotas of the oceanic strains, and this effect was dependent on Cu level and phylum.

### **6.2.2 The copper requirements of Fe-limited phytoplankton are higher than those of Fe-sufficient cells**

In the last decade, diatoms have been shown to have mechanisms to increase Fe nutrition: some possess Fe storage mechanisms (Marchetti et al. 2009), while others have a high affinity Fe transport system that allows them to access organically bound Fe, the greatest pool of dissolved Fe in seawater. This high affinity Fe transport system requires Cu in the putative multi-Cu containing iron oxidases (Peers et al. 2005, Wells et al. 2005, Maldonado et al. 2006). Thus, some diatoms have higher Cu requirements when Fe-limited (Annett et al. 2008). To test whether phytoplankton belonging to other phyla also have higher Cu requirements when Fe limited, I examined the Cu:C of Fe limited phytoplankton relative to Fe-sufficient ones. However, only two strains out of 10 tested, the coastal *Synechococcus* and coastal *Chrysochromulina*, had increased Cu quotas when Fe was limiting (Chapter 2). My results may suggest that either the Cu demand for the proper functioning of the high-affinity Fe transport system is relatively low, or that the role of Cu in the high-affinity Fe uptake system is not universal among phytoplankton phyla. Alternative Fe acquisition pathways may be found in marine phytoplankton, including Fe<sup>2+</sup> uptake systems, unspecific divalent ion uptake systems, and direct Fe siderophore transport (Kustka et al. 2007, Lane et al. 2008, Palenik et al. 2007, Allen et al. 2008, Sutak et al. 2010). Further studies on Fe transport mechanisms of diverse

phytoplankton may help our understanding of the cellular functions of Cu.

### **6.2.3 Copper quotas are higher for eukaryotic phytoplankton of the green plastid than the red plastid superfamilies. *Synechococcus* have the lowest Cu quotas, as they evolved in a low Cu environment and are very sensitive to high Cu levels**

Under Fe/Cu sufficiency, the Cu quotas of multiple phytoplankton genera ranged from 0.36 to 3.8  $\mu\text{mol Cu mol}^{-1}\text{ C}$ , with the Sargasso Sea cyanobacterium *Synechococcus* sp (WH7803) having the highest Cu quotas and the oceanic dinoflagellate *Prorocentrum* the lowest (Chapter 2). The average Cu quotas of Bacillariophyceae, Cyanophyceae, Prymnesiophyceae and Dinophyceae under Fe/Cu sufficient condition were  $2.41 \pm 0.74$ ,  $2.13 \pm 2.37$ ,  $1.78 \pm 0.86$  and  $0.52 \pm 0.22$   $\mu\text{mol Cu} \cdot \text{mol}^{-1}\text{ C}$ , respectively. This order, from high to low, is in disagreement with that found in Ho et al. study (2003), where the average Cu quotas (Cu:C) of Dinophyceae ( $4.18 \pm 4.06$   $\mu\text{mol Cu} \cdot \text{mol}^{-1}\text{ C}$ ) were higher than those of Bacillariophyceae ( $2.83 \pm 0.74$   $\mu\text{mol Cu} \cdot \text{mol}^{-1}\text{ C}$ ) and Prymnesiophyceae ( $1.32 \pm 0.56$   $\mu\text{mol Cu} \cdot \text{mol}^{-1}\text{ C}$ ).

Changes in ocean redox state have been suggested to have influenced trace metal stoichiometry in marine phytoplankton (Quigg et al. 2003, Ho et al. 2003, and Saito et al. 2003). Differences in the Cu requirements of marine eukaryotic phytoplankton have been observed between the red and the green plastid superfamilies, with the former having, in general, lower Cu quotas than the latter (Quigg et al. 2003, Ho et al. 2003). In addition, metal preferences (e.g. for Fe) and sensitivities (e.g. to Cu) of Cyanophyceae have been suggested to reflect their evolution in an ancient sulfidic ocean, where the availability of Fe was high and that of Cu was low (Saito et al. 2003). My limited data set supports the notion that *Synechococcus* spp. have relatively high Fe requirements, as the two *Synechococcus* strains exhibited the greatest reduction in growth rates due to Fe limitation. However, contrary to my expected high Cu sensitivities of *Synechococcus*, the highest Cu:C quotas were found in the Sargasso Sea *Synechococcus*. In spite of these high Cu:C ratios, this strain achieved fast growth rates ( $\sim 1.0\text{ d}^{-1}$ ). These results imply

that this strain, which supposedly evolved in a low Cu environment, is unaffected by the accumulation of high intracellular Cu levels.

Another important consideration is that apparent taxonomic patterns in trace metal quotas may depend upon the element used as a proxy for phytoplankton biomass when normalizing metal concentrations. To compare my Cu:C ratios to those presented in Ho et al. (2003), I converted their Cu:P to Cu:C using the cellular concentrations of C presented in Table 2 in Ho et al. (2003). The calculated Cu:C ratios do not support Ho et al.'s conclusion (2003) that systematic differences in trace metal quotas (including Cu) exist between the green algae and that of Prymnesiophyceae and Bacillariophyceae. In addition, the phylogenetic difference in Cu requirements (Cu:P) between the red and green plastid superfamilies described by Quigg et al. (2003) is not observed if the Cu quotas are normalized to C. Thus, though phytoplankton trace metal concentrations are often normalized to cellular P concentrations, using P as a biomass proxy is not ideal, given its plasticity (Sterner and Elser 2002), and its tendency to adsorb to cell surfaces (Sanudo-Wilhelmy et al. 2004). Similar conclusions were reached by Twining et al. 2004. These combined results highlight the urgent need for a more consistent proxy for phytoplankton cellular biomass.

Some interesting phylogenetic trends were observed with respect to Fe nutrition. Phytoplankton in the Prymnesiophyceae exhibited the least average growth rate reduction due to low Fe while the Cyanophyceae exhibited the most. This suggests that Prymnesiophyceae requires little Fe for growth, while Cyanophyceae requires high Fe. The low Fe demand of Prymnesiophytes and the high Fe demand of Cyanophyceae may explain their increased and decreased abundance, respectively, along Line P, a natural Fe availability gradient from Fe rich coastal waters off British Columbia to the well studied offshore Fe limited station (OSP). These results illustrate how my findings on the effects of Fe and/or Cu availability on phytoplankton growth may help our understanding of the distribution of various phytoplankton taxa in regions of the world ocean.

#### **6.2.4 Marine diatoms possess a high- and a low-affinity Cu transport system, and these systems are controlled differently by Fe and/or Cu availability**

This thesis presents the first evidence of the co-occurrence of a high- and a low-affinity Cu transport system in marine phytoplankton (Chapter 3). In the diatoms, *T. oceanica* and *T. pseudonana*, used as model organisms, Michaelis-Menten type kinetics and biphasic uptake kinetics as a function of Cu concentration were observed. Moreover, the Cu uptake systems in the two diatom species are different. Under sufficient Fe and Cu condition, the  $K_m$  values of the low- and high-affinity Cu transport systems for *T. oceanica* differ by 50-fold (2410 nM versus 48 nM total Cu). These  $K_m$  values are very similar to those of the freshwater green alga *Scenedesmus subspicatus* (Knauer et al. 1997) but distinct from those of the green algae *C. reinhardtii* (Hill et al. 1996). Interestingly, the low-affinity Cu transport system in *T. pseudonana* did not saturate at Cu concentrations of 2  $\mu$ M, while the  $K_m$  of the high-affinity Cu transport system is higher (3-3.5 fold) than the  $K_m$  of *T. oceanica* and *S. subspicatus*. These results suggest that the oceanic isolate has higher affinity for Cu than the coastal isolate. In contrast, the coastal isolate seems to have more efficient intracellular Cu homeostasis mechanisms. These physiological differences between the coastal and oceanic diatoms illustrate the adaptive evolution of these organisms to their respective high and low Cu environments.

Moreover, the Cu uptake systems of these two diatoms are differentially controlled by Cu and/or Fe nutrition. For example, as observed in other phytoplankton (Hill et al. 1996), *T. oceanica* increased the  $V_{max}$  of the low-affinity Cu transport system in response to low Cu, while *T. pseudonana* decreased its  $V_{max}$ . However, both diatoms downregulated their high affinity Cu transport systems under Fe-limitation. This study showed that the responses of Cu uptake kinetics to different Fe and/or Cu conditions are complex, providing more support for the dynamic interactions between Fe and Cu in diatom physiology.

### **6.2.5 Copper uptake rate is determined by the concentration of total Cu and not that of free Cu<sup>2+</sup>**

Using CuEDTA as a model organic Cu complex, my results suggest that phytoplankton might be able to access Cu bound within organic complexes. There are three lines of evidence in support of this. First, lowering the total Cu concentration in the media 10-fold decreased the steady-state Cu uptake rates and cellular Cu:C by 5.3 and 4.5 fold, respectively (Chapter 2). These average decreases match the reduction in the total Cu (5 fold decrease between Cu-sufficient and low-Cu treatment) but not in free Cu<sup>2+</sup> concentration (10 fold decrease). Second, the Cu uptake rates measured in this thesis ( $\rho_{\text{Cu}}$ ) are 1.5 to 15.1 fold faster than the flux of inorganic Cu to the cell surface ( $J_{\text{D}}$ ) (Chapter 3). The mean ratio of  $\rho_{\text{Cu}}: J_{\text{D}}$  ratio was 7.2 and 3.3 for *T. oceanica* and *T. pseudonana*, respectively. Third, the gene expression of the Fe reductases (*TpFRE2*) was down-regulated after a Cu addition (Chapter 4). Iron reductases can function as cupric reductases in the high affinity Cu transport system (Hassett and Kosman 1995, Georgatsou et al. 1997, Weger, 1999, Yi and Guerinot 1996; Robinson et al. 1999). The lower Cu reduction activity in the presence of high Cu, suggests that when Cu is low organically bound Cu is reduced enzymatically in order to release it from the organic complexes and ultimately enhance Cu uptake. Cupric reductase activity at the cell surface of some marine phytoplankton has been observed (Jones et al. 1987). Thus, the dissociation of Cu from organic ligands may be mediated by cupric reductase involved in the high affinity Cu uptake system in marine phytoplankton, as previously observed in other eukaryotes (Hill et al. 1996, Puig et al. 2007). This combined evidence confirms previous conclusions from lab and field studies that Cu acquisition is controlled by the concentration of organically complexed Cu instead of free Cu<sup>2+</sup> (Hudson 1998, Quigg et al. 2006, Annett et al. 2008, Semeniuk et al. 2009). Hence, total Cu concentration in the sea may be a better indicator of Cu availability than free Cu<sup>2+</sup>.

### **6.2.6 The putative genes encoding high- and low-affinity Cu transport systems, as well as for Cu chaperones are present in the genome of *T. pseudonana*. Their gene expressions are affected by Cu and/or Fe availability**

The putative genes encoding potential components of Cu acquisition and homeostasis mechanisms (including CTR-like Cu transport proteins, Cu transporting P-type ATPases, Cu chaperones and putative Zn transporters) were identified in the genome of the centric diatom *T. pseudonana* (Chapter 4), using known transmembrane domains and conserved Cu or Zn binding motifs in homologs of fungi, green algae, plants and animals (Kim and Thiele, 2004, Puig et al. 2007, Merchant et al. 2006). In addition, changes in the expression of these genes in response to adjustments in Fe and/or Cu availability were investigated. Two CTR-like transporters, two putative Cu transporting P-type ATPases, two putative Cu chaperones and one of Fe reductases, were down-regulated after the addition of excess Cu (500 nM), suggesting that they were involved in Cu acquisition and homeostasis when Cu level is low. Under long-term Fe limitation and/or starvation, most of the identified genes were up-regulated, while low Cu either had no effect or the effect was dependent on Fe availability. In addition, one ZIP-like gene was up-regulated by Cu deficiency when Fe was also low, suggesting that Zn transporter may be involved in Cu uptake under low Fe condition. A significant role for Fe in controlling the expression of Cu-related genes is evident, as well as a complex interaction of Cu and Fe response networks.

### **6.2.7 The putative high affinity, CTR-like Cu transporters in *T. pseudonana* are novel**

Two putative Cu transport CTR genes (*TpCTR|24275* and *TpCTR|9391*) were identified in *T. pseudonana* using conserved structures and motifs for CTR family Cu transporters (Chapter 4). In addition, the down-regulation of their expression after the addition of excess Cu suggests their involvement in the high-affinity Cu uptake system. However, their gene sequences show low similarity with other known homologues from model

organisms (e.g. *Saccharomyces cerevisiae*, *Arabidopsis thaliana* and *Chlamydomonas reinhardtii*). The N-terminus of these two CTR-like proteins is atypical, though they have metal-binding motifs containing Cys, Met and His. The N-terminal sequence of *TpCTR|24275* is more like the homologs of *Phaeodactylum tricornutum*, *Ostreococcus lucimarinus*, *Micromonas pusilla* and *Perkinsus marinus*. They share a number of putative conserved Cu-binding residues and motifs, including HxH, C<sub>x6/7</sub>C<sub>xxx</sub>C, H<sub>xxx</sub>C and C<sub>x5/8</sub>M<sub>x</sub>M, which are different from those of yeast in which Met-rich motifs (M<sub>xx</sub>M and/or M<sub>x</sub>M) are typical. This may be significant in view of the suggestion that diatoms acquired a significant number of genes by lateral gene transfer from members of the Mamiellales (Prasinophyceae) to which *Ostreococcus* and *Micromonas* belong (Moustafa et al. 2009). The protein sequence of *TpCTR|9391* does not share these N-terminal motifs with *TpCTR|24275*, but is more similar to that of COPT1 in the green alga *Chlamydomonas* (Page et al. 2009) and plant *Arabidopsis* (Kampfenkel et al. 1995) in which the N-terminal domain contains His and Met-rich Cu binding motifs. Given that the gene sequences of these *T. pseudonana* CTRs seem novel and have low similarity with other known homologues, I investigated whether these genes were encoding high-affinity Cu transporters using functional complementation experiments with *Saccharomyces cerevisiae* *ctr1Δctr3Δ* mutant (MPY17), a high-affinity Cu transport mutant (Chapter 5). However, the results of these experiments did not confirm that these CTR-like genes were involved in high-affinity Cu transport. Some possible explanations for these negative results include their locations, in the tonoplasts instead of the plasma membrane, or a complex Cu transport protein structure. As observed in *S. pombe* and rice *Oryza sativa*, some CTR family proteins are unable to transport Cu unless other components, that aid in the formation of a heteromeric protein, are present (Zhou and Thiele 2001, Loannoni et al. 2010, Yuan et al. 2011). This type of heteromeric protein complex may also exist in *T. pseudonana* to perform the Cu transport function, and may not have properly assembled during the yeast functional complementation experiments.

## 6.3 Future research

The results of this dissertation provide the basis for some future projects on trace metals physiology of marine phytoplankton.

1) The coastal *E. huxleyi* was the most sensitive species to low Cu and the least sensitive to low Fe. At present, I am unable to explain these findings. Although other phytoplankton species have been shown to be very resilient to Fe limitation as a result of extremely low Fe requirements (i.e. the Antarctic diatoms; Timmermans 2001, 2004, Lane et al. 2009, Strezepek et al. 2011), this is the first time that a phytoplankton species with extremely low Fe and high Cu demand have been described. This species might be an ideal model to investigate possible substitutions of Fe with Cu in phytoplankton metabolic pathways, using EST libraries and differential proteomics.

2) The responses of Cu uptake kinetics to different Fe and/or Cu culture conditions are complex. However, while performing my Cu uptake kinetic experiments, due to the limited amount of  $^{67}\text{Cu}$  received during each delivery, I was only able to measure uptake rates at 8 different Cu concentrations. This experimental design resulted in some uncertainties. For example, I was unable to saturate Cu uptake in *T. pseudonana* at my highest Cu concentration (2000 nM). Future kinetic studies, incorporating more Cu concentrations, at both, low and high Cu levels, might be able to provide better estimates of the  $K_m$  and  $V_{max}$  of the high- and/or the low-affinity Cu uptake system in marine diatoms and/or other phytoplankton. To further improve our understanding of the availability of various Cu species for phytoplankton uptake, future investigations should examine Cu uptake in the presence of a variety of organic Cu complexes with a range of stability constants for Cu.

3) Putative genes encoding CTR-like Cu transporters, Zn transporters, and Cu chaperones in *T. pseudonana* were identified in this thesis. However, their potential functions and regulations in response to Cu or other trace metals are still unclear. Future

research should elucidate the location of the putative CTR transporters and P-type Cu transport ATPases. To test the function of these transporters, yeast complementation experiments could also be useful, as well as metal uptake assays and competition experiments. Investigating how these potential proteins are regulated at the post-translation level might provide some insights into their regulation by Cu and/or Fe availability. The function of my identified *T. pseudonana* Cu chaperones is unknown, though they are expected to perform intracellular trafficking of Cu. Some putative Zn transporters were identified to be involved in Cu transport. Considering the essential role of Zn in the physiology of marine phytoplankton, and the complex interactions between Zn and Cu, further studies can be conducted. For example, a project on the effects of Zn deficiency or toxicity on the gene expression of potential Fe and Cu transport proteins and homeostasis could be of interest.

To establish the function of these potential metal transporters, genes could be overexpressed by using an expression plasmid, as has been developed in *P. tricornutum* (Siaut et al. 2007), or be knocked down to inactivate the function using RNA interference (RNAi, De Riso et al. 2009). The consequences of overexpressing or knocking down specific genes would elucidate their functions. Expression vectors of a putative protein could also be fused with a fluorophore in order to identify its intracellular location and regulation in response to changes in Fe and/or Cu availability.

4) Recent studies, as well as my dissertation, demonstrate that Cu is more important for the growth of the oceanic diatom *T. oceanica* than its coastal counterpart, *T. pseudonana*. In addition, the kinetics of Cu uptake in *T. oceanica* suggest that this oceanic isolate has higher affinity for Cu than the coastal isolate, suggesting that oceanic diatoms have evolved to acquire Cu efficiently. Considering these oceanic-coastal differences, *T. oceanica* may be an excellent model oceanic phytoplankton to study Cu acquisition and homeostasis mechanisms. Since the genome of *T. oceanica* has not been sequenced, to investigate its trace metal related gene make up, Expressed Sequence Tag (EST) libraries can be constructed for various trace metal culture conditions (metal replete condition, Cu-

and/or Fe-limitation). These EST libraries can provide detailed information on the gene expression profiles of *T. oceanica* grown under these conditions, and will give us powerful insight into how oceanic phytoplankton adapt biochemically to Fe and/or Cu deficiency. These *T. oceanica* EST libraries could then be used to identify and quantify the differential expression of proteins, using stable-isotope labeling and LC-MS/MS. If novel metalloproteins are identified in *T. oceanica*, their biochemistry and crystallography could be determined in order to elucidate the function and structure of these novel enzymes.

5) Most studies on Cu requirements and uptake kinetics in phytoplankton have focused on centric diatoms, while little is known about pennate diatoms. The genome sequence of the pennate diatom, *P. tricornutum*, has been completed recently (<http://genome.jgi-psf.org/Phatr2/Phatr2.home.html>). Thus, *P. tricornutum* can now be used as a model organism for the mechanistic understanding of the relationship between trace metal nutrition and phytoplankton physiology. More specifically, using its genome, we could now identify the components of Cu transport and homeostasis, and study their regulations. Like *T. oceanica*, *P. tricornutum* can tolerate much lower (50 times lower) Fe concentrations than *T. pseudonana* (Kustka et al. 2007). Under Fe-limiting conditions, two metal related genes are overexpressed in *P. tricornutum*, a Cu-related gene TYR1 (Cu-tyrosinase) and a Fe-related one, ISIP1 (Allen et al. 2008). Copper-containing tyrosinase is an enzyme present in plant and animal tissues that catalyzes the production of melanin, which absorbs harmful UV-radiation and transforms the energy into harmless heat, and other pigments from tyrosine by oxidation. However, the functions of TYR1 and ISIP1 in *P. tricornutum* are presently unknown. To investigate their function, methods of gene overexpression and knocking down (RNAi) could also be used in *P. tricornutum*.

## Bibliography

- Abdel-Ghany, S. E., Müller-Moulé, P., Niyogi, K. K., Pilon, M. & Shikanai, T. 2005. Two P-type ATPases are required for copper delivery in *Arabidopsis thaliana* chloroplasts. *Plant Cell* 17:1233–51.
- Ahner, B. A. & Morel, F. M. M. 1995. Phytochelatin production in marine algae: II. Induction by various metals. *Limnol. Oceanogr.* 40: 658-65.
- Ahner, B. A., Morel, F. M. M. & Moffett, J. W. 1997. Trace metal control of phytochelatin production in coastal waters. *Limnol. Oceanogr.* 42:601–608
- Ahner, B. A., Price, N. M. & Morel, F. M. M. 1994. Phytochelatin production by marine phytoplankton at low free metal ion concentrations: laboratory studies and field data from Massachusetts Bay. *Proc. Natl. Acad. Sci. U.S.A.* 91:8433–8436.
- Ahner, B. A., Wei, L. P., Oleson, J. R. & Ogura, N. 2002. Glutathione and other low molecular weight thiols in marine phytoplankton under metal stress. *Mar. Ecol. Prog. Ser.* 232:93-103.
- Allen, A. E., LaRoche, J., Maheswari U., Lommer, M., Schauer N., Lpez. P. J., Finazzi, G., Fernie, A. R. & Bowler, C. 2008. Whole-cell response of the pennate diatom *Phaeodactylum tricornutum* to iron starvation. *Proc. Natl Acad. Sci. USA* 105, 10438–43.
- Aller, S.G. & Unger, V. M. 2006. Projection structure of the human copper transporter CTR1 at 6-Å resolution reveals a compact trimer with a novel channel-like architecture. *Proc. Natl. Acad. Sci. USA* 103:3627–32.
- Annett, A., Lapi, S., Ruth, T. J. & Maldonado, M. T. 2008. The effects of Cu and Fe availability on the growth and Cu:C ratios of marine diatoms. *Limnol. Oceanogr.* 53:2451-61.
- Armbrust, E. V., and Others. 2004. The genome of the diatom *Thalassiosira pseudonana*: Ecology, evolution, and metabolism. *Science* 306: 79–86.
- Askwith, C., Eide, D., Van Ho, A., Bernard, P. S., Li, L., Davis-Kaplan, S., Sipe, D. M. & Kaplan, J. 1994. The FET3 gene of *S. cerevisiae* encodes a multicopper oxidase required for ferrous iron uptake. *Cell* 76:403-10.

- Austenfeld, F.-A. & Veltrup, W. 1983. Multiphasic uptake systems in cell suspension cultures. *Plant Cell Rep.* 2:5-6.
- Banci, L., Bertini, I., Ciofi-Baffoni, S., Janicka, A., Martinelli, M., Kozłowski, H. & Palumaa, P. 2008. A structural-dynamical characterization of human Cox17. *J. Biol. Chem.* 283:7912-20.
- Bashkin, V. N., 2002. Modern Biogeochemistry. Kluwer Academic Publishers, Dordrecht, The Netherlands.
- Beaudoin, J., Laliberte, J. & Labbe, S. 2006. Functional dissection of Ctr4 and Ctr5 amino-terminal regions reveals motifs with redundant roles in copper transport. *Microbiology-Sgm* 152:209-22.
- Bekker A, Holland, H. D., Wang, P. L., Rumble, D., Stein, H. J., Hannah, J. L., Coetzee, L. L. & Beukes, N. J. 2004. Dating the rise of atmospheric oxygen. *Nature* 427:117–20.
- Bellemare, D. R., Shaner, L., Morano, K. A., Beaudoin, J., Langlois, J. & Labbe, S. 2002. Ctr6, a vacuolar membrane copper transporter in *Schizosaccharomyces pombe*. *J Biol Chem.* 277:46676-86.
- Boyd, P. W., Muggli, D. L., Varela, D. E., Goldblatt, R. H., Chretien, R., Orians, K. J. & Harrison, P. J. 1996. In vitro iron enrichment experiments in the NE subarctic Pacific. *Mar. Ecol. Prog. Ser.* 136: 179-93.
- Boyd, P. W., Watson, A. J., Law, C. S., Abraham, E. R., Trull, T., Murdoch, r., Bakker, D. C. E., Bowie, A. R., Buessler, K. O., Chang, H., Charette, M., Croot, P., Downing, K., Frew, R., Gall, M., Hadfield, M., Hall, J., Harvey, M., Jameson, G., LaRoche, J., Liddicoat, M., Ling, R., Maldonado, M. T., McKay, R. M., Nodder, S., Pickmere, S., Pridmore, R., Rintoul, S., Safi, K., Sutton, P., Strzepek, R., Tanneberger, K., Turner, S., Waite, A. & Zeldis, J. 2000. A mesoscale phytoplankton bloom in the polar Southern Ocean Stimulated by iron fertilization. *Nature* 407:695-702.
- Boyle, E. A., Husted, S. S. & Jones, S. P. 1981. On the distribution of copper, nickel, and cadmium in the surface waters of the North Atlantic and North Pacific Ocean.

- J. Geophys. Res.* 86:8048-66.
- Brand, L. E. 1991. Minimum iron requirements of marine phytoplankton and the implications for the biogeochemical control of new production. *Limnol. Oceanogr.* 36:1756-71.
- Brand, L. E., Guillard, R. R. L. & Murphy, L. S. 1981. A method for the rapid and precise determination of acclimated phytoplankton reproduction rates. *J. Plankton Res.* 3:193-201.
- Brand, L. E., Sunda, W. G. and Guillard, R. R. L. 1983. Limitation of marine phytoplankton reproductive rates by zinc, manganese and iron. *Limnol. Oceanogr.* 28: 1182 – 98.
- Brand, L. E., Sunda, W. G. and Guillard, R. R. L. 1986. Reduction of marine phytoplankton reproduction rates by copper and cadmium. *J. Exp. Mar. Biol. Ecol.* 96: 225-50.
- Bruland, K. W. & Franks, R. P. 1983. Mn, Cu, Ni, Zn, and Cd in the western North-Atlantic, *In* Wong, C. S., Boyle, E. A., Bruland, K. W. & Goldberg, E. D. [Eds.] *Trace Metals in Seawater*. Plenum Press, New York, pp. 395–413.
- Bruland K.W. & Lohan, M.C. 2003. Controls of trace metals in seawater. *In*: H. Elderfield, Editor, *The Oceans and Marine Geochemistry (Treatise on Geochemistry)* vol. 6, Elsevier, Amsterdam, pp. 23–47.
- Boulter, D., Haslett, B. G., Peacock, D., Ramshaw, J. A. M. & Scawen, M. D. 1977. Chemistry, function and evolution of plastocyanins. *Intl Rev Biochem.* 13:1-40.
- Buck, K. N., Ross, J. R. M., Russell Flegal, A. & Bruland, K. W. 2007. A review of total dissolved copper and its chemical speciation in San Francisco Bay, California. *Environ. Res.* 105:5-19
- Buckhout, T. J., Yang, T. J. & Schmidt, W. 2009. Early iron-deficiency-induced transcriptional changes in *Arabidopsis* roots as revealed by microarray analyses. *BMC Genomics* 10: 147-62.
- Campbell, P. G. C. 1995. Interactions between trace metals and aquatic organisms: a critique of the freeion activity model. *In* A. Tessier, & D. R. Turner (Eds.), *Metal*

- Speciation and Bioavailability in Aquatic Systems (pp. 45–102). Chichester, UK: John Wiley & Sons.
- Campbell, L. & Carpenter, E. J. 1987. Characterisation of phycoerythrin-containing *Synechococcus* spp. populations by immunofluorescence. *J. Plankton Res.* 9: 1167-81.
- Carr, H. S., George, G. N. & Winge, D. R. 2002. Yeast Cox11, a protein essential for cytochrome c oxidase assembly, is a Cu(I) binding protein. *J. Biol. Chem.* 277:31237-42.
- Castruita, M., Casero, D., Karpowicz, S. J., Kropat, J., Vieler, A., Hsieh, S. I., Yan, W., Cokus, S., Loo, J. A., Benning, C., Pellegrini, M. & Merchant, S. S. 2011. Systems biology approach in *Chlamydomonas* reveals connections between copper nutrition and multiple metabolic steps. *Plant Cell.* 23: doi: 10.1105/tpc.111.084400.
- Chadd, H. E., Newman, J., Mann, N. H. & Carr, N. G. 1996. Identification of iron superoxide dismutase and a copper/zinc superoxide dismutase enzyme activity within the marine cyanobacterium *Synechococcus* sp WH 7803. *FEMS Microbiol. Lett.* 138:161-5.
- Chang, S.I. & Reinfelder, J. R. 2000. Bioaccumulation, subcellular distribution and trophic transfer of copper in a coastal marine diatom. *Environ. Sci. Technol.* 34:4931-5.
- Chen, Y. F., Randlett, M. D., Findell, J. L. & Schaller, G. E. 2002. Localization of the ethylene receptor ETR1 to the endoplasmic reticulum of *Arabidopsis*. *J. Biol. Chem.* 277:19861-66.
- Cid, A., Herrero, C., Torres, E. & Abalde, J. 1995. Copper toxicity on the marine microalga *Phaeodactylum tricoratum*: effects on photosynthesis and related parameters. *Aquat. Toxicol.* 31:165–174
- Clemens, S. 2001. Molecular mechanisms of plant metal tolerance and homeostasis. *Planta* 212:475-86.
- Cloud, P. 1973. Paleoecological significance of the banded iron formation. *Econ Geol* 68:1135-43

- Coale, K. H. & Bruland, K. W. 1988. Copper complexation in the Northeast Pacific. *Limnol. Oceanogr.* 33:1084-101.
- Coale, K. H. & Bruland, K. W. 1990. Spatial and temporal variability in copper complexation in the North Pacific. *Deep-Sea Res.* 37:317-36.
- Coale, K. H., Fitzwater, S. E., Gordon, R. M., Johnson, K. S. & Barber, R. T. 1996a. Control of community growth and export production by upwelled iron in the equatorial Pacific Ocean. *Nature* 379:621-4.
- Coale, K. H., Johnson, K. S., Fitzwater S. E., Gordon R. M., Tanner, S., Chavez, F. P., Ferioli, L., Sakamoto, C., Rogers, P., Millero, F., Steinberg, P., Nightingale, P., Cooper, D., Cochlan W. P., Landry, M. R., Constantinou, J, Rollwagen, G., Trasvina, A. & Kudela, R. 1996b. A massive phytoplankton bloom induced by an ecosystem-scale iron fertilization experiment in the equatorial Pacific Ocean. *Nature* 383:495-501.
- Coble, P., Hu, C., Gould, R. W. J., Chang, G. & Wood, A. M. 2004. Colored dissolved organic matter in the coastal ocean: An optical tool for coastal zone environmental assessment and management. *Oceanography* 17: 50-9.
- Cohen, C. K., Norvell, W. A. & Kochian, L. V. 1997. Induction of root cell plasma membrane ferric reductase. An exclusive role for Fe and Cu. *Plant Physiol.* 114:1061-9.
- Collos, Y., Vaquer, A., Bibent, B., Slawy, G., Garcia, N. & Souchu, P. 1997. Variability in nitrate uptake kinetics of phytoplankton communities in a Mediterranean coastal lagoon. *Estuar. Coast. Shelf Sci.* 44:369-75.
- Crawford, D. W., Lipsen, M. S., Purdie, D. A., Lohan, M. C., Statham, P. J., Whitney, F. A., Putland, J. N., Johnson, W. K., Sutherland, N., Peterson, T. D., Harrison, P. J. & Wong, C. S. 2003. Influence of zinc and iron enrichments on phytoplankton growth in the northeastern subarctic Pacific. *Limnol. Oceanogr.* 48: 1583-600.
- Croot, P. L. 2003. Seasonal cycle of copper speciation in Gullmar Fjord, Sweden. *Limnol. Oceanogr.* 48:764-76.
- Croot, P. L., Karlson, B., Van Elteren, J. T. & Kroon, J. J. 1999. Uptake of <sup>64</sup>Cu-oxine by

- marine phytoplankton. *Environ. Sci. Technol.* 33:3615-21.
- Croot, P. L., Karlson, B., van Elteren, J. T. & Kroon, J. J. 2003. Uptake and efflux of  $^{64}\text{Cu}$  by the marine cyanobacterium *Synechococcus* (WH7803). *Limnol. Oceanogr.* 48:179-88.
- Croot, P. L., Moffett, J. W. & Brand, L. E. 2000. Production of extracellular Cu complexing ligands by eucaryotic phytoplankton in response to Cu stress. *Limnol. Oceanogr.* 45: 619– 27.
- Culotta, V. C., Klomp, L. W., Strain, J., Casareno, R. L., Krems, B., and Gitlin, J. D. 1997. The copper chaperone for superoxide dismutase *J. Biol. Chem.* 272: 23469–72.
- Curie, C. & Briat, J. F. 2003. Iron transport and signaling in plants. *Annu. Rev. Plant Biol.* 54:183-206.
- Dancis, A., Haile, D., Yuan, D. S. & Klausner, R. D. 1994a. The *Saccharomyces cerevisiae* copper transport protein (Ctr1p). Biochemical characterization, regulation by copper, and physiologic role in copper uptake. *J. Biol. Chem.* 269:25660-7.
- Dancis, A., Yuan, D. S., Haile, D., Askwith, C., Eide, D., Moehle, C., Kaplan, J. & Klausner, R. D. 1994b. Molecular characterization of a copper transport protein in *S. cerevisiae*: an unexpected role for copper in iron transport. *Cell* 76:393-402.
- Da Silva J. J. R. F. & R. J. P. Williams, 1991. *The Biological Chemistry of the Elements: The Inorganic Chemistry of Life*, Oxford University Press, Oxford.
- Davis, A. K., Hildebrand, M. & Palenik, B. 2006. Gene expression induced by copper stress in the diatom *Thalassiosira pseudonana*. *Eukaryot. Cell* 5:1157-68.
- De Feo, C. J., Aller, S. G. & Unger, V. M. 2007. A structural perspective on copper uptake in eukaryotes. *Biometals* 20:705–16.
- DeRome, L. & Gadd, G. M. 1987. Measurement of copper uptake in *Saccharomyces cerevisiae* using a  $\text{Cu}^{2+}$ -selective electrode. *FEMS Microbiol. Lett.* 43:283-87.

- De Riso V, Raniello R, Maumus F, Rogato A, Bowler C, Falciatore A. 2009. Gene silencing in the marine diatom *Phaeodactylum tricornutum*. *Nucl. Acids Res.* 37:e96
- Dix, D., Bridgham, J., Broderius, M. & Eide, D. 1997. Characterization of the FET4 protein of yeast. Evidence for a direct role in the transport of iron. *J. Biol. Chem.* 272:11770-7.
- Donat, J. R., & Bruland, K. W. 1995. Trace elements in the oceans. *In* Steinnes, E. [Ed.], Trace Elements in Natural Waters, CRC, pp. 347-281.
- Duce, R. A. & Tindale, N. W. 1991. Atmospheric transport of iron and its deposition in the ocean, *Limnol. Oceanogr.* 36 :1715-26.
- Dumay, Q. C., Debut, A. J., Mansour, N. M. & Saier, M. H. 2006. The copper transporter (Ctr) family of Cu<sup>+</sup> uptake systems. *J Mol Microbiol Biotechnol*, 11: 10–9.
- Dupont, C. L., Barbeau, K. & Palenik, B. 2008. Ni uptake and limitation in marine *Synechococcus* strains. *Appl. Environ. Microbiol.* 74: 23-31.
- Edwardsen, B. & Paasche, E. 1998. Bloom dynamics and physiology of *Prymnesium* and *Chrysochromulina*. *In* Anderson, D. M., Cembella, A. D. & Hallegraeff, G. M. [Eds.] *Physiological Ecology of Harmful Algal Blooms*, Vol 41. Springer, Heidelberg, Germany, pp. 193-208.
- Eide, D. J. 1998. The molecular biology of metal ion transport in *Saccharomyces cerevisiae*. *Annu. Rev. Nutr.* 18: 441-69.
- Eide, D. J. 2006. Zinc transporters and the cellular trafficking of zinc. *Biochim. Biophys. Acta* 1763:711–22.
- Eisses, J.F. & J.H. Kaplan. 2002. Molecular characterization of hCTR1, the human copper uptake protein. *J. Biol. Chem.* 277: 29162-71.
- Epstein, E., Elzam, O. E. & Rains, D. W. 1963. Resolution of dual mechanisms of potassium absorption by barley roots. *Proc. Natl. Acad. Sci.U.S.A.* 49:684-92.
- Falkowski, P. G. 1994. The role of phytoplankton photosynthesis in global biogeochemical cycles. *Photosynth. Res.* 39:235-58.

- Falkowski, P. G., Barber, R. T. & Smetacek, V. 1998. Biogeochemical controls and feedbacks on ocean primary production. *Science* 281: 200-6.
- Field, C., Behrenfeld, M., Randerson, J. & Falkowski, P. 1998. Primary production of the biosphere: integrating terrestrial and oceanic components. *Science* 281:237-40.
- Fu, D., Beeler, T. J. & Dunn, T. M. 1995. Sequence, mapping and disruption of CCC2, a gene that cross-complements the Ca<sup>(2+)</sup>-sensitive phenotype of *csg1* mutants and encodes a P-type ATPase belonging to the Cu<sup>(2+)</sup>-ATPase subfamily. *Yeast* 11:283-92.
- Gaither, L. A. & Eide, D. J. 2000. Functional expression of the human hZIP2 zinc transporter. *J. Biol. Chem.* 275:5560-4.
- Gaither, L. A. & Eide, D. J. 2001. Eukaryotic zinc transporters and their regulation. *BioMetals*. 14: 251-70.
- Geider, R. J. & LaRoche, J. 1994. The role of iron in phytoplankton photosynthesis, and the potential for iron-limitation of primary productivity in the sea. *Photosynth. Res.* 39:275-301.
- Georgatsou, E., Mavrogiannis, L. A., Fragiadakis, G. S. & Alexandraki, D. 1997. The yeast Fre1p/Fre2p cupric reductases facilitate copper uptake and are regulated by the copper-modulated Mac1p activator. *J. Biol. Chem.* 272:13786-92.
- Gervais, F., Riebesell, U. & Gorbunov, M. Y., 2002. Changes in primary productivity and chlorophyll a in response to iron fertilization in the Southern Polar Frontal Zone. *Limnol. Oceanogr.* 47:1324-35.
- Glantz, S. A. & Slinker, B. K. 2001. Primer of applied regression and analysis of variance, 2nd ed. McGraw-Hill Book Co., New York, 949 pp.
- Gledhill, M., Nimmo, M., Hill, S. J. & Brown, M.T., 1999. The release of coppercomplexing ligands by the brown alga *Fucus vesiculosus* (*Phaeophyceae*) in response to increasing total copper levels. *J. Phycol.* 35, 501–9.
- Glerum, D. M., Shtanko, A. & Tzagoloff, A. 1996. Characterization of *COX17*, a yeast gene involved in copper metabolism and assembly of cytochrome oxidase. *J. Biol. Chem.* 271:14504–09.

- Gnassia-Barelli, M. & Hardstedt-Romeo, M. 1982. Short-term time series study of copper and cadmium uptake by *Criscophaera elongata* (Droop) Braarud. *J. Exp. Mar. Biol. Ecol.* 61: 287–298
- Gordon, A. S., Dyer, B. J., Kango, R. A. & Donat, J. R. 1996. Copper ligands isolated from estuarine water by immobilized metal affinity chromatography: temporal variability and partial characterization. *Mar Chem.* 53:163–72.
- Grotz, N., Fox, T., Connolly, E., Park, W., Guerinot, M.L. & Eide, D. 1998. Identification of a family of zinc transporter genes from *Arabidopsis* that respond to zinc deficiency. *Proc. Natl. Acad. Sci. U.S.A.* 95:7220-4.
- Guerinot, M. L. 2000. The ZIP family of metal transporters. *Biochim. Biophys. Acta* 1465:190-8.
- Gunshin, H., Mackenzie, B., Berger, U. V., Gunshin, Y., Romero, M. F., Boron, W. F., Nussberger, S., Gollan, J. L. & Hediger, M. A. 1997. Cloning and characterization of a mammalian proton-coupled metal-ion transporter. *Nature* 388:482-8.
- Guo, J., Annett, A. L., Taylor, R. L., Lapi, S., Ruth, T. J. & Maldonado, M. T. 2010. Copper uptake kinetics of coastal and oceanic diatoms. *J. Phycol.* 46: 1218-28.
- Guo, J., Lapi, S., Ruth, T.J. & Maldonado, M.T. 2012. The effects of iron and copper availability on the Cu stoichiometry of marine phytoplankton *J. Phycol.* (In press).
- Halliwell, B. & Gutteridge, J. M. 1984. Oxygen toxicity, oxygen radicals, transition metals and disease. *J. Biochem.* 219:1-14.
- Hamm, C. E. 2000. Architecture, ecology and biogeochemistry of *Phaeocystis* colonies. *J. Sea Res.* 43:307-15.
- Hanikenne, M., Merchant, S. S. & Hamel, P. P. 2008. Transition metal nutrition: a balance between deficiency and toxicity. In Stern D. [Ed], *The Chlamydomonas Sourcebook*, Ed2, Vol. 2, Academic Press, San Diego, USA, pp. 333-400.
- Harrison, M. D., Jones, C. E. & Dameron, C. T. 1999. Copper chaperones: function, structure and copper-binding properties. *Biol. Inorg. Chem.* 4:145-53.
- Hassett, R., Dix, D. R., Eide, D. J. & Kosman, D. J. 2000. The Fe(II) permease Fet4p functions as a low affinity copper transporter and supports normal copper

- trafficking in *Saccharomyces cerevisiae*. *J. Biochem.* 351:477-84.
- Hassett, R. & Kosman, D. J. 1995. Evidence for Cu(II) reduction as a component of copper uptake by *Saccharomyces cerevisiae*. *J. Biol. Chem.* 270:128-34.
- Heaton, D., Nittis, T., Srinivasan, C. & Winge, D. R. 2000. Mutational analysis of the mitochondrial copper metallochaperone Cox17. *J. Biol. Chem.* 275:37582-7.
- Heil, C. A., Glibert, P. M. & Fan, C. L. 2005. *Prorocentrum minimum* (Pavillard) Schiller - A review of a harmful algal bloom species of growing worldwide importance. *Harmful Algae* 4:449-70.
- Hell, R. & Stephan, U. W. 2003. Iron uptake, trafficking and homeostasis in plants. *Planta* 216:541-51.
- Hill, K. L., Hassett, R., Kosman, D. & Merchant, S. 1996. Regulated copper uptake in *Chlamydomonas reinhardtii* in response to copper availability. *Plant Physiol.* 112:697-704.
- Hirayama, T., Kieber, J. J., Hirayama, N., Kogan, M., Guzman, P., Nourizadeh, S., Alonso, J. M., Dailey, W. P., Dancis, A. & Ecker, J.R. 1999. RESPONSIVE-TO-ANTAGONIST1, a Menkes/Wilson disease-related copper transporter, is required for ethylene signaling in *Arabidopsis*. *Cell* 97:383-93.
- Ho, K. K. & Krogmann, D. W. 1984. Electron donors to P700 in cyanobacteria and algae. An instance of unusual genetic variability. *Biochim. Biophys. Acta* 766:310-6.
- Ho, T. Y., Quigg, A., Finkel, Z. V., Milligan, A. J., Wyman, K., Falkowski, P. G. & Morel, F. M. M. 2003. The elemental composition of some marine phytoplankton. *J. Phycol.* 39:1145-59.
- Hudson, R. J. M. 1998. Which aqueous species control the rates of trace metal uptake by aquatic biota? Observations and predictions of non-equilibrium effects. *Sci. Total Environ.* 219:95-115.
- Hudson, R. J. M. 2005. Trace metal uptake, natural organic matter, and the free-ion model. *J. Phycol.* 41:1-4.
- Hudson, R.J.M. & Morel, F.M.M. 1990. Iron transport in marine phytoplankton: Kinetics of cellular and medium coordination kinetics. *Limnol Oceanogr.* 35:1002-20.

- Hudson, R.J.M. & Morel, F.M.M. 1993. Trace metal transport by marine microorganisms: implications of metal coordination kinetics. *Deep-Sea Res.* 40: 129-150.
- Huizenga, D. L., & Kester, D. R. 1983. The distribution of total and electrochemically available copper in the northwestern Atlantic Ocean. *Mar. Chem.* 13: 28 1-91.
- Jickells, T. D. & Burton, J. D. 1988. Cobalt, copper, manganese and nickel in the Sargasso Sea. *Mar. Chem.* 23:131-44.
- Johnson K.S., Gordon, R. M. & Coale, K. H. 1997. What controls dissolved iron concentrations in the world ocean? *Marine Chemistry* 57: 137-61.
- Jones, G. J., Palenik, B. P. & Morel, F. M. M. 1987. Trace metal reduction by phytoplankton: The role of plasmalemma redox enzymes. *J. Phycol.* 23:237-44.
- Kajikawa, H., Amari, M. & Masaki, S. 1997. Glucose transport by mixed ruminal bacteria from a cow. *Appl. Environ. Microbiol.* 63:1847-1851.
- Kampfenkel, K., Kushnir, S., Babiyshuk, E., Inze, D. & Van Montagu, M. 1995. Molecular characterization of a putative *Arabidopsis thaliana* copper transporter and its yeast homolog. *J. Biophys. Acta* 1763:646-51.
- Kanamaru, K., Kashiwagi, S. & Mizuno, T. 1994. A copper-transporting P-type atpase found in the thylakoid membrane of the Cyanobacterium *Synechococcus* species Pcc7942. *Mol. Microbiol.* 13:369-77.
- Kim, B. E., Nevitt, T. & Thiele, D. J. 2008. Mechanisms for Copper Acquisition, Distribution and Regulation. *Nat. Chem. Biol.* 4:176-85.
- Knauer, K., Behra, R. & Sigg, L. 1997. Adsorption and uptake of copper by the green alga *Scenedesmus subspicatus* (Chlorophyta). *J. Phycol.* 33:596-601.
- Knight, S., Labbe, S., Kwon, L. F., Kosman, D. J. & Thiele, D. J. 1996. A widespread transposable element masks expression of a yeast copper transport gene. *Genes and Develop* 10:1917-29.
- Koch, K. A., Pena, M. M. & Thiele, D. J. 1997. Copper-binding motifs in catalysis, transport, detoxification and signaling. *Chem Biol* 4: 549-60.
- Komor, E. & Tanner, W. 1975. Simulation of a high-affinity and low-affinity sugar-uptake system in chlorella by a pH-dependent change in  $K_m$  of uptake system.

*Planta* 123:195-98.

- Korshunova, Y. O, Eide, D., Clark, W. G., Guerinot, M. L. & Pakrasi, H. B. 1999. The IRT1 protein from *Arabidopsis thaliana* is a metal transporter with a broad substrate range. *Plant Mol. Biol.* 40:37-44.
- Kramer, C. J. M. 1986. Apparent copper complexation capacity and conditional stability constants in North Atlantic waters. *Mar. Chem.* 18: 335- 49.
- Kustka, A. B., Allen, A. & Morel, F. M. M. 2007. Sequence analysis and regulation of iron acquisition genes in two marine diatoms. *J. Phycol.* 43:715-29.
- La Fontaine, S., Quinn, J. M., Nakamoto, S. S., Page, M. D., Gohre, V., Moseley, J. L., Kropat, J. & Merchant, S. 2002. Copper-dependent iron assimilation pathway in the model photosynthetic eukaryote *Chlamydomonas reinhardtii*. *Eukaryot. Cell* 1:736-57.
- Labbe, S., Zhu, Z. & Thiele, D. J. 1997. Copper-specific transcriptional repression of yeast genes encoding critical components in the copper transport pathway. *J. Biol. Chem.* 272:15951-8.
- Labbe, S. & Thiele, D. J. 1999. Pipes and wiring: The regulation of copper uptake and distribution in yeast. *Trends Microbiol.* 7: 500-5.
- Lam, P. J. & Bishop, J. K. B. 2008, The continental margin is a key source of iron to the HNLC North Pacific Ocean. *Geophys. Res. Lett.* 35 L07608.
- Lane, E. S., Jane, K., Cullen, J. T. & Maldonado, M. T. 2008. The interaction between inorganic iron and cadmium uptake in the marine diatom *Thalassiosira oceanica*. *Limol. Oceanogr.* 53:1784-9.
- Lane, E. S., Semeniuk, D. M., Strzepek, R. F., Cullen, J. T. & Maldonado, M. T. 2009. Effects of iron limitation on intracellular cadmium of cultured phytoplankton: Implications for surface dissolved cadmium to phosphate ratios. *Mar. Chem.* 115: 155–62
- Laudenbach, D. E., Herbert, S. K., McDowell, C., Fork, D. C., Grossman, A. R. & Straus, N. A. 1990. Cytochrome c553 is not required for photosynthetic activity in the cyanobacterium *Synechococcus*. *Plant Cell* 2:913-24.

- Leal M. F. C., Vasconcelos, M. T. S. D. & Van den Berg, C. M. G. 1999. Copper-induced release of complexing ligands similar to thiols by *Emiliana huxleyi* in seawater cultures. *Limnol. Oceanogr.* 44:1750–62.
- Lee, J., Pena, M. M. O., Nose, Y. & Thiele, D. J. 2002. Biochemical characterization of the human copper transporter Ctr1. *J Biol Chem.* 277:4380-7.
- Lee, J., Prohaska, J. R., Dagenais, S. L., Glover, T. W. & Thiele, D. J. 2000. Isolation of a murine copper transporter gene, tissue specific expression and functional complementation of a yeast copper transport mutant. *Gene* 254:87-96
- Le Gall C. A. & Van den Berg, C. M. G. 1998. Folic acid and glutathione in the water column of the north east Atlantic. *Deep-Sea Res Part I* 45:1903–18
- Li, H.H. & Merchant, S. 1995. Degradation of plastocyanin in copper-deficient *Chlamydomonas reinhardtii*: evidence for a protease-susceptible conformation of the apoprotein and regulated proteolysis. *J. Biol. Chem.* 270:23504-10.
- Lin, C. M. & Kosman, D. J. 1990. Copper uptake in wild type and copper metallothionein-deficient *Saccharomyces cerevisiae*. Kinetics and mechanism. *J. Biol. Chem.* 265:9194-200.
- Lin, S. J., Pufahl, R. A., Dancis, A., O'Halloran, T. V. & Culotta, V. C. 1997. A role for the *Saccharomyces cerevisiae* ATX1 gene in copper trafficking and iron transport. *J. Biol. Chem.* 272: 9215–20
- Liu, X. F., Supek, F., Nelson, N. & Culotta, V. C. 1997. Negative control of heavy metal uptake by the *Saccharomyces cerevisiae* BSD2 gene. *J. Biol. Chem.* 272:11763-9.
- Livak, K. J. & Schmittgen, T. D. 2001. Analysis of relative gene expression data using real-time quantitative PCR and the  $2^{-\Delta\Delta CT}$  method. *Methods.* 25: 402-8.
- Loannoni, R., Beaudoin, J., Mercier, A. & Labbe S. 2010. Copper-dependent trafficking of the Ctr4-Ctr5 copper transporting complex. *Plos One*, 5: e11964.
- Lutsenko, S. & Kaplan, J. H. 1995. Organization of P-type ATPases: significance of structural diversity. *Biochem.* 34:15608–13.
- Lutsenko, S. & Petris, M. J. 2003. Function and regulation of the mammalian copper-transporting ATPases: insights from biochemical and cell biological approaches, *J.*

*Membr. Biol.* 191:1–12.

- Mackenzie, N. C., Brito, M., Reyes, A. E. & Allende, M. L. 2004. Cloning, expression pattern and essentiality of the high-affinity copper transporter 1 (ctr1) gene in zebrafish. *Gene* 328:113-20.
- Maldonado, M. T., Allen, A. E., Chong, J. S., Lin, K., Leus, D., Karpenko, N. & Harris, S. L. 2006. Copper-dependent iron transport in coastal and oceanic diatoms. *Limnol. Oceanogr.* 51:1729-43.
- Maldonado, M. T. & Price, N. M. 1996. Influence of N substrate on Fe requirements of marine centric diatoms. *Mar. Ecol. Prog. Ser.* 141:161-72.
- Maldonado, M. T. & Price, N. M. 1999. Utilization of iron bound to strong organic ligands by plankton communities in the subarctic Pacific Ocean. *Deep-Sea Res. II* 46:2447-73.
- Maldonado, M. T. & Price, N. M. 2001. Reduction and transport of organically bound iron by *Thalassiosira oceanica* (Bacillariophyceae). *J. Phycol.* 37:298-310.
- Mann, E.L., Ahlgren, N.A., Moffett, J.W., Chishom, S.W., 2002. Copper toxicity and cyanobacteria ecology in the sargasso sea. *Limnol. Oceanogr.* 47: 976–88.
- Marchetti, A, Parker, M. S., Moccia, L. P., Lin, E. O., Arrieta, A. L., Ribalet, F., Murphy, M. E. P., Maldonado, M. T. & Armbrust, E. V. 2009. Ferritin is used for iron storage in bloom-forming marine pennate diatoms. *Nature* 457:467–70.
- Martin, J. H Coale, ., K. H., Johnson, K. S., Fitzwater, S. E., Gordon, R. M., Tanner, S. J., Hunter, C. N., Elrod, V. A., Nowicki, J. L., Cooley, T. L., Barber, R. T., Lindley, S., Watson, A. J., Van Scoy, K. & Law. C. S. 1994. Testing the iron hypothesis in ecosystems of the Equatorial Pacific Ocean. *Nature* 371: 123-29
- Martin, J. H. & Fitzwater, S. E. 1988. Iron deficiency limits phytoplankton growth in the north-east Pacific subarctic. *Nature* 331: 341–3.
- Martin, J. H., Gordon, R. M., Fitzwater, S. E. & Broenkow, W. W. 1989. Vertex: phytoplankton/iron studies in the Gulf of Alaska. *Deep Sea Res I.* 36: 649-80.
- Merchant, S. 1998. Synthesis of Metalloproteins Involved in Photosynthesis. In *Molecular Biology of Chlamydomonas: Chloroplasts and Mitochondria.* Advances

- in Photosynthesis (Govindjee, series ed.), Kluwer Academic Publishers, pp. 597-611.
- Merchant, S. 2006. Trace metal utilization in chloroplasts. *In* Wise, R. R. & Hooper, J. K. [Eds.] *The Structure and Function of Plastids*, Springer, Netherlands, pp. 199-218.
- Merchant, S. S., Allen, M. D., Kropat, J., Moseley, J. L., Long, J. C., Tottey, S. & Terauchi, A. M. 2006. Between a rock and a hard place: trace element nutrition in *Chlamydomonas*. *Biochim. Biophys. Acta* 1763:578-94.
- Merchant S, & Bogorad, L. 1986. Regulation by copper of the expression of plastocyanin and cytochrome c552 in *Chlamydomonas reinhardi*. *Mol Cell Biol.* 6:462–9.
- Merchant, S., Hill, K. & Howe, G. 1991. Dynamic interplay between two Cu-titrating components in the transcriptional regulation of cytochrome c6. *The EMBO J.* 10:1383-9.
- Miao, A., Wang, W. X. & Juneau, P. 2005. Comparison of Cd, Cu, and Zn toxic effects on four marine phytoplankton by pulse-amplitude-modulated fluorometry. *Environmental Toxicology and Chemistry.* 24: 2603-11.
- Millero, F. J. 2006. *Chemical Oceanography*. Third Edition, CRC Press, Boca Raton. Page 91
- Moffett, J. W. 1995. Temporal and spatial variability of copper complexation by strong chelators in the Sargasso-Sea. *Deep-Sea Res. Part I. Oceanogr. Res. Pap.* 42:1273-95.
- Moffett, J. W. & Brand, L. E. 1996. Production of strong, extracellular Cu chelators by marine cyanobacteria in response to Cu stress. *Limnol. Oceanogr.* 41: 388–95.
- Moffett, J.W., Brand, L. E., Croot, P. L. & Barbeau, K. A. 1997. Cu speciation and cyanobacterial distribution in harbors subject to anthropogenic Cu inputs. *Limnol. and Oceanogr.* 42:789–99.
- Moffett, J. W. & Dupont, C. 2007. Cu complexation by organic ligands in the sub-arctic NW Pacific and Bering Sea. *Deep-Sea Res. Part I. Oceanogr. Res. Pap.* 54:586-95.
- Moffett, J. W, Zika, R. G. & Brand, L. E. 1990. Distribution and potential sources and sinks of copper chelators in the Sargasso Sea. *Deep-Sea Res.* 37:27–36.

- Morel, A. 1997. Consequences of a *Synechococcus* bloom upon the optical properties of oceanic (case 1) waters. *Limnol. and Oceanogra.* 42, 1746-54.
- Morel, F. M. M. 1983. Principles of Aquatic Chemistry. Wiley-Interscience, New-York NY, 446 p.
- Morel, F. M. M. 1987. Kinetics of Nutrient-Uptake and Growth in Phytoplankton. *J. Phycol.* 23:137-50.
- Morel, F. M. M., Milligan, A. J. & Saito, M. A. 2003. Marine Bioinorganic Chemistry: The Role of Trace of Metals in the Oceanic Cycles of Major Nutrients in Treatise on Geochemistry, Vol. 6, edited by Turekian, K K. & Holland, H. D. Elsevier Science Ltd, Cambridge, UK, p. 113-43.
- Morel, F. M. M., Rueter, J. G. & Price, N. M. 1991. Iron nutrition of phytoplankton and its possible importance in the ecology of ocean regions with high nutrient and low biomass. *Oceanography* 4: 56-61.
- Morelli, E. & Scarano, G. 2004. Copper-induced changes of non-protein thiols and antioxidant enzymes in the marine microalga *Phaeodactylum tricornutum*. *Plant Sci.* 167:289–296.
- Moustafa, A., Beszteri, B., Maier, U. G., Bowler, C., Valentin, K. & Bhattacharya, D. 2009. Genomic footprints of a cryptic plastid endosymbiosis in diatoms. *Science* 324:1724-6.
- Muggli, D. L. & Harrison, P. J. 1996. Effects of nitrogen source on the physiology and metal nutrition of *Emiliana huxleyi* grown under different iron and light conditions. *Mar. Ecol. Prog. Ser.* 130:255-67.
- Natarajan, P. & Endicott, J. F. 1973. Photoredox behavior of transition metal-ethylenediaminetetraacetate complexes. A comparison of some group VIII metals. *J. Phys. Chem.* 77:2049–54.
- Nissen, P. 1991. Multiphasic uptake mechanisms in plants. *Int. Rev. of Cytol.-a Survey of Cell Biology* 126:89-134.

- Nose, Y., Kim, B.E. & Thiele, D. J. 2006. Ctr1 drives intestinal copper absorption and is essential for growth, iron metabolism, and neonatal cardiac function. *Cell Metab.* 4: 235-44.
- Nosenko, T., Lidie, K. L., Van Dolah, F. M., Lindquist, E., Cheng, J. F. & Bhattacharya, D. 2006. Chimeric plastid proteome in the florida "red tide" dinoflagellate *Karenia brevis*. *Mol. Biol. Evol.* 23:2026-38.
- Nriagu, J. O. 1979. Copper in the Environment, *Part I: Ecological Cycling*. Wiley-Interscience, New York.
- Ooi, C. E., Rabinovich, E., Dancis, A., Bonifacino, J. S. & Klausner, R. D. 1996 Copper dependent degradation of the *Saccharomyces cerevisiae* plasma membrane copper transporter Ctr1p in the apparent absence of endocytosis. *EMBO J* 15:3515–23.
- Paasche, E. 2001. A review of the coccolithophorid *Emiliana huxleyi* (Prymnesiophyceae), with particular reference to growth, coccolith formation, and calcification-photosynthesis interactions. *Phycologia* 40:503-29.
- Page, M. D., Kropat, J., Hamel, P. P. & Merchant, S. S. 2009. Two *Chlamydomonas* CTR copper transporters with a novel cys-met motif are localized to the plasma membrane and function in copper assimilation. *Plant Cell* 21:928-43.
- Palenik, B., Brahamsha, B., Larimer, F. W., Land, M., Hauser, L., Chain, P., Lamerdin, J., Regala, W., Allen, E. E., McCarren, J., Paulsen, I., Dufresne, A., Partensky, F., Webb, E. A. & Waterbury, J. 2003. The genome of a motile marine *Synechococcus*. *Nature* 424:1037-42.
- Palenik, B., Grimwood, J., Aerts, A., Rouzé, P., Salamov, A., Putnam, N., Dupont, C., Jorgensen, R., Derelle, E., Rombauts, S., Zhou, K., Otiillar, R., Merchant, S., Podell, S., Gaasterland, T., Napoli, C., Gendler, K., Manuell, A., Tai, V., Vallon, O., Piganeau, G., Jancek, S., Heijde, M., Jabbari, K., Bowler, C., Lohr, M., Robbens, S., Werner, G., Dubchak, I., Pazour, G., Ren, Q., Paulsen, I., Delwiche, C., Schmutz, J., Rokhsar, D., Van de Peer, Y., Moreau, H. & Grigoriev, I. 2007. The tiny eukaryote *Ostreococcus* provides genomic insights into the paradox of plankton speciation. *Proc. Natl. Acad. Sci. USA* 104:7705–10.

- Palenik, B., Kieber, D. & Morel, F. M. M. 1988-1989. Dissolved organic nitrogen use by phytoplankton: The role of cell-surface enzymes. *Biol. Oceanogr.* 6:347-54.
- Palenik, B., Ren, Q. H., Dupont, C. L., Myers, G. S., Heidelberg, J. F., Badger, J. H., Madupu, R., Nelson, W. C., Brinkac, L. M., Dodson, R. J., Durkin, A. S., Daugherty, S. C., Sullivan, S. A., Khouri, H., Mohamoud, Y., Halpin, R., & Paulsen, I. T. 2006. Genome sequence of *Synechococcus* CC9311: insights into adaptation to a coastal environment. *Proc. Natl. Acad. Sci. USA* 103:13555-59.
- Pandey, P. K., Singh, S. P. & Bisen, P. S. 1997. Cu<sup>2+</sup> efflux and its regulation in Cu-resistant (Cur) cyanobacterium *Nostoc calcicola* BREB. *J. Basic Microbiol.* 37:355-360.
- Peers, G. & Price, N. M. 2006. Copper-containing plastocyanin used for electron transport by an oceanic diatom. *Nature* 441:341-44.
- Peers, G., Quesnel, S. A. & Price, N. M. 2005. Copper requirements for iron acquisition and growth of coastal and oceanic diatoms. *Limnol. Oceanogr.* 50:1149-58.
- Pena, M. M. O., Koch, K. A. & Thiele, D. J. 1998. Dynamic regulation of copper uptake and detoxification genes in *Saccharomyces cerevisiae*. *Mol. Cell. Biol.* 18:2514-23.
- Pena, M. M., Puig, S. & Thiele, D. J. 2000. Characterization of the *Saccharomyces cerevisiae* high affinity copper transporter Ctr3. *J. Biol. Chem.* 275:33244-51.
- Peñas, M. M., Azparren, G., Domínguez, A., Sommer, H., Ramírez L. & Pisabarro, A. G. 2005. Identification and functional characterisation of ctr1, a *Pleurotus ostreatus* gene coding for a copper transporter. *Mol. Genet. Genomics.* 274:402-9.
- Perez-Llorens, J. L. & Niell, F. X. 1995. Short-term phosphate-uptake kinetics in *Zostera noltii* Hornem - a comparison between excised leaves and sediment-rooted plants. *Hydrobiologia* 297:17-27.
- Persson, P., Shrimpton, J. M., McCormick, S. D. & Bjornsson, B. T. 2000. The presence of high-affinity, low-capacity estradiol-17 $\beta$  binding in rainbow Trout Scale indicates a possible endocrine route for the regulation of scale resorption. *Gen. Comp. Endocrinol.* 120:35-43.

- Petris, M.J., Smith, K., Lee, J. & Thiele, D. J. 2003. Copper-stimulated endocytosis and degradation of the human copper transporter, hCtr1. *J. Biol. Chem.* 278, 9639–46.
- Phung, L. T., Ajlani, G. & Haselkorn, R. 1994. P-Type atpase from the cyanobacterium *Synechococcus-7942* related to the human Menkes and Wilson Disease gene-products. *Proc. Natl. Acad. Sci. U.S.A.* 91:9651-54.
- Pilon, M., Abdel-Ghany, S. E., Cohu, C. M., Gogolin, K. A. & Ye, H. 2006. Copper cofactor delivery in plant cells. *Curr. Opin. Plant Biol.* 9:256-63.
- Pistocchi R, Guerrini, F., Balboni, V. & Boni, L. 1997. Copper toxicity and carbohydrate production in the microalgae *Cylindrotheca fusiformis* and *Gymnodinium* sp. *Eur. J. Phycol.* 32: 125–32.
- Price, N. M., Harrison, G. I., Hering, J. G., Hudson, R. J., Nirel, P. M. V., Palenik, B. & Morel, F. M. M. 1989. Preparation and chemistry of the artificial algal culture medium Aquil. *Biological Oceanography* 6:443-61.
- Pufahl, R. A., Singer, C. P., Peariso, K. L., Lin, S. J., Schmidt, P., Fahrni, C., Cizewski-Culotta, V., Penner-Hahn, J. E. & O'Halloran, T. V. 1997. Metal ion chaperone function of the soluble Cu(I) receptor, Atx1. *Science* 278: 853-6.
- Puig, S., Andres-Colas, N., Garcia-Molina, A. & Penarrubia, L. 2007. Copper and iron homeostasis in *Arabidopsis*: responses to metal deficiencies, interactions and biotechnological applications. *Plant Cell and Environ.* 30:271-90.
- Puig, S., Lee, J., Lau, M. & Thiele, D. J. 2002. Biochemical and genetic analyses of yeast and human high affinity copper transporters suggest a conserved mechanism for copper uptake. *J. Biol. Chem.* 277: 26021-30.
- Puig, S. & Thiele, D. J. 2002. Molecular mechanisms of copper uptake and distribution. *Curr. Opin. Chem. Biol.* 6:171-80.
- Quigg, A., Finkel, Z. V., Irwin, A. J., Rosenthal, Y., Ho, T. Y., Reinfelder, J. R., Schofield, O., Morel, F. M. M. & Falkowski, P. G. 2003. The evolutionary inheritance of elemental stoichiometry in marine phytoplankton. *Nature* 425:291-94.
- Quigg, A., Reinfelder, J. R. & Fisher, N. S. 2006. Copper uptake kinetics in diverse

- marine phytoplankton. *Limnol. Oceanogr.* 51:893-99.
- Ramesh, S. A., Shin, R., Eide, D. J. & Schachtman, D. P. 2003. Differential metal selectivity and gene expression of two zinc transporters from rice. *Plant Physiol.* 133:126-34
- Raven, J. A., Evans, M. C. & Korb, R. E. 1999. The role of trace metals in photosynthetic electron transport in O<sub>2</sub>-evolving organisms. *Photosynthesis Res.* 60:111-50.
- Raymont, J. E. G. 1980. Plankton and productivity in the oceans: Phytoplankton. 2nd ed. Pergamon Press, Oxford, 489 pp.
- Redfield, A. C., Ketchum, B. H. & Richards, F. A. 1963. The influence of organisms on the composition of sea-water, p. 2G77. In M. N. Hill [Ed.], *The Sea*, v. 2. Wiley.
- Rees, E.M. & Thiele, D.J. 2004. From aging to virulence: forging connections through the study of copper homeostasis in eukaryotic microorganisms. *Curr. Opin. Microbiol.* 7:175-84.
- Reinfelder, J. R., Jablonka, R. E. & Cheney, M. 2000. Metabolic responses to subacute toxicity of trace metals in a marine microalga (*Thalassiosira weissflogii*) measured by calorimetry. *Environmental Toxicology and Chemistry.* 19: 448-53.
- Riggio, M., Lee, J., Scudiero, R., Parisi, E., Thiele, D. J. & Filosa, S. 2002. High affinity copper transport protein in the lizard *Podarcis sicula*: molecular cloning, functional characterization and expression in somatic tissues, follicular oocytes and eggs. *Biochim Biophys Acta*, 1576:127-35.
- Robinson, N. J., Proctor, C. M., Connolly, E. L. & Guerinot, M. L. 1999. A ferric-chelate reductase for iron uptake from soils. *Nature* 397:694-7.
- Rodriguez, F. I., Esch, J. J., Hall, A. E., Binder, B. M., Schaller, G. E. & Bleecker, A. B. 1999. A copper cofactor for the ethylene receptor ETR1 from *Arabidopsis*. *Science* 283:996-8.
- Rogers, E.E., Eide, D.J. & Guerinot, M.L. 2000. Altered selectivity in an Arabidopsis metal transporter, *Proc. Natl. Acad. Sci. U.S.A.* 97:12356-60.
- Ross, A. R. S., Ikonomou, M. G. & K. J. Orians. 2003. Characterization of copper-complexing ligands in seawater using immobilized copper (II)-ion affinity

- chromatography and electrospray ionization mass spectrometry. *Mar. Chem.* 83: 47–58.
- Rubino, J. T., Chenkin, M. P., Keller, M., Riggs-Gelasco, P. & Franz, K. J. 2011. A comparison of methionine, histidine and cysteine in copper (I)-binding peptides reveals differences relevant to copper uptake by organisms in diverse environments, *Metallomics* 3:61-73.
- Rue, E. L., & Bruland, K. W. 1995. Complexation of iron(III) by natural organic-ligands in the central north pacific as determined by a new competitive ligand equilibration adsorptive cathodic stripping voltammetric method. *Marine Chemistry* 50: 117-38.
- Rueter J. G., McCarthy, J. J. & Carpenter, E. J. 1979. The toxic effect of copper on *Oscillatoria. (Trichodesmium) theibautii*. *Limnol. Oceanogr.* 24:558-62.
- Rutgers van der Loeff, M., Helmers, E. & Kattner, G. 1997. Continuous transects of cadmium, copper, and aluminum in surface waters of the Atlantic ocean, 50°N to 50° S: Correspondence and contrast with nutrient-like behaviour. *Geochim. Cosmochim. Acta.* 61: 47-61.
- Ryther, J. H. & Kramer, D. D. 1961. Relative iron requirements of some coastal and offshore plankton algae. *Ecology* 42: 444-6.
- Saito, M. A., Sigman, D. M. & Morel, F. M. M. 2003. The bioinorganic chemistry of the ancient ocean: the co-evolution of cyanobacterial metal requirements and biogeochemical cycles at the Archean - Proterozoic boundary? *Inorganica Chimica Acta* 356C:308-18.
- Sancenon, V., Puig, S., Mateu-Andres, I., Dorcey, E., Thiele, D. J. & Peñarrubia, L. 2004. The *Arabidopsis* copper transporter COPT1 functions in root elongation and pollen development. *J. Biol. Chem.* 279: 15348-55.
- Sancenon, V., Puig, S., Mira, H., Thiele, D. J. & Peñarrubia, L. 2003. Identification of a copper transporter family in *Arabidopsis thaliana*. *Plant Mol. Biol.* 51: 577-87.
- Sandmann, G., Reck, H., Kessler, E. & Boger, P. 1983. Distribution of plastocyanin and soluble plastidic cytochrome-C in various classes of algae. *Arch. Microbiol.* 134:23-7.

- Sanudo-Wilhelmy, S. A., Tovar-Sanchez, A., Fu, F. X., Capone, D. G., Carpenter, E. J. & Hutchins, D. A. 2004. The impact of surface-adsorbed phosphorus on phytoplankton Redfield stoichiometry. *Nature* 432: 897-901.
- Schneide, R. P. & Wiley, W. R. 1971. Regulation of sugar transport in *Neurospora-Crassa*. *J. Bacteriol.* 106:487-92.
- Semeniuk, D. M., Cullen, J. T., Johnson, W. K., Gagnon, K., Ruth, T. J. & Maldonado, M. T. 2009. Plankton copper requirements and uptake in the subarctic Northeast Pacific Ocean. *Deep-Sea Res. Part I Oceanogr. Res. Pap.* 56:1130-42.
- Shaked, Y., Kustka, A. B. & Morel, F. M. M. 2005. A general kinetic model for iron acquisition by eukaryotic phytoplankton. *Limnol. Oceanogr.* 50:872-82.
- Shikanai, T., Muller-Moule, P., Munekage, Y., Niyogi K. K., & Pilon, M. 2003. PAA1, a P-type ATPase of *Arabidopsis*, functions in copper transport in chloroplast, *Plant Cell* 15:1333-46.
- Siaut, M., Heijde, M., Mangogna, M., Montsant, A., Coesel, S., Allen, A., Manfredonia, A., Falciatore, A. & Bowler, C. 2007. Molecular toolbox for studying diatom biology in *Phaeodactylum tricornutum*. *Gene* 406:23-5.
- Solioz, M. & Vulpe, C. 1996. CPx-type ATPase: a class of P-type ATPase that pump heavy metals, *Trends Biochem. Sci.* 21:237-41.
- Sterner, R. W. & Elser, J. J. 2002. Ecological stoichiometry. *Ecological Stoichiometry: the Biology of Elements from Molecules to the Biosphere*. Princeton University Press, Princeton, 584 pp.
- Strzepek, R. F. & Harrison, P. J. 2004. Photosynthetic architecture differs in coastal and oceanic diatoms. *Nature* 431: 689-92.
- Strzepek, R.F., Maldonado, M.T., Hunter, K.A., Frew, R.D. & Boyd, P.W. 2011. Adaptive strategies by Southern Ocean phytoplankton to lessen iron limitation: Uptake of organically-complexed iron and reduced cellular iron requirements. *Limnol. Oceanogr.* 56:1983-2002.
- Stuart, R. K., Dupont, C. L., Johnson, D. A., Paulsen, I. T., & Palenik, B. 2009. Coastal strains of marine *Synechococcus* species exhibit increased tolerance to copper

- shock and a distinctive transcriptional response relative to those of open-ocean strains. *Appl. Environ. Microbiol.* 75: 5047–57.
- Sunda, W. G. 1994. Trace metal/phytoplankton interactions in the sea. In G. Bidoglio and W. Stumm [eds.], *Chemistry of aquatic systems: Local and global perspectives*. Kluwer Academic. p. 213–47.
- Sunda, W. G., & Ferguson, R. L. 1983. Sensitivity of natural bacterial communities to additions of copper and to cupric ion activity: A bioassay of copper complexation in seawater, p. 871- 890. *Zn Trace metals in sea water*. NATO Conf. Ser. 4, Mar. Sci. V. 9. Plenum.
- Sunda, W. G. & Huntsman, S. A. 1983. Effect of competitive interactions between manganese and copper on cellular manganese and growth in estuarine and oceanic species of the diatom *Thalassiosira*. *Limnol. Oceanogr.* 28:924-34.
- Sunda, W. G. & Huntsman, S. A. 1995a. Iron uptake and growth limitation in oceanic and coastal phytoplankton. *Mar. Chem.* 50:189-206.
- Sunda, W. G. & Huntsman, S. A. 1995b. Regulation of copper concentration in the oceanic nutricline by phytoplankton uptake and regeneration cycles. *Limnol. Oceanogr.* 40:132-37.
- Sunda, W. G. & Huntsman, S. A. 1996. Antagonisms between cadmium and zinc toxicity and manganese limitation in a coastal diatom. *Limnol. Oceanogr.* 41:373-87.
- Sunda, W. G. & Huntsman, S. A. 1998a. Interactive effects of external manganese, the toxic metals copper and zinc, and light in controlling cellular manganese and growth in a coastal diatom. *Limnol. Oceanogr.* 43:1467–75.
- Sunda, W. G. & Huntsman, S. A. 1998b. Interactions among  $\text{Cu}^{2+}$ ,  $\text{Zn}^{2+}$ , and  $\text{Mn}^{2+}$  in controlling cellular Mn, Zn, and growth rate in the coastal alga *Chlamydomonas*. *Limnol. Oceanogr.* 43:1055-64.
- Sunda, W. G. & Huntsman, S. A. 1998c. Processes regulating cellular metal accumulation and physiological effects: Phytoplankton as model systems. *Sci. Total Environ.* 219:165-81.
- Sunda, W. G., Price, N. M. & Morel, F. M. M. 2005. Trace metal ion buffers and their

- use in culture studies. In: Anderson, R. A. [Ed.] *Algal Culturing Techniques*. Elsevier, Amsterdam, pp. 35-63.
- Sunda, W. G., Swift, D. G. & Huntsman, S. A. 1991. Low iron requirement for growth in oceanic phytoplankton. *Nature* 351:55-7.
- Sunda, W. G., Tester, P. A. & Huntsman, S. A. 1990. Toxicity of trace metals to *Acartia tonsa* in the Elizabeth River and southern Chesapeake Bay. *Estuar. Coast. and Shelf Sci.* 30:207-21.
- Sutak, R., Slapeta, J., San Roman, M., Camadro, J. M., Lesuisse, E. 2010. Nonreductive iron uptake mechanism in the marine alveolate *Chromera velia*. *Plant Physiol.* 154:991-1000.
- Tang D., Hung, C. C, Warnken, K. W. & Santschi, P. H. 2000. The distribution of biogenic thiols in surface waters of Galveston Bay. *Limnol Oceanogr* 45:1289–97.
- Tennant, J., Stansfield, M., Yamaji, S., Srari, S. K. & Sharp, P. 2002. Effects of copper on the expression of metal transporters in human intestinal Caco-2 cells. *FEBS Letters* 527, 239–44.
- Timmermans, K. R., Gerringa, L. J. A., De Baar, H. J. W., Van Der Wagt B., Veldhuis, M. J. W., De Jong, J. T. M., & Croot, P. L. 2001. Growth rates of large and small Southern Ocean diatoms in relation to availability of iron in natural seawater. *Limnol. Oceanogr.* 46: 260–6.
- Timmermans, K. R., Van Der Wagt B. & De Baar, H. J. W. 2004. Growth rates, half-saturation constants, and silicate, nitrate, and phosphate depletion in relation to iron availability of four large, open-ocean diatoms from the Southern Ocean. *Limnol. Oceanogr.* 49: 2141–51.
- Toledo, G., Palenik, B. & Brahamsha. B. 1999. Swimming marine *Synechococcus* strains with widely different photosynthetic pigment ratios form a monophyletic group. *Appl. Environ. Microbiol.* 65: 5247-51.
- Tsuda, A., Takeda, S., Saito, H., Nishioka, J., Nojiri, Y., Kudo, I., Kiwosawa, H., Shiimoto, A., Imai, K., Ono, T., Shiamoto, A., Tsumune, D., Yoshimura, T., Aono, T., Hinuma, A., Kinugasa, M., Suzuki, K., Sohrin, Y., Noiri, Y., Tani, H.,

- Deguchi, Y., Tsurushima, N., Ogawa, H., Fukami, K., Kuma, K. & Saino, T. 2003. A mesoscale iron enrichment in the western subarctic Pacific induces a large centric diatom bloom. *Science* 300: 958-961.
- Twining, B.S., Baines, S.B. & Fisher, N.S. 2004. Element stoichiometries of individual plankton cells collected during the Southern Ocean Iron Experiment (SOFeX). *Limnol.Oceanogr.* 49: 2115-28.
- Tzagoloff, A., Nobrega, M., Gorman, N. & Sinclair, P. 1993. On the function of yeast COX10 and COX11 gene products. *Biochem. Mol. Biol. Int.* 31:593– 98.
- Van Den Berg. 1984. Determination of the complexing capacity and conditional stability constants of complexes of copper(B) with natural organic ligands in seawater by cathodic stripping voltammetry of copper-catechol complex ions. *Mar. Chem.* 15: 1- 18.
- Van Den Berg, C. M. G., Merks, A. G. A. & Duursma, E. K. 1987. Organic complexation and its control of the dissolved concentrations of copper and zinc in the Scheldt Estuary. *Estuar Coast Shelf Sci.* 24:785–97.
- Van der Loeff M. R., Helmers, E. & Kattner, G. 1997. Continuous transects of cadmium, copper, and aluminium in surface waters of the Atlantic Ocean, 50°N to 50°S: Correspondence and contrast with nutrient-like behaviour *Geochimica et Cosmochimica Acta* 61:47-61
- Verma, S. K. & Singh H. N. 1991. Evidence for energy-dependent copper efflux as a mechanism of Cu<sup>2+</sup> resistance in the cyanobacterium *Nostoc calcicola*. *FEMS Microbiol. Lett.* 84: 291–294.
- Walker J. C. G, Klein, C., Schidlowski, M., Schopf, J. W., Stevenson, D. J. & Walter, M. R. 1983. Environmental evolution of the Archean-early Proterozoic Earth. In: Schopf JW (Ed) *Earth's Earliest Biosphere: Its Origin and Evolution*, Princeton Univ Press, Princeton. pp 260-90.
- Waterbury, J. B., Watson, S. W., Valois, F. W. & Franks, D. G. 1986. Biological and ecological characterization of the marine unicellular cyanobacterium *Synechococcus*. In Platt, T. & Li, W. [Eds.] *Photosynthetic picoplankton*, Vol 214.

- Can. J. Fish. Aquat. Sci. Bull., Ottawa, Canada, pp 71-120.
- Waters, B.M. & Eide, D.J. 2002. Combinatorial control of yeast FET4 gene expression by iron, zinc, and oxygen. *J. Biol. Chem.* 277:33749–57.
- Weger, H. G. 1999. Ferric and cupric reductase activities in the green alga *Chlamydomonas reinhardtii*: experiments using iron-limited chemostats. *Planta*. 207:377-84.
- Welch, R. M., Norvell, W. A., Schaefer, S. C., Shaff, J. E. & Kochian, L. V. 1993. Induction of iron (III) and copper (II) reduction in pea (*Pisum sativum* L.) roots by Fe and Cu status: Does the root-cell plasmalemma Fe(III)-chelate reductase perform a general role in regulating cation uptake? *Planta* 190:555-61.
- Wells, M. L., Trick, C. G., Cochlan, W. P., Hughes, M. P. & Trainer, V. L. 2005. Domoic acid: The synergy of iron, copper, and the toxicity of diatoms. *Limnol. Oceanogr.* 50:1908-17.
- Welschmeyer, N., Goericke, R., Strom, S. & Peterson, W. 1991. Phytoplankton growth and herbivory in the sub-Arctic Pacific - a chemotaxonomic analysis. *Limnol. Oceanogr.* 36:1631-49.
- Wintz, H., Fox, T., Wu, Y. Y., Feng, V., Chen, W., Chang, H. S., Zhu, T. & Vulpe, C. 2003. Expression profiles of *Arabidopsis thaliana* in mineral deficiencies reveal novel transporters involved in metal homeostasis. *J. Biol. Chem.* 278:47644-53.
- Wintz, H. & Vulpe, C. 2002. Intracellular trafficking: plant copper chaperones. *Biochem. Soc. Trans.* 30:732-5.
- Wiramanaden, C. I. E., Cullen, J. T., Ross, A. R. S. & Orians, K. J.. 2008. Cyanobacterial copper-binding ligands isolated from artificial seawater cultures. *Marine Chemistry* 110:28-41.
- Wood, P. M., 1978. Interchangeable copper and iron proteins in algal photosynthesis. Studies on plastocyanin and cytochrome c-552 in *Chlamydomonas*. *Eur. J. Biochem.* 87: 8-19.
- Woeste, K.E. & Kieber, J. J. 2000. A strong loss-of-function mutation in *RAN1* results in constitutive activation of the ethylene response pathway as well as a rosette-lethal

- phenotype. *Plant Cell*. 12, 443-55.
- Wu, J. & Luther, G. W. 1996. Spatial and temporal distribution of iron in the surface water of the northwestern Atlantic Ocean. *Geochim Cosmochim Acta* 60:2729-41.
- Wu, J., & Luther, G.W. 1995. Complexation of Fe (III) by natural organic ligands in the northwest Atlantic Ocean by a competitive ligand equilibrium method and a kinetic approach, *Mar. Chem.* 50, 159– 177.
- Xiao, Z. & Wedd, A. G. 2002. A C-terminal domain of the membrane copper pump Ctr1 exchanges copper (I) with the copper chaperone Atx1. *Chem. Commun.* 21:588-9.
- Yamaguchi-Iwai, Y., Serpe, M., Haile, D., Yang, W., Kosman, D. J., Klausner, R.D. & Dancis, A., 1997. Homeostatic regulation of copper uptake in yeast via direct binding of MAC1 protein to upstream regulatory sequences of FRE1 and CTR1. *J. Biol. Chem.* 272, 17711– 8.
- Yang, T. J, Lin, W. D. & Schmidt, W. 2010. Transcriptional profiling of the Arabidopsis iron deficiency response reveals conserved transition metal homeostasis networks. *Plant Physiol.* 152:2130-41.
- Yi, Y. & Guerinot, M. L. 1996. Genetic evidence that induction of root Fe(III) chelate reductase activity is necessary for iron uptake under iron deficiency. *Plant J.* 10:835-44.
- Yuan, M., Chu, Z., Li, X. & Xu, C. 2010. Wang S: The bacterial pathogen *Xanthomonas oryzae* overcomes rice defenses by regulating host copper redistribution. *Plant Cell* 22:3164-3176.
- Yuan, M., Li, X., Xiao, J. & Wang, S. 2011. Molecular and functional analyses of COPT/Ctr type copper transporter-like gene family in rice. *Plant Biology* 11:69-81.
- Zerkle, A. L, House, C. H., Cox, R. P. & Canfield, D. E. 2006. Metal limitation of cyanobacterial N<sub>2</sub> fixation and implications for the Precambrian nitrogen cycle. *Geobiology* 4, 285–297.
- Zhou, H., Cadigan, K. M. & Thiele, D. J. 2003. A copper-regulated transporter required for copper acquisition, pigmentation, and specific stages of development in *Drosophila melanogaster*. *J Biol Chem.* 278:48210-8.

- Zhou, B. & Gitschier, J. 1997. hCTR1: a human gene for copper uptake identified by complementation in yeast. *Proc. Natl. Acad. Sci. U.S.A.* 94:7481-6
- Zhou, H. & Thiele, D. J. 2001. Identification of a novel high affinity copper transport complex in the fission yeast *Schizosaccharomyces pombe*. *J Biol Chem* 276:20529-35.
- Zhu, S. H., Guo, J., Maldonado, M. T. & Green, B. R. 2010. Effects of iron and copper deficiency on the expression of members of the light-harvesting family in the diatom *Thalassiosira pseudonana*. *J. Phycol.* 46: 974-81.

## Appendix A

Supplemental table 1. A list of all genes and primer sequences used in this study. Each gene name is as given in the text with its protein identification number (ID) in the *T. pseudonana* genome. The protein ID and chromosome locations were obtained from <http://genome.jgi-psf.org/Thaps3/Thaps3.home.html>. Sequences of forward and reverse primers are given. Asterisks indicate the sequences for the primers that have been published previously (Kustka et al. 2007).

Candidate genes	Annotation	Primer sequence (5'–3') (forward/reverse)	Genome locus
<i>Tp</i> CTR 24275	Putative CTR-like Cu transporter	GCATGCGTCGGCTTATTCTA	chr_11a:66327-68695
<i>Tp</i> CTR 9391		CACATGACCTGCCATCATTC	
<i>Tp</i> CTP 263051	Putative Cu- transporting p-type ATPase	GTCAAATGCTCTGTCCAGCA	chr_13:305077-306438
<i>Tp</i> CTP 264357		CGTTTGATCCATTTGGAGGT	
<i>Tp</i> CTP 264357		GTGCTGAGCAGACAGTGAGC	
<i>Tp</i> COX17 264096	Putative Cu chaperone	GCAGATAGACAACGGCGATT	chr_7:97839-101400
<i>Tp</i> COX11 37139		TTGACAAGACGGGAACCATT	
<i>Tp</i> COX11 37139		TTCCTGCCCAGGGTAAATC	
<i>Tp</i> FRE1 (11375)	Putative Fe reductase	AAAGTGGGCATCAAATCAGG	chr_14:17090-17324
<i>Tp</i> FRE2 (3129)		CTCTTACAATCCGCGTCCTC	
<i>Tp</i> FRE2 (3129)		AGTCGCCACCTACAATGTCC	
<i>Tp</i> FET3 (5574)	Putative multi- copper oxidase	ACTGGCATATCCACCGTTTC	chr_13:211685-212026
<i>Tp</i> FTR1(268009)		GCCGTAAGCTGCAATGCTGA*	
<i>Tp</i> NRAMP (9840)	Putative NRAMP protein	GTTTCGCAATGCAACTTTCT	chr_19c_29:203384-205714
<i>Tp</i> ZIP 32375		ATCGGAAGCTTCGCTGTTTT *	
<i>Tp</i> ZIP 268980	Putative ZIP transporter	GGCCTGCTGTAGCTGACTTG*	chr_3:199111-202275
<i>Tp</i> ZIP 22351		GTCGTCGAGCAAGTTTCGTT *	
<i>Tp</i> ZIP 263800		GGGAGCAACGTGGATAACAT *	chr_5:1547780-1553454
<i>Tp</i> ZIP 11826		GCTGGCTTGTGTTTGGGAATTGT *	
<i>Tp</i> Actin (25772)		CACCTTCCTCTGCCTCGTTGA *	chr_1:1226465-1227728
<i>Tp</i> Actin (25772)		ATCGCCCAAGACGACAGAGTTGA *	
<i>Tp</i> Actin (25772)		CACCGCTCCTAGAATCCAGTAATG *	chr_14:507218-508928
<i>Tp</i> Actin (25772)	AACGTAGGAACAGCCCTCCT		
<i>Tp</i> Actin (25772)	ATGACACCTGCCGACAAAC	chr_2:430621-431896	
<i>Tp</i> Actin (25772)	TGGTGTGTGGTCACTTCGTT		
<i>Tp</i> Actin (25772)	GCCTCCAACAACAACCTCCAT	chr_5:2224263-2225620	
<i>Tp</i> Actin (25772)	CAACGCAGACGAAGAAAACA		
<i>Tp</i> Actin (25772)	GGGAACGCATACTTCGACAT	chr_4:1529303-1531395	
<i>Tp</i> Actin (25772)	GCCATTGCTCAAACCGTATT		
<i>Tp</i> Actin (25772)	CTTAGCCGCAAGACCAAATC	chr_11a:519107-520118	
<i>Tp</i> Actin (25772)	CATTGGTTGCAGCACTATCG		
<i>Tp</i> Actin (25772)	CGACAATCGTTTACCAAGCA	chr_22:553746-555404	
<i>Tp</i> Actin (25772)	ACTGGATTGGAGATGGATGG *		
<i>Tp</i> Actin (25772)	CAAAGCCGTAATCTCCTTCG *	chr_22:804575-806436	